Title
Characterization of the Behavior and Regulation of Pioneer Microtubules at the Larval Drosophila Neuromuscular Junction

Author
Pawson, Catherine Tara

Publication Date
2008

Characterization of the Behavior and Regulation of Pioneer Microtubules at the Larval Drosophila Neuromuscular Junction.

by

Catherine Pawson

DISSERTATION

Submitted in partial satisfaction of the requirements for the degree of

DOCTOR OF PHILOSOPHY

in

Cell Biology

in the

GRADUATE DIVISION

of the

UNIVERSITY OF CALIFORNIA, SAN FRANCISCO

To Grae, my unending thanks for your help and support.
To Mum and Dad for always believing. To Tyler for always supporting. To CRKL, WL, AH, IH, AMC, AC, EH, and SA for always listening.

A portion of the text of this dissertation is a reprint of material as it appeared in the October 29th 2008 issue of the Journal of Neuroscience 28(44):11111-23, under the title "Formin-dependent synaptic growth: evidence that Dlar signals via Diaphanous to modulate synaptic actin and dynamic pioneer microtubules", and is reproduced here with the permission of the journal. The co-author listed in this publication, Dr. Benjamin Eaton, also made significant contributions to the work appearing in this paper.

ABSTRACT

Here live imaging and genetic manipulations are combined to visualize and quantitatively characterize a population of dynamic pioneer microtubules within the *Drosophila* neuromuscular junction (NMJ). First, a GFP-tagged microtubule plus-end binding protein, EB1-GFP, was used to qualitatively and quantitatively characterize the growth and invasion of dynamic axonal and synaptic microtubule plus-ends *in vivo*. Axonal microtubules were found to be uniformly oriented. EB1-GFP movement in the axons was processive and constrained to a straight path. Interestingly, plus-end growth was found to be significantly slower in sensory (3.02 μm/minute ± 0.12) compared to motor (4.12 μm/min ± 0.038) axons, and is significantly faster within the NMJ (4.66 μm/min ± 0.10) compared to the motor axon. Unlike axonal movement, plus-end movement at the synapse was of mixed orientation. Genetic and imaging analysis revealed the movement of dynamic plus-ends to be largely independent of the Map1b-like protein Futsch, though the dynein/dynactin complex was shown to be required for normal plus-end growth. EB1-GFP labeled puncta are often observed exploring nascent and newly formed synaptic regions, an exploratory behavior that may play a role in synapse development. Supporting movies are presented as supplemental data. This tool was next applied to the study of the formin protein, *diaphanous (dia)*, a gene identified in a screen for mutations effecting growth at the NMJ. Diaphanous is present both pre- and postsynaptically however, genetic rescue and interaction experiments support the conclusion that *dia* is necessary presynaptically for normal NMJ growth. Formin family proteins are potent regulators of the cytoskeleton and defects in cytoskeletal organization or regulation could correlate with the synaptic growth defect. Live imaging of dynamic

microtubules and actin revealed defects in both cytoskeletal elements at the synapse. Finally, genetic evidence is presented demonstrating Dia functions downstream of the presynaptic receptor tyrosine phosphatase Dlar and the Rho-type GEF *trio* to control NMJ growth. Based upon the established function of DRFs as Rho-GTPase dependent regulators of the cell cytoskeleton, a model is proposed in which Diaphanous links receptor tyrosine phosphatase signaling at the plasma membrane to growth-dependent modulation of the synaptic actin and microtubule cytoskeletons.

Table of Contents

List of Figures

List of Tables

INTRODUCTION

Within the nervous system, information is integrated and transferred across synapses, specialized sites of cell-cell contact between neurons. Stimulation of a presynaptic neuron leads to the release of packets of chemical neurotransmitters at the synapse, in turn stimulating the post-synaptic cell, ultimately resulting in a functional output such as movement or new synapse formation. The normal development of appropriate synaptic connections is therefore essential to maintaining the efficiency and fidelity of information transfer. Accordingly, defects in synapse formation and function are often associated with, and believed to functionally underlie, disorders of cognition, behavior and movement (Reiner et al., 1993; Comery et al., 1997; Lo Nigro et al., 1997; Goldstein et al., 2003; Munch et al., 2004). In addition, synapses remodel by adding or eliminating connections in response to changes in stimulation frequency and strength. This structural plasticity at the synapse plays an important role in learning and memory (Lisman and Raghavachari, 2006; De Roo et al., 2008). Although the development of synapses is clearly essential for the function of the nervous system, much remains to be elucidated about the mechanisms underlying the structural development of synapse.

There have been a number of hints from study of human diseases that microtubules and microtubule-associated proteins (MAPs) have important roles in the development and maintenance of synapses. For example, in the neurological disorder, lisencephaly, cortical neurons do not migrate to their proper positions, resulting in decreased cortical complexity and giving the surface of the brain a smooth appearance (Reiner et al., 1993; Lo Nigro et al., 1997). Although the mechanisms underlying the migration defects are not clear, there is evidence to support the hypothesis that they arise

from changes in microtubule based motility (Vallee and Tsai, 2008). Recent work has linked mutations in a dynein interacting protein, Lis1 to the development of classical type 1 lisencephaly. The interactions between Lis1 and dynein are complex and it is speculated that Lis1 association may serve to regulate the function of the minus end directed motor protein (Reiner et al., 1993; Lo Nigro et al., 1997). In a second example, P150/Glued, a member of the microtubule associated dynactin complex, has been associated with a reduction in synapse growth and stability (Eaton et al., 2002; LaMonte et al., 2002; Puls et al., 2003; Munch et al., 2004). The decrease in synaptic connections seen in animals with this mutation seem to arise from both defects in synapse development and the degeneration of existing synapses a number of systems (Eaton et al., 2002; LaMonte et al., 2002; Puls et al., 2003). Further, mutations in this gene have been linked to a hereditary form of ALS, a disease marked by loss of synaptic connections, in human patients (Munch et al., 2004). Mutations in additional MAPs have also been associated with altered synapse development and maintenance underlying various disease states (Roos et al., 2000; Garcia and Cleveland, 2001; Zhang et al., 2001; Lu et al., 2004; Bettencourt da Cruz et al., 2005; Pielage et al., 2008). Together these studies provide evidence that the regulation of the microtubule cytoskeleton may be essential for the regulation of synapse formation.

There are a number of ways in which disruption of the integrity of the microtubule cytoskeleton could alter synapse development. A stable core of microtubules provides a track for the trafficking of proteins and vesicles to different regions of the cell. It has been demonstrated that disrupting microtubule based trafficking can alter synapse development . In some cases this occurs by disrupting the

trophic signaling required for continued synapse growth and maintenance. The long-term consolidation of trophic signals requires the retrograde trafficking of signaling intermediaries from the synapse to the nucleus. It has been demonstrated that disrupting the integrity of the axonal microtubule core or retrograde microtubule motor function leads to a decrease in the nuclear translocation of transcription factors downstream of trophic signals, this in turn results in defects in synaptic expansion (Aberle et al., 2002; Eaton et al., 2002; Eaton et al., 2005; Zweifel et al., 2005). In addition to providing tracks for protein trafficking, the microtubule core of most cell types provides global structural support of cell shape. It would therefore be anticipated that altering the integrity of the microtubule core would impair growth of the synapse. While the analysis of MAP mutations in the mammalian nervous system has provided some insight into the role of microtubules in synapse development, a great deal of useful information has been gained from a far simpler model system.

The glutamatergic synapse of the *Drosophila melanogaster* larval neuromuscular junction (NMJ) has been widely used as a tool for studying mechanisms of synaptic development (Brunner and O'Kane, 1997; Featherstone and Broadie, 2000; Rose and Chiba, 2000; Keshishian and Kim, 2004; Schuster, 2006). In this system, the innervation pattern of individual motor neurons has been well characterized and is highly stereotyped (Schuster et al., 1996; Zito et al., 1999). The synapses of the NMJ are composed of discrete spherical swellings of the presynaptic membrane, known as boutons, connected by thin membrane extensions (Jan and Jan, 1976). The presynaptic release machinery is organized into active zones housed within the boutons (Jan and Jan, 1976). Over the course of larval development, the NMJ continuously adds new boutons to maintain an

appropriate level of stimulation of the muscle. This is required as the post-synaptic muscle surface expands up to 100-fold, from the early first to late third larval instars, decreasing the resistance of the muscle surface. To maintain the synaptic efficacy required to stimulate the expanding muscles, new boutons, and thus new release sites, are added (Schuster et al., 1996). This continuous growth has allowed for the straightforward identification of new molecules involved in synapse development. Further, visualization of the expansion of individual synapses from the mid-second to the late larval instar stages has provided some hints as to the cellular mechanisms involved in synapse growth (Zito et al., 1999). The addition of new boutons follows a proximal to distal gradient with newer boutons found at the distal end of a branch (Zito et al., 1999). Although new boutons are occasionally added by intercalation between two extant boutons in more central regions of the synapse, much of the new growth observed occurs at the distal end of a branch. Here new boutons are added either by splitting from a pre-existing bouton in a manner similar to yeast budding, or by *de novo* formation (Zito et al., 1999). The stereotyped pattern of the NMJ, coupled with this basic understanding of the chronology of bouton addition, makes the *Drosophila* NMJ a good system in which to assess the importance of the microtubule cytoskeleton in synapse growth and maintenance.

The organization of the synaptic microtubule cytoskeleton has been well described at the NMJ. In this system, bundling and stabilization of the microtubule core requires the MAP1B-like molecule Futsch (Hummel et al., 2000; Roos et al., 2000). Futsch staining co-localizes with acetylated tubulin staining at the NMJ (Roos et al., 2000). Together these data indicate that the pattern of Futsch staining at the NMJ reflects the organization of a synaptic population of stable microtubules. Consequently, Futsch

staining has been used to visualize and describe the organization of the microtubule cytoskeleton within the NMJ (Roos et al., 2000; Pennetta et al., 2002; Ruiz-Canada et al., 2004; Sherwood et al., 2004; Trotta et al., 2004; Pielage et al., 2005; Zhang et al., 2005; Viquez et al., 2006). The organization revealed by both Futsch and tubulin staining of the NMJInitial characterization is a tightly bundled core that runs throughout the length of the NMJ (Roos et al., 2000). Within some boutons, the microtubules are observed to take on a loop like structure. This organization allows microtubules to provide structural and trafficking support for all regions of the synapse. Interestingly, this core is thickest in the proximal region of the synapse, at the point of nerve entry on the muscle, and tapers dramatically such that the distal most boutons contain little to no Futsch staining (Roos et al., 2000; Pennetta et al., 2002; Ruiz-Canada et al., 2004). This is reminiscent of the pattern of synapse expansion and bouton addition. It has therefore been hypothesized that Futsch invasion is a mark of synapse stability or maturity (Roos et al., 2000; Pennetta et al., 2002). Further, Futsch loops are often observed in branching or newly added boutons, suggesting that this conformation of microtubules correlates with dynamic boutons (Roos et al., 2000). Thus the presence of stable microtubules within a bouton may be an indicator of maturity or stability and may be required for sustained synapse growth.

Disruption of the organization of the Futsch-labeled microtubule core correlates with defects in synapse growth. This correlation was first demonstrated in a *futsch* null background (Roos et al., 2000). In this background the thread-like microtubule core is unbundled and fragmented and microtubule loops within boutons are absent. Additionally, there is a significant decrease in synapse expansion likely as a result of

decreased structural and trafficking support at the NMJ. Following this initial finding, microtubules were shown to be disrupted in a number of mutations associated with decreased synaptic growth. For example, in the backgrounds of DVAP-33A, aPKC, and p150/Glued the integrity of the synaptic microtubule core is compromised corresponding with severely impaired NMJ growth (Eaton et al., 2002; Pennetta et al., 2002; Ruiz-Canada et al., 2004). It is therefore clear that, in the context of the NMJ, the development and organization of a stable microtubule core is required to support and consolidate synapse growth.

More recent work has demonstrated that the integrity of the microtubule cytoskeleton is also essential for the maintenance of the presynaptic terminal at the *Drosophila* NMJ. Synaptic instability at the NMJ can be measured using a "footprint" assay where the presence of organized post-synaptic staining in the absence of a corresponding pre-synaptic stain and structure indicates the retraction of a bouton (Eaton et al., 2002). In two separate retraction backgrounds, the microtubule cytoskeleton is severely altered in the region of synapse loss. Perhaps the most dramatic synaptic retractions observed to date occur in the background of the loss of pre-synaptic α-spectrin, where retraction of entire NMJs can be observed (Pielage et al., 2005). In this background, the organization of the microtubule core is altered throughout the synapse and Futsch-labeled microtubules are absent or fragmented in the region of the synapse most proximal to the retraction event. Similarly, pre-synaptic expression of a dominant negative p150/Glued construct resulted in the fragmentation of the Futsch-labeled microtubule core proximal to footprints (Eaton et al., 2002). It has been demonstrated that the Futsch-labeled microtubule core is among the earliest structures to withdraw

from the region of a retraction, suggesting that disruption of the stable microtubule core in a mature bouton could be a causative event in synapse loss (Pielage et al., 2005; Pielage et al., 2008). Taken together these data support the conclusion that a stable microtubule core is required for normal synaptic development and maintenance.

However, in addition to the stable core, recent evidence has emerged implicating a population of dynamic microtubules in the regulation of synapse growth in a number of other systems. If, as previously believed, microtubules act primarily as structural support for the synapse, increased microtubule stability would be anticipated to lead to an increase in synaptic growth. Instead some mutations that result in an overly stable microtubule core are in some cases associated with defective synaptic growth. For example, increased microtubule stability, as measured by increased levels of MAP1-B or Futsch, underlies synaptic growth defects in models of Fragile X Mental Retardation (Zhang et al., 2001; Lu et al., 2004; Menon et al., 2008). In at least one model system the morphological synaptic defects associated with loss of FMR function could be rescued by decreasing the levels of the MAP (Zhang et al., 2001). In a second example, mutations in Spastin have been linked to changes in synapse development in the *Drosophila* NMJ (Sherwood et al., 2004; Trotta et al., 2004). Defects in Spastin function affect synapse development in a variety of systems as mutations in this protein are linked with the development of dominant hereditary spastic paraplegia, a disorder that results in the loss of synapses from the long axons of the spinal cord (Hazan et al., 1999). As Spastin is able to sever stable microtubules in a number of systems, the loss of this protein within synapses likely increases the stability of the microtubule cytoskeleton (Hartman et al., 1998; Hazan et al., 1999; Errico et al., 2002; Roll-Mecak and Vale, 2005, 2008). In a

final example, increased aPKC results in significant growth defects at the *Drosophila* NMJ (Ruiz-Canada et al., 2004). Pre-synaptic expression of an activated aPKC increased the association of Futsch with microtubules, thereby increasing microtubule stability throughout the NMJ (Ruiz-Canada et al., 2004). Together, these studies demonstrate that altering microtubule stability can be associated with decreased synaptic growth. These observations raise the possibility that a population of dynamic microtubules exists at the synapse and that the balance between this population and the bundled, stable microtubules is important for synapse growth and maintenance.

It is first important to understand the characteristics of microtubule dynamics in order to better understand how such a population could be involved in regulating synapse development. Microtubules are structurally and biochemically asymmetric polymers marked by distinct "plus" and "minus" ends. The structural asymmetry arises from the head-to-tail arrangement of α-β tubulin subunits along the length of the filament. The addition of these hetero-dimers occurs preferentially at the "plus end" of the filament, as kinetics at the "minus end" favor depolymerization or dimer loss. (Desai and Mitchison, 1997; Nogales, 1999) To prevent the abolishment of a filament due to subunit loss, the minus end is typically capped or anchored, largely restricting dynamics to the plus end (Waterman-Storer and Salmon, 1997a; Drewes et al., 1998). Here, the microtubule growth is characterized by a phenomenon known as dynamic instability (Desai and Mitchison, 1997). This is marked by periods of sustained growth interrupted by periods of rapid shrinking. The transitions from growth to shrinking are known as catastrophe events (Cassimeris et al., 1987). Catastrophe events can lead to the complete depolymerization of a filament from the plus end, however, in some instances growth can

be renewed at the plus end through the spontaneous addition of new α-β dimers, a transition referred to as rescue. The constant transitions between growth and shrinking allow individual plus ends to efficiently explore the three dimensional volume of the cell. It has been hypothesized that this exploratory behavior is used by the cell to find and capture rare structures, such as activated signaling receptors or kinetochores (Dent and Gertler, 2003; Dehmelt and Halpain, 2004; Suter et al., 2004; Odde, 2005). Interestingly, microtubules in the axon and synapse are known to be oriented with their plus ends pointed away from the cell body and towards the synapse. This organization could theoretically allow plus ends to invade the full volume of the synapse acquiring information about the intra- and extra-cellular environment.

Some hints as to how dynamic microtubules could influence synapse development can be found by examining their roles in growth cone guidance. The navigation of a growth cone to a target relies on the acquisition of chemical cues, which occurs primarily at filopodial extensions of the growth cone lamella. Interestingly, dynamic microtubules are observed throughout the lamella and entering filopodia (Sabry et al., 1991; Dent et al., 1999; Schaefer et al., 2002). This extensive exploration of the growth cone lamella is necessary for normal growth cone advance as pharmacological disruption of microtubules stalls growth cone advance. Interestingly, this occurs even at very low drug concentrations that effect only plus end dynamics and not the relatively stable central core of microtubules (Buck and Zheng, 2002). Early analysis of cytoskeletal organization using immuno-staining revealed that stable microtubules accumulate in the direction of growth cone turning (Tanaka et al., 1995; Dent et al., 1999; Buck and Zheng, 2002; Zhou et al., 2002; Dent and Gertler, 2003). Additionally, the acquisition and integration of

some guidance cues requires a dynamic microtubule population (Challacombe et al., 1997; Kabir et al., 2001; Dent and Gertler, 2003; Suter et al., 2004). While these studies have focused on *in vitro* analysis of axon guidance, recent data supports a role for dynamic microtubules in axon guidance *in vivo*. Specifically, the loss of the microtubule binding protein Orbit/Mast was shown to alter axon pathfinding downstream of Slit-Robo signaling in *Drosophila* (Lee et al., 2004). Together these data support the hypothesis that a small population of dynamic microtubules are able to effect large changes in the morphology of a cell.

The distal most bouton within the *Drosophila* NMJ may be considered as the synaptic equivalent to the growth cone lamella, as this area is considered to be the most dynamic of the synapse (Zito et al., 1999; Roos et al., 2000). Interestingly, within the distal most bouton microtubules adopt a splayed morphology reminiscent of that observed in the growth cone (Ruiz-Canada et al., 2004). Although the importance of this morphology at the NMJ is not clear, it is possible that these unbundled microtubules are actively searching the membrane for trophic signals or sites permissive for growth, similar to dynamic microtubules in the growth cone lamella. The ability of dynamic microtubules to efficiently invade and explore the full volume of a bouton would therefore be anticipated to be important for the growth of the synapse. Upon identification of active signaling, the dynamic plus ends could initiate actin remodeling and membrane extension.

A number of observations suggest that a population of dynamic microtubules exist within synapse of the NMJ. At the *Drosophila* NMJ, a small population of microtubules has recently been observed to invade the distal most, and thus youngest,

regions of the synapse. These microtubules are not bundled and instead exhibit a splayed organization, similar to dynamic microtubules observed in a number of other systems, including the lamella of the advancing growth cone (Pennetta et al., 2002; Ruiz-Canada et al., 2004). Initial studies did not identify this population as it is not bundled by Futsch. Together the splayed organization and the absence of MAP binding suggest that this population may represent a dynamic subset of microtubules at the NMJ. In support of this, a recent FRAP study revealed the existence of growing microtubules within the NMJ of third instar larvae (Yan and Broadie, 2007). Further, in a range of organisms from Drosophila to mouse, fluorescently labeled plus end markers have been used to identify populations of growing microtubules in mature neurons both *in vitro* and *in vivo* (Chang et al., 1999; Stepanova et al., 2001; Ma et al., 2004; Rolls et al., 2007). Although these observations make it clear that a population of dynamic microtubules is maintained within neurons, the role of this population in synapse growth remains unclear. It is possible this population plays a housekeeping role, becoming incorporated into the stable core over time, thereby strengthening the structural and trafficking support of the neuron. However, it is equally possible that the presence of a small, unbundled population of microtubules in actively growing regions of the synapse is reflective of a more active role for dynamic microtubules in synapse development.

Despite the hints of a role for dynamic microtubules in synapses growth in a variety of systems, the most basic characteristics of the behavior of dynamic microtubules within an *in vivo* synapse are unknown. While live imaging studies in neuronal culture have defined some behaviors of dynamic microtubules in neurons, it has not been possible image synaptic connections in this system. In contrast work on mature

synapses has relied on fixed tissue staining, precluding analysis of a dynamic microtubule population. Thus, no study to date has focused on the behavior or regulation of this population specifically within a synapse. As a result a number of key questions remain unanswered. For example, although it has been suggested that changes in the stable microtubule core reflect changes in the dynamic behavior of microtubules, the relationship between these populations has never been thoroughly examined at the synapse. It is possible that these populations play separate roles in synaptic development as they do in axon guidance. However, it is equally possible that the sole role of dynamic microtubules at the synapse is to supply new subunits to the stable core. Also, while dynamic microtubules influence a number of cellular processes important for synapse development, such as migration and polarization, it is unclear whether synaptic microtubules display this behavior. It would also be of interest to understand the regulation of microtubule dynamics at the synapse.

In the following studies, the behavior and regulation of dynamic microtubules is examined within the larval third instar *Drosophila* NMJ. Two recent studies have used a combination of techniques to confirm the existence of a dynamic microtubule population within the nervous system, and the NMJ (Rolls et al., 2007; Yan and Broadie, 2007). In one study, a microtubule plus-end binding protein, EB1-GFP was used to visualize individual microtubule ends in various neural compartments (Rolls et al., 2007). However this study did not focus on behavior within the synapse. A second study (Yan and Broadie, 2007) demonstrated that microtubule polymerization occurred within the NMJ, suggesting that a population of dynamic microtubules could be found within the synapse. However the technique used in this study precluded analysis of individual plus-

ends. Here, EB1-GFP is used to characterize the behavior and regulation of dynamic microtubules within the NMJ. These studies will characterize the basic behavior of dynamic microtubules within the axon and synapse of motoneurons, including examination of growth polarity, invasive behavior of plus ends and the relationship of pioneer and stable microtubules in these compartments. Next, the regulation of both microtubule dynamics and the invasive behavior of pioneer microtubules will be examined. A special focus will be placed on the ability of Diaphanous and its related formin molecules to regulate both the microtubule and actin cytoskeleton at the synapse. In these studies, a preliminary examination of the role of pioneer microtubules in synapse growth will be presented, along with a model of how this dynamic population may contribute to synapse outgrowth will be presented. Together, these studies represent the first attempt to describe and quantitate pioneer microtubules within a mature synapse.

Quantitative *in vivo* Live Imaging of Axonal and Synaptic Microtubules; Neuronal Type and Synapse-Specific Regulation

INTRODUCTION

The microtubule cytoskeleton is a fundamental component of the nerve cell, providing structural support for the dendrites, axon, growth cone and synapse (Mitchison and Kirschner, 1988; Lin et al., 1994; Mandell and Banker, 1996). Additionally, stable microtubules act as conduits for protein traffic throughout the cell. Much is known about the roles and regulation of the stable microtubule population. However, a second less well understood dynamic population of microtubules also exists within many cells types, including neurons (Wadsworth, 1999). In the growth cone dynamic microtubules are important in turning and directional changes (Tanaka et al., 1995). Furthermore, this population may be required to link transient signaling events at the plasma membrane to signal transduction in the cell interior in neural and other cell types (Kirschner and Mitchison, 1986). The ability of dynamic microtubules to acquire information about the intra and extra cellular environment, as well as to influence cell outgrowth raises intriguing possibilities as to their role at the synapse. However, to date no study has been made of the role of dynamic microtubules in synapse growth and stability.

Much of the current understanding of neural microtubules has come largely from the study of *in vitro* systems and immuno-staining studies in fixed tissues. The use of cultured neurons has allowed for the direct visualization and characterization of the inherently dynamic microtubule cytoskeleton (Tanaka et al., 1995; Stepanova et al., 2003). However a limitation of the in vitro systems has been the inability to examine this population within a mature synapse. In contrast, studies focused on the imaging of synaptic microtubules have relied on the use of fixed tissue staining in a variety of different genetic backgrounds. Combining microscopy with genetic studies has

demonstrated that the synaptic microtubule cytoskeleton plays an important role during synaptic growth, remodeling, and neurodegenerative disease (Lucas et al., 1998; Hall et al., 2000; Roos et al., 2000; Garcia and Cleveland, 2001; Zhang et al., 2001; Eaton et al., 2002; Pennetta et al., 2002; Goldstein, 2003). However, the use of fixed tissue staining precludes the observation of dynamic microtubules. Instead, alterations in tubulin or MAP staining patterns have been used as a means to draw conclusions about the regulation and behavior of this population *in vivo*. Thus to better understand the behavior and regulation of the dynamic microtubules at the nerve terminal, it was important to observe this population *in vivo* in a functional synapse. This requires a synapse that is amenable to live imaging and experimental manipulation. The size, stereotyped development and ease of genetic manipulation make the *Drosophila* NMJ a good model system for live imaging and study of synaptic cytoskeletal elements (Jan and Jan, 1976).

The ability to visualize and quantify microtubule movement and dynamics in an *in vivo* system has historically been hampered by technical hurdles. For example, most recent work examining microtubule dynamics *in vitro* use fluorescently labeled tubulin, injected at low concentration into a cell, to "speckle" microtubules with fluorescence (Waterman-Storer et al., 1998; Salmon et al., 2002; Schaefer et al., 2002). However, the small size of *Drosophila* neurons precludes micro-injection. Furthermore, it has not been possible to optimize the transgenic expression of GFP-tubulin to allow microtubule speckling while still attaining sufficient signal for *in vivo* imaging. However, two recent studies in *Drosophila* have paved the way for a quantitative analysis of dynamic microtubules in a living synapse. In one study a GFP-tagged microtubule plus-end binding protein, EB1, was expressed in central neurons. The use of EB1-GFP allowed

the authors to identify, and characterize the organization of, a dynamic population of microtubules in different cellular compartments including the axons, dendrites and cell bodies of mature neurons (Rolls et al., 2007) *in vivo*. However, in this study the authors chose not to focus on this population within a synaptic terminal. A second study made use of live imaging of GFP-tubulin to specifically examine synaptic microtubules (Yan and Broadie, 2007). Using the rate of fluorescence recovery after photobleaching the GFP-tubulin at the NMJ, the authors were able to conclude that two distinct populations of microtubules exist at the synapse, both a dynamic and a stable population. However, as GFP-tubulin is equally incorporated in the dynamic and stable microtubule populations, the use of this tool precluded specific examination of the behavior of dynamic microtubules. While these studies together demonstrate that dynamic microtubules are present in mature neurons and at the NMJ, much work remains to provide a full understanding of the behavior and regulation of this population at the synapse.

In the following study neural expression of the microtubule plus-end binding protein, EB1-GFP, is used as a means of specifically examining dynamic microtubules within the axon and presynaptic nerve terminal of third instar *Drosophila* larvae. By combining live imaging and *Drosophila* genetics the *in vivo* behavior of this population can be characterized and quantified. Areas of particular interest include: the basic behavior and regulation of dynamic microtubules, the relationship between dynamic and stable microtubules at the synapse, and the role of this population in synaptic growth. It is demonstrated that the regulation of dynamic microtubule behavior depends on both the neuronal cell type and compartment within individual neurons. Time-lapse imaging and

genetic manipulations are further combined to identify a number of molecules involved in regulating dynamic microtubule behavior at the NMJ. These data provide evidence that the EB1-GFP labeled-microtubules are independent of the well-studied, stable core that extends from the soma to the synapse and may represent a pioneer population of microtubules within the NMJ. Finally, the link between the regulation of dynamic microtubules and the growth and maintenance of the synapse is probed.

MATERIALS AND METHODS

Generation of UAS-EB1-GFP Transgenic *Drosophila*

C-terminal fusion of green fluorescent protein with *Drosophila* EB1 (EB1-GFP) was obtained from Steve Rogers (SR and RV unpublished data) and cloned into the pUAST vector using standard methodology. Transgenic *Drosophila* lines were obtained with homozygous viable *UAS-EB1-GFP* transgenes inserted on the second and third chromosomes.

Cell Culture

All *Drosophila* S2 cell protocols were performed as described in the *Drosophila* Expression System Manual (Stratagene; La Jolla, CA). Briefly, *Drosophila* S2 cells were cultured in Schneider's Medium supplemented with 10% fetal calf serum at 25°C. Cells stably expressing the Gal4 transcription factor were transiently transfected with the pUAST-EB1-GFP plasmid using a standard calcium phosphate transfection protocol. Transfected cells were incubated normally for 48 hrs prior to plating on ConA (0.5 mg/ml stock; Sigma) coated coverslips for live imaging and subsequent analysis (Rogers et al., 2002).

Genetics

Drosophila strains were maintained at 25ºC on normal food. The following strains were used in this study: 1) $futsch^{N94}/futsch^{N94}$; *UAS-EB1-GFP/UAS-EB1-GFP* 2) *UAS-DN* $Glued^{84}$ (Allen et al., 1999) 3) *dhc* $64C^{4-19}$*/Tm6b* (Gepner et al., 1996) 4) *UAS-syb-GFP* (Sean Sweeney, unpublished reagent) 5) *UAS-Kin-DAD/Tm6b*. For CNS expression *UAS-*

EB1-GFP flies were crossed to one of three Gal4 lines: 1) *elaV*^{c155}*-GAL4* (pan neuronal) 2) *OK6-GAL4* (motor neuron specific (Aberle et al., 2002) and 3) *D42-GAL4* (Parkes et al., 1998). *Pickpocket-Gal4* was used to drive expression specifically in the PNS (Unpublished reagent, generous gift from C. Yang, W.B. Grueber, L.Y. Jan and Y.N. Jan).

Live imaging and kymograph analysis

Wandering third instar larvae were dissected in HL3 saline (0.5mM Ca^{++}) and stably positioned on glass slides using pressure pins held in place using a magnetic surface surrounding the glass slide. EB1-GFP labeled microtubules were imaged using a GFP filter set (Chroma) with a 100x (0.97 NA) AchroPlan water immersion objective (Zeiss). Images were acquired with a Quantix cooled CCD camera (Roper Scientific) and Kodak EEV57 back thinned chip (Roper Scientific) mounted on a fixed–stage upright microscope (Zeiss Axioskop 2). The sample was illuminated using a 100W Xenon light source (Sutter Instruments) and liquid light guide (Sutter Instruments). In general, EB1-GFP puncta were visualized using a 500ms exposure and a 500ms frame rate (rapid capture mode to prevent shutter closing during imaging). Synaptobrevin-GFP puncta were imaged using a 750ms exposure and either a 1s or a 5 s frame rate. Individual imaging sessions lasted a maximum of one hour per larva. The camera, shutter and filter were controlled by Slidebook software (Intelligent Imaging Innovations). Images were collected at room temperature (18ºC).

Kymograph analysis was used to determine rates of movement in axons and synapses. Axons in the segmental nerve overlaying muscle four were imaged and used in kymograph analysis. Images were deconvolved using a no neighbors algorithm prior to

analysis. To generate axonal kymographs a one pixel wide mask was drawn over a length of axon in the first time point. This mask was copied to all time points and kymographs were generated using the smooth curve analysis function of SlideBook 4. This function aligns the masked regions from each time point. Any movement that occurs in the masked region over the time imaged appears as a diagonal line through the kymograph. The slope of this line was measured using Slidebook software to determine the rate of movement. Synaptobrevin images were taken from the same region of the axon, and movement was analyzed as described above. Images were acquired from the segmental nerve overlaying muscle four. Reversals were defined as a directional change in the slope of the kymograph. The synapse on muscle four was selected for imaging and analysis as it was possible to image several boutons in the same plane of focus. Puncta in the synapse often took a curved path in a bouton compared to the linear path in the axon. To generate kymographs for the synapse the mask was created over the specific path of an individual puncta resulting in a curved line for many of the masks. These masks were then treated in the same way as the axonal masks. For a given segment of axon or synapse, all puncta that remained in the plane of focus for at least 5 frames were analyzed.

Only puncta that moved were selected for the measurement of comet tail length. Length was measured across the long axis of the comet from the tip of fluorescence to the back edge of the tail using Slidebook software.

Pharmacology

Taxol (Sigma) was dissolved in DMSO to a concentration of 1mM to create a stock. The taxol stock solution was diluted to a final concentration of 1μM in HL3 saline (0.5mM Ca^{++}). This concentration was settled upon after testing a range of concentrations from 0.1 to 25μM. Disruption of EB1 puncta was observed at .5μM and above. For control experiments DMSO alone was diluted into HL3 at an identical concentration to that used in the experimental condition. Wandering third instar larvae were dissected in HL3 (0.5mM Ca^{++}) and incubated for 10 minutes at room temperature in either DMSO (control) or taxol (experimental). Preps were then imaged and kymographs made to analyze the presence of moving EB1 puncta.

A 10mM stock solution of nocodazole (Sigma) was diluted to a final concentration of 100μM in HL3 saline (0.5mM Ca^{++}). Disruption of EB1 puncta was observed at 10μM and above. For control experiments DMSO alone was diluted into HL3 to an identical concentration. Wandering third instar larvae were dissected in HL3 (0.5mM Ca^{++}) and incubated in either DMSO or nocodazole for ten minutes at room temperature. Preps were then imaged and kymographs analyzed for the presence of moving EB1 puncta.

Antibody staining

Primary antibodies used in this study include mAb 22C10 (1:50; obtained from the Developmental Studies Hybridoma Bank, University of Iowa), Cy3 conjugated HRP (1:200; obtained from ICN/Cappel), anti-brp (1:10, gift of Erich Buchner), anti-DAP-160 (1:200), anti-FLAG (1:200, obtained from Sigma). Secondary antibodies used were FITC

labeled anti-mouse (1:200), Cy3 conjugated anti-mouse (1:200), and Cy5 conjugated anti-rabbit (1:200). All secondary antibodies were obtained from ICN/Cappel.

RESULTS

EB1-GFP as a tool for live imaging.

The expression of GFP tagged EB1 protein has been used to visualize the plus-ends of individual growing microtubules *in vitro* and, more recently *in vivo* (Morrison et al., 2002; Ma et al., 2004; Piehl et al., 2004; Wen et al., 2004). EB1 binds preferentially to a site within the GTP cap of growing microtubule plus-ends providing a punctate, live marker that is suitable for quantitative live imaging of microtubules (Mimori-Kiyosue et al., 2000; Schuyler and Pellman, 2001; Rogers et al., 2002; Tirnauer et al., 2002). Importantly, this preferential binding allows for specific examination of the dynamic population of microtubules undergoing plus-end polymerization (Mimori-Kiyosue et al., 2000; Rogers et al., 2002; Tirnauer et al., 2002). Low levels of EB1-GFP also decorate the length of microtubules through a mechanism that is thought to be distinct from the preferential plus-end binding (Tirnauer et al., 2002). This tool has recently been used successfully to probe the organization of dynamic microtubules within different neural compartments (Rolls et al., 2007). EB1-GFP was therefore used in this study to quantify the *in vivo* behavior of a dynamic population of microtubules in the developing axons and neuromuscular synapse of the third instar *Drosophila* larvae.

Prior to the generation of a transgenic *Drosophila* line, it was important to demonstrate that expression of EB1-GFP marks the plus-ends of growing microtubules, *in vitro*, in a manner that is quantitatively and qualitatively similar to prior work in mammalian cell systems (Morrison et al., 1998; Mimori-Kiyosue et al., 2000; Morrison et al., 2002; Tirnauer et al., 2002). In cultured *Drosophila* S2 cells, EB1-GFP puncta

generally originate near the center of the cell, at the microtubule organizing center (MTOC), and move toward the cell periphery as observed in other systems (Supplemental Movie 1-1) (Morrison et al., 1998; Mimori-Kiyosue et al., 2000; Tirnauer et al., 2002). Each puncta is a defined spot present at the microtubule plus-end with a characteristic comet tail (Figure 1-1A, inset). This comet tail is believed to reflect the gradual release of EB1-GFP along the length of the growing microtubule as the GTP cap is hydrolyzed (Rogers et al., 2002; Tirnauer et al., 2002; Stepanova et al., 2003; Wen et al., 2004). The rate of EB1-GFP puncta movement in the S2 cells was measured and found to be consistent with the microtubule growth rates observed in other *in vitro* cell types (6.62 μm/min ± 0.17; Figure 1-1B) (Tanaka et al., 1995; Tirnauer et al., 2002). Perhaps more importantly, the rate observed in S2 cells in this study was found to be consistent with the previously measured rate for microtubule polymerization in this cell type (Tanaka et al., 1995; Rogers et al., 2002; Tirnauer et al., 2002). As the EB1-GFP construct appears to report microtubule polymerization in this *in vitro* system, transgenic *Drosophila* lines were generated harboring this construct under UAS control to allow characterization of dynamic microtubules *in vivo* (Brand et al., 1994).

Microtubule Orientation and Growth in *Drosophila* Sensory and Motor Axons.

To begin an analysis of dynamic microtubules *in vivo,* the behavior of EB1-GFP puncta in axons within the segmental nerve of third instar *Drosophila* larvae was examined. EB1-GFP was expressed under the control of the pan-neuronal *elaV-Gal4*^{c155} driver to ensure a high level of expression for imaging. The segmental nerve bundle was chosen for this analysis. EB1-GFP comets were observed to localize as distinct puncta or

comets and move throughout the length of the segmental nerve, consistent with the observations from recent work in *Drosophila* (Rolls et al., 2007) (Figure 1-2A, arrowheads). Interestingly, when *UAS-EB1-GFP* is expressed pan-neuronally using the *elaV-GAL4*^{C155} driver, individual EB1-GFP puncta can be observed moving both anterogradely, toward the periphery, and retrogradely, toward the central nervous systems (CNS) (Supplemental Movie 2). This observation raised the possibility that microtubules in the axons have a mixed orientation as hypothesized by a recent study. This work, using cultured neurons from *Xenopus laevis*, suggests that up to 10% of axonal microtubules may be inversely oriented, with their plus-ends positioned towards the cell body (Ma et al., 2004). As the segmental nerve bundle contains both motoneurons (cell body in the CNS) and sensory neurons (cell body in the periphery) it is not possible, using the *elaVGAL4*^{c155} driver, to determine the orientation of microtubule plus-ends within individual axons. Therefore, cell-type specific GAL4 lines were used to drive *UAS-EB1-GFP* expression selectively in motoneurons, using *OK6-GAL4* (Aberle et al., 2002), or sensory neurons, using *ppk-GAL4* (unpublished data). Motoneuron specific expression revealed uniform movement toward the periphery by observable EB1-GFP comets. Similarly sensory neuron specific expression also revealed uniform movement of EB1-GFP this time traveling from the periphery toward the CNS. These data are therefore consistent with numerous studies describing a uniform, anterograde orientation of microtubules within axons (Topp et al., 1994; Signor and Scholey, 2000; Rolls et al., 2007). The existence of a small number of retrogradely oriented microtubules at the *Drosophila* NMJ could not be ruled out by these observations, however no evidence of this population was found under the conditions used in this study. In all subsequent motor

axon analyses using *elaV-Gal4* only the movement of EB1-GFP puncta toward the NMJ, is used.

Prior to the quantification of EB1-GFP rate of advance, a series of control experiments were performed to ensure that the EB1-GFP puncta observed *in vivo* do reflect the microtubule plus-end and not transport of the protein (Chang et al., 1999; Ma et al., 2004). As this marker is to be used to identify and quantitatively characterize dynamic microtubules with the axon and synapse, it is crucial that all puncta measured reflect the movement of a growing plus-end. The preferential plus-end localization of EB1-GFP has been shown to require intact and growing microtubules (Mimori-Kiyosue et al., 2000; Ligon et al., 2003). Thus disruption of either stability or growth should eliminate observable GFP comets in the axon. In contrast, movement originating from protein trafficking would require only the presence of an intact microtubule cytoskeleton. In order to distinguish between microtubule growth and transport of EB1-GFP, larvae were treated with one of two pharmacological agents that alter the state of the microtubule cytoskeleton. Larvae were first dissected and incubated in the microtubule-destabilizing drug, nocodazole. A second group of larvae were incubated in vehicle alone (DMSO) as a negative control. Axons from both groups were then imaged to detect the presence any EB1-GFP puncta. Treatment with nocodazol resulted in the loss of observable EB1-GFP puncta. This is in contrast to DMSO treatment, which had no discernable effect on EB1-GFP localization (Figure 1-3A, A'). Furthermore, kymographs generated from time-lapse series of the axons from larvae treated with vehicle alone revealed normal EB1-GFP movement, while incubation in nocodazole resulted in no distinguishable movement in kymographs (Figure 1-3B,B'). This is

consistent with a requirement for an intact microtubule cytoskeleton for normal localization and movement of EB1-GFP in the axon. However it remains possible the observed movement is due to the active, motor-driven trafficking of vesicles containing excess EB1-GFP and is not reflective of microtubule growth in this system. To address this question, the same series of experiments were conducted in the presence of taxol, to stabilize microtubules, or in vehicle alone. In addition to stabilizing microtubules, taxol also prevents the addition of new GTP-tubulin dimers to the plus-end, preventing further dynamic instability or growth. Thus, if the observed EB1-GFP puncta reflect the growth of microtubule plus-ends, taxol treatment should result in a loss of the EB1-GFP puncta, active vesicle transport in contrast should be unaffected by this treatment. Consistent with the former hypothesis, a complete loss of discrete EB1-GFP puncta following taxol, but not DMSO, treatment was observed (Figure 1-3C,C'). Instead, EB1-GFP re-localizes to bind the entire length of the microtubule cytoskeleton (Mimori-Kiyosue et al., 2000; Tirnauer et al., 2002). Kymographs generated from time lapse series of DMSO treated larvae reveals normal movement, while no discernable movement was detected following taxol treatment (Figure 1-3D,D'). These data support the conclusion that in this system, EB1-GFP is behaving in a manner consistent with prior *in vitro* and *in vivo* data.

In a second control experiment, the rate and nature of EB1-GFP movement was directly compared with that of neuronally expressed synaptobrevin-GFP. Synaptobrevin has been shown to traffic within a transport vesicle in axons (Li et al., 1996). Live imaging of neuronally expressed synaptobrevin-GFP revealed a number of characteristics that were markedly different from EB1-GFP. Initial comparison of the movement of synaptobrevin-GFP and EB1-GFP revealed that synaptobrevin GFP puncta pause and

frequently reverse direction within the axon. This behavior is consistent with the microtubule motor-driven transport of vesicles within axons (Figure 1-4E,G). In contrast, EB1-GFP puncta movement is processive and is never observed to reverse direction (Figure 1-4F,G). Note that microtubules undergoing catastrophe loose the GTP cap resulting in the loss of discrete EB1-GFP comets (Mimori-Kiyosue et al., 2000; Ma et al., 2004). For this reason, a catastrophe event will not result in a reversal of direction as reported by EB1-GFP puncta. This difference in behavior is apparent in projections of time-lapse image series of EB1-GFP (Figure 1-4A) and syb-GFP puncta (Figure 1-4B). In addition the characteristic geometry of both proteins is clearly different. While the comet tail is a defining characteristic of EB1-GFP localization, the individual synaptobrevin-GFP puncta are well-defined spheres and lack (Figure 1-4C,D). These data are consistent with the conclusion that observed EB1-GFP movement reflects the advance of microtubule plus-ends in this *in vivo* system. Therefore, this tool was used for the qualitative and quantitative characterization of the behavior and regulation of dynamic microtubules within the axons and NMJ of third instar *Drosophila* larvae.

EB1-GFP Movement is Slower in Sensory Compared to Motor Axons.

The above experiments largely represent a qualitative analysis of the movement of EB1-GFP labeled microtubule plus-ends within axons. To more quantitatively characterize this population, the rate of EB1-GFP movement within motor and sensory neuron axons was measured. For these and all subsequent experiments >100 individual EB1-GFP puncta from at least 10 different animals were measured for each genetic combination. The rate of EB1-GFP puncta movement was determined by kymography

(see methods). Using this method of quantification EB1-GFP puncta were calculated to move at a rate of 4.10 μm/min when expressed within axons of *Drosophila* motor neurons using *OK6-Gal4*. Interestingly, the average rate of EB1-GFP movement was observed to be significantly slower in sensory neurons compared to that observed in motor neurons; 3.02 μm per minute in sensory neurons compared to 4.10 μm per minute in motoneurons (Figure 1-2B). In this experiment sensory neuron specific expression of UAS-EB1-GFP was accomplished using the pickpocket (*ppk*) Gal4 driver. Thus, neurons of different modality, *in vivo*, can have significantly different rates of microtubule plus-end movement. Due to the nature of EB1 binding, the difference in these rates likely reflects differences in the rate of microtubule polymerization. However, it has also been hypothesized that short microtubule segments are trans-located down the axon by motor driven transport. The movement observed in axons could therefore be due to polymerization, translocation or a mix of both phenomena (Baas and Brown, 1997; Hirokawa, 1997; Baas, 2002; Ma et al., 2004; Baas et al., 2006). In this study the observed rates of EB1-GFP advance are more consistent with known polymerization rates than those of motor driven transport, which is often up to an order of magnitude faster (Svoboda et al., 1993; Svoboda and Block, 1994; Kotani et al., 2007). However, the possibility that a small population of transported, dynamic microtubules exist within axons and contributes to the rates measured in this study cannot completely be ruled out.

Plus-end-binding proteins are known to regulate the dynamics of microtubule plus-ends (Akhmanova et al., 2001; Ligon et al., 2003; Akhmanova and Steinmetz, 2008). The majority of data in vertebrate cell cultures systems and in *Drosophila* S2 cells demonstrate that the EB1 protein itself does not modulate the rate of microtubule

polymerization (Rogers et al., 2002; Tirnauer et al., 2002; Ligon et al., 2003). Instead, EB1 has been shown to primarily modulate the balance of catastrophe versus pausing or rescue events in dynamic microtubules. However, it remains possible that differences in EB1 expression levels could change polymerization rates either directly, or by displacing endogenous microtubule plus-end binding proteins. If this were the case in this *in vivo* system, one would predict that differences in expression levels should alter the observed rate of EB1-GFP movement. To test this prediction, the rate of EB1-GFP movement was measured in motor axons using three GAL4 drivers with different expression levels (low expression=*OK6-GAL4/+*, medium expression=*D42-GAL4/+*, high expression=*elaV-GAL4^{C155}/Y*). A comparison of the polymerization rates in these backgrounds revealed no significant difference (Figure 1-2C). Thus, EB1-GFP labeled plus-end growth is independent of EB1-GFP levels over the range of expression levels tested and used throughout these studies.

To test this further, experiments were performed to determine whether the differences in the rate of EB1-GFP in the sensory versus motor neurons could be accounted for by the use of GAL4 drivers with varying expression levels in the different cell types. First, EB1-GFP was expressed using the pan-neuronal *elaVGal4^{C155}* driver and puncta movement was examined in sensory and motor axons. Using a single GAL4 driver the rate of EB1-GFP puncta movement in sensory neurons remains slower than that observed in motor neurons (*elaV-Gal4^{c155}* sensory = 3.09 μm/min ± 0.091, n=159; *elaV-Gal4^{c155}* motor neuron = 4.12 μm/min ± 0.038, n=1121. K-S $p < 0.01$, T-test $p<0.001$) (Figure 1-2B). Next, the rate of EB1-GFP puncta movement in sensory neurons was compared for two different expression backgrounds. Despite the high level

of expression of EB1-GFP in the *elaV-GAL4*^{C155} background compared to *PPK*, the rate of plus-end movement was not significantly different (*PPK/+* =3.02 μm/min ± 0.12, *elaV-GAL4*^{C155}*/Y* =3.09 μm/min ± .091. K-S=0.256, T-test p=0.724) (Figure 1-2B). These data suggest that there are fundamental differences in the cell biological mechanisms that control the polymerization of microtubules in different neuronal types. The results of this initial examination reveal that EB1-GFP can be effectively used to probe the behavior of dynamic microtubules within the axon *in vivo*. Time-lapse imaging was next applied to the synapse at the NMJ to characterize the behavior and regulation of the dynamic microtubules recently identified within the presynaptic nerve terminal at the NMJ (Yan and Broadie, 2007).

Characterization of Dynamic, EB1-GFP Labeled Microtubules at the NMJ.

The regulation and organization of the microtubule cytoskeleton is essential for the development and stability of the NMJ (Roos et al., 2000; Pennetta et al., 2002; Ruiz-Canada et al., 2004; Eaton and Davis, 2005; Viquez et al., 2006; Pielage et al., 2008). Mutations in MAPs are often associated with defects in synapse growth. It was therefore necessary to ensure that expression of EB1-GFP did not alter the development of the NMJ. To test the gross morphological development of the synapse, bouton number and size were both quantified. These specific parameters were tested as they have previously been shown to be sensitive to disruption of microtubules. In the background of high levels of EB1-GFP expression, both parameters were found to be normal relative to wild type (bouton number; wt =15.9 ± 1.02, n =19 synapses; *UAS-EB1-GFP* =16.7 ± 1.05, n =19 synapses. Bouton size; wt =2.22 ± 0.084 μm^2, n =191 boutons; *UAS-EB1-GFP* =2.22

± 0.80 μm^2, n =188 boutons) (Figure 1-5A,B). Immuno-staining of active zone (brp) and peri-active zone (Dap160) markers was used to more closely analyze the development of synapses in a wild type background (C,C') and the background of EB1-GFP expression under the control of *elaV-Gal4*^{C155} (D,D') (Roos and Kelly, 1998; Wagh et al., 2006). Both markers were found to be qualitatively and quantitatively normal relative to wild type controls. These data demonstrate that neuronal expression of EB1-GFP does not interfere with normal synaptic development. Therefore, EB1 can be used as a tool to monitor the behavior and regulation of dynamic microtubules within a normal synapse *in vivo*.

To begin this analysis the rate of plus-end growth at the NMJ was determined. Time-lapse imaging revealed EB1-GFP puncta moving throughout the synapse, invading all boutons (Figure 1-6A, Supplemental Movie 5). No proximal or distal bias was observed in the density of invading EB1-GFP comets. Kymographs were then generated to measure the rate of EB1-GFP movement (Figure 1-6B). Interestingly, the average rate of EB1-GFP puncta movement within the presynaptic nerve terminal is slightly but significantly faster than that observed in the motor axon (Synapse =4.66μm/min ± 0.10, n=337. Axon = 4.12 μm/min ± 0.038, n=1121. Kolmogrov-Smirnov $p<0.01$, Student's T-test = 5.44×10^{-6}) (Figure 1-6C). As the movement of EB1-GFP reflects the growth of microtubule plus-ends, the observed increase at the synapse is likely to reflect a difference in polymerization rates between the axon and NMJ. The length of EB1-GFP comet tails has been used in the past as an indicator of polymerization rates (Stepanova et al., 2003; Wen et al., 2004). A longer tail is thought to reflect a more rapid addition of tubulin dimmers, and thus increased polymerization. A comparison of the length of EB1-

GFP comet tails in the axon and synapse revealed significantly longer comets in the synapse as compared to the axon (axon = 0.31μm ± 0.006, n =264; synapse = 0.36 μm ± 0.008, n=235. Student's T-test p =$1.48x10^{-7}$) (Figure 1-6D). This is consistent with the idea that microtubule polymerization is enhanced within the synapse. The synapse may therefore represent a unique sub-cellular domain for the regulation of microtubule dynamics. In the future, it may be of interest to investigate whether there are synapse specific MAPs that regulate microtubule growth in this compartment.

The Dynein/Dynactin Complex Regulates Dynamic Microtubules in the Axon and NMJ.

A wide complement of microtubule-associated proteins is known to affect microtubule polymerization and organization (Carvalho et al., 2003; Wittman and Desai, 2005; Morrison, 2007). One such molecule, the dynactin complex member p150/Glued, is known to bind the microtubule plus-end where it has been shown to regulate microtubule dynamics and cell signaling in a variety of cellular contexts (Berrueta et al ., 1999; Vaughan et al., 1999; Eaton et al., 2002; Ligon et al., 2003; McCabe et al., 2003). Of particular interest to this study, recent work has demonstrated that the dynactin complex, and specifically p150, is important for the normal development and maintenance of the NMJ (Eaton et al., 2002; McCabe et al., 2003). The stable microtubule core is disrupted in the absence of p150/Glued, a fact that may contribute to the synaptic growth defect. However, the role of p150/Glued in regulating dynamic microtubules at the *Drosophila* NMJ has not been tested. To determine whether this

member of the dynactin complex regulates the dynamic behavior of growing plus-ends at the NMJ, EB1-GFP was expressed in the background of impaired p150/Glued function.

Due to the essential nature of the dynactin complex, null mutations in p150 result in early lethality of the embryo. To allow for the examination of larval axons and synapses, a dominant negative p150 transgene, referred to here as *DN-glued* was used (Reddy et al., 1997; Allen et al., 1999). This construct acts dominantly to block the interaction of p150 with microtubules (Reddy et al., 1997; Allen et al., 1999; Martin et al., 1999; Eaton et al., 2002). Previous work in *in vitro* systems has implicated P150/Glued in the nucleation of new microtubules (Ligon et al., 2003). If this role is conserved at the *Drosophila* NMJ one would anticipate a decrease in the density of EB1-GFP puncta in larvae expressing the *DN-glued* construct. Thus, the density of visible EB1-GFP puncta within axonal and synaptic segments was measured. No significant change in the density of visible EB1-GFP labeled plus-ends was observed in the axons of DN-glued larvae relative to wild type (wt axon=0.73$\pm$0.04 puncta/μm^2, p150 axon=0.69$\pm$0.03 puncta/μm^2). Likewise, no significant decrease in puncta density was observed within the NMJ of *DN-glued* larvae (wt synapse=0.84$\pm$0.06 puncta/μm^2; p150 synapse=0.99$\pm$0.06 puncta/μm^2). These data suggest that the function of p150/Glued is not essential for the initiation of new microtubules within the axon or NMJ.

Next, the ability of p150 to regulate the rate of dynamic microtubule growth was examined. In the presence of the *DN-Glued* construct EB1-GFP movement is slowed to approximately half the rate observed in wild type axons. The decrease in plus-end advance is clearly illustrated in projections of the time lapse imaging series where the entire path of an individual plus-end can be observed (Figure 1-7A,B). Quantification of

the rate of microtubule plus-end advance confirmed that there is a significant decrease in background of *DN-Glued* relative to wild type (wild type=4.12± 0.038µm/min n=1121; *DN-Glued*= 2.89±0.03µm/min, n=1249) (Figure 1-7D). Similarly, disruption of P150/Glued function also affected the growth of microtubules within the NMJ. As with the axon, projection images generated from synaptic time lapse series showed a clear decrease in the distance traveled by EB1-GFP puncta from the *DN-glued* background relative to wild type synapses (Figure 1-7E, F). Again, quantification of the rate of plus-end advance within the synapse reveals a significant decrease in the DN-Glued background (wild type= 4.66µm/min ± 0.10, n=337; *DN-Glued*= 2.69 µm/min ± 0.070, n=381) (Figure 1-7H). These data are consistent with p150/Glued playing a role in the regulation of the rate of polymerization at the plus-end. Interestingly, the neuronal expression of *DN-Glued* also changes the nature of polymerization compared to that seen in wild type animals. Pause events are observed in kymographs from the synapses and axons of the transgenic larvae. These events are not observed in wild type larvae (Figure 1-7I). The pause events likely reflect either a stall in polymerization, or rescue of a catastrophe, these events would be indistinguishable in this assay. In kymographs where a pause event was observed, the rate of EB1 advance both before and after the pause event were measured and averaged. In this way the period of pause did not contribute to the overall calculation of the rate of plus-end polymerization in the *DN-Glued* background. The exclusion of these events may have lead to a slight overestimation of the growth rate of microtubules in the *DN-glued* background. Taken together the results of this time-lapse imaging revealed that p150/Glued is required for the normal regulation of polymerization, but not nucleation, of microtubules in the motoneuron axon and NMJ.

Further, the processivity of growth is disrupted in the absence of normal p150/Glued function.

The dynactin complex often functions in conjunction with the minus-end directed microtubule motor protein dynein (Tinsley et al., 1996; Karki and Holzbaur, 1999; Howell et al., 2001; LaMonte et al., 2002). It was therefore of interest to understand whether the p150/Glued dependent regulation of dynamic microtubule growth in *Drosophila* motor neurons is a dynein dependent or independent function. If the dynactin complex acts in concert with the dynein motor complex to regulate dynamic microtubules, one would expect that disruption of dynein function would result in a similar phenotype to that observed in *DN-Glued*. To test this possibility EB1-GFP labeled microtubule plus-ends were monitored in dynein heavy chain (dhc) mutant animals. As homozygous dynein heavy chain mutations (*dhc/dhc*) are embryonic lethal, a heterozygous *dhc* background was used. Previous work in *Drosophila* have shown that heterozygous *Dhc* mutations ($dhc64C^{4-19}$/+) are sensitized to axonal transport defects and thus have an observable disruption in motor function (Gepner et al., 1996; Martin et al., 1999). It was therefore likely that loss of a single copy of the dynein heavy chain would disrupt motor function sufficiently to be revealed in quantitative measurements. Heterozygous $dhc64C^{4-19}$/+ mutations slowed EB1-GFP movement in a manner that was qualitatively and quantitatively similar to expression of the *DN-Glued* transgene both in the axon (wild type=4.12μm/min ± 0.038, n=1121, $dhc64C^{4-19}$/+= 2.90 μm/min ± 0.031, n=1091, p-value=1.10×10^{-53}) (Figure 1-7C, D) and the synapse (wild type= 4.66μm/min ± 0.10, n=337; $dhc64C^{4-19}$/+= 2.68 μm/min ± 0.067, n=377) (Figure 1-7G,H). These data are consistent with the hypothesis that the dynactin complex acts in concert with the

dynein motor complex to modulate the growth of pioneer microtubules within motor axons and the NMJ.

As noted above, the rate of microtubule polymerization in the axons of wild type larvae is dependant on the specific neural type. Differences in the specific complement of MAPs, and the concentration of free tubulin and possibly the volume of the different compartments, are likely to account for the different pioneer microtubule growth rates in sensory and motor neurons (Lopez and Sheetz, 1993; Heidary and Fortini, 2001; Seitz et al., 2002; Mandelkow et al., 2004; Janulevicius et al., 2006). The microtubule plus-ends within sensory axons were shown to have a significantly slower rate of advance when compared to those within motor axons. One possible explanation for this phenomenon is the existence of a different complement of microtubule-associated proteins regulating polymerization each cell type. It was therefore noteworthy that the measured rate of EB1-GFP movement in the motor axons of *DN-Glued* or dynein heavy chain mutations is quantitatively similar to that observed in wild type sensory neurons. This may indicate that the dynein/dynactin complex plays no role in the regulation of microtubule growth in sensory neurons, and the ability to effect polymerization may be specific to their actions in motor axons. In turn, the rate of EB1-GFP movement within the sensory neurons could represent the base rate of microtubule polymerization in axons (*PPK/+* =3.02 μm/min ± 0.12, n=129; *DN-Glued*= 2.89±0.03μm/min, n=1249; $dhc64C^{4\text{-}19}$/+= 2.90 μm/min ± 0.031, n=1091). To examine the role of the dynein-dynactin complex in regulating microtubule polymerization in other neuronal lineages, the rate of plus end advance was measured in sensory neurons in wild type, *DN-Glued* and $dhc64C^{4\text{-}19}$/+ backgrounds. A significant reduction in EB1-GFP movement was observed in the

sensory axons in both mutant backgrounds relative to wild type (Figure 1-7J). These data do not support the hypothesis that the dynein-dynactin complex is not required for plus-end growth in sensory neurons. Instead these observations are consistent with the dynein/dynactin complex actin as a common regulator of microtubule polymerization in both neural lineages.

Characterization of Presynaptic, Futsch-independent Pioneer Microtubules at the NMJ.

In *Drosophila*, the microtubule cytoskeleton can be visualized with a monoclonal antibody that recognizes a large MAP1b-like protein termed Futsch (Hummel et al., 2000; Roos et al., 2000). The microtubules labeled by the monoclonal antibody recognizing Futsch are found throughout the central and peripheral nervous systems. The anti-Futsch staining identifies a large fraction of the synaptic microtubules as anti-tyrosinated or anti-acetylated tubulin staining co-localizes with the anti-Futsch pattern (Roos et al., 2000). Within the neuromuscular synapse, anti-Futsch staining identifies a tightly bundled core of microtubules that are present throughout the synapse, tapering gradually from the point of nerve entry to the distal end (Roos et al., 2000). Upon entry into boutons this core may be re-organized, becoming splayed or forming loop-structures. Interestingly, these reorganizations tend to occur in “dynamic boutons”, that is newly formed or growing boutons. Although altered anti-Futsch staining in fixed tissue has been interpreted to reveal changes in microtubule dynamics (Roos et al., 2000; Zhang et al., 2001; Pennetta et al., 2002; Ruiz-Canada et al., 2004) the relationship between the

Futsch labeled core of microtubules and dynamic microtubules remains to be investigated.

To better understand this relationship, the live behavior of EB1-GFP was compared with the fixed pattern of Futsch staining. Specifically, it was of interest to determine whether the movement of the EB1-GFP labeled microtubules was confined to the Futsch-labeled core. It might be expected that if Futsch staining accurately reflects the behavior of the dynamic microtubules, EB1-GFP labeled plus-end advance would be constrained to the Futsch core. To compare the EB1-GFP advance with the Futsch core, live imaging was used to visualize microtubule plus-ends in individual NMJs. This was followed immediately by fixation and immuno-staining for Futsch. In this way the movement of EB1-GFP puncta can be directly compared to Futsch labeled microtubules in the same synapse (Figures 1-8 and 1-9; Supplemental Movies 1-6 and 1-7 correspond to the fixed images shown in these figures). As shown above, EB1-GFP puncta can be observed to move throughout the synapse (Figure 1-6A, Supplemental Movie 1-5). Consistent with the idea that fixed Futsch staining reflects dynamic microtubule behavior, puncta are often observed to follow the path laid down by the Futsch-labeled core (not shown) and Futsch loops (see arrowheads in Figure 1-8). However upon closer analysis it was observed that EB1-GFP labeled plus ends did not always respect the boundary of the Futsch labeled core. For example, in many instances microtubule plus-ends are clearly observed to traverse across the open center of a Futsch loop (data not shown). Surprisingly, EB1-GFP puncta are also observed to travel within a given Futsch-loop in opposing directions. In some examples EB1-GFP puncta are observed to travel in opposite directions within a single bouton simultaneously, crossing paths as they move

(Figure 1-9A,B arrowheads, Supplemental Movie 1-7). In other examples EB1-GFP puncta traverse opposite sides of a single microtubule loop, traveling in the same direction (Figure 1-8B, arrowhead, Supplemental Movie 1-6). These behaviors would not be predicted if EB1-GFP labeled plus-ends were physically constrained to the Futsch-labeled microtubule core. This is particularly true of the behavior of plus ends within Futsch-loops, which are proposed to represent closed, unidirectional structures. Interestingly, the uniformly polarized movement of plus-ends observed in the axon is not observed at the synapse where approximately 10% of puncta moving in a retrograde direction. Thus microtubules within the synapse appeared to be less constrained relative to the axon, possibly allowing greater exploration of the synaptic volume.

The observation that EB1-GFP puncta can traverse across a microtubule loop suggests that dynamic microtubule movement is not confined to, and may in fact be independent of the Futsch-labeled core. This is further supported by the observation that EB1-GFP puncta are present within regions of the synapse that lack Futsch-positive microtubules. EB1-GFP puncta were commonly observed to track the bouton periphery, moving in regions that lack anti-Futsch staining. In one intriguing example microtubules are observed entering a nascent bouton bud in a central region of the NMJ (Figure 1-9 Aii,iii arrowheads, C). This is also the case within the distal most synaptic bouton, referred to here as the terminal bouton. Within the terminal bouton EB1-GFP puncta track to the periphery, and interact with the cortex of the bouton membrane (Figure 1-8B, compare open and closed arrows). Interestingly while anti-Futsch staining diminishes greatly prior to the terminal bouton, there is no obvious decrease in the abundance of EB1-GFP puncta within the distal compared to proximal regions of the synapse (Figure

1-8A). The ability of dynamic plus-ends to enter regions of the synapse lacking Futsch immunoreactivity is consistent with the hypothesis that EB1-GFP labeled microtubules represent a previously uncharacterized population of microtubules at the NMJ.

The above observations raise the possibility of two distinct populations of microtubules at the synapse. From the direct comparison of Futsch and EB1-GFP labeled microtubules within the same NMJ it appears the movement of dynamic microtubule plus-ends is neither dependent on, nor constrained by, the stable core. However, the possibility that Futsch is present at undetectable levels in the distal boutons imaged in the above experiment cannot be completely ruled out. To directly test the possibility of two independent microtubule populations, the movement of EB1-GFP-labeled plus-ends was examined in synapses of *futsch* mutant animals. If in fact the EB1-GFP labeled plus-ends represented an independent population of microtubules, one would expect no significant change in the behavior of this population in the absence of Futsch. To determine whether this was the case, plus-end advance and invasion were observed in the third instar NMJ of *futsch*^{N94} mutant larvae.

The behavior of dynamic EB1-GFP labeled plus-ends within the NMJ was first analyzed in the *futsch* mutant background. As previously described, Futsch staining is not visible at the NMJ of *futsch*^{N94} mutant larvae (Fig. 1-10A,B). Additionally the synaptic microtubule core is dramatically disrupted in this background, with a loss of the bundling and loops (not shown, Roos et al., 2000). Despite the disorganization of the bundled core however, the invasive behavior of the EB1-GFP-labeled dynamic microtubule population is unaltered in this background as monitored by time-lapse imaging. EB1-GFP puncta are still observed to move throughout the entirety of the NMJ

and to target the cortex of the distal most boutons. Additionally, the normal processive advance of EB1-labeled plus ends in *futsch*^{N94} NMJs is readily apparent in projection images generated from time-lapse series (Figure 1-10G, H). These observations are inconsistent with the idea that a disrupted Futsch-labeled microtubule core at the synapse inherently reflects a change in the underlying dynamic behavior of microtubules. Instead, the behavior of the EB1-GFP-labeled microtubule population appears to be largely independent of the Futsch core.

To further analyze the relationship between dynamic and stable microtubules the rate of plus-end growth within the axon and NMJ of *futsch*^{N94} was examined. As with the synapse, no significant change in the processivity of growth or behavior of EB1-GFP comets is observed in projections from the axons of *futsch*^{N94}/+ or *futsch*^{N94} relative to wild type axons (Figure 1-10 C-E). Additionally, the rate of growth of EB1-GFP labeled plus-ends within the axon is unaltered in the *futsch*^{N94} mutants relative to either heterozygous sibling and wild type controls (wild type=4.46 μm/min ± 0.022, n=140. *futsch*^{N94}/+=4.44μm/min ± 0.09, n=221. *futsch*^{N94}= 4.81 μm/min ± 0.02, n=139) (Figure 1-10B). Curiously, a slight but significant increase in the rate of synaptic plus-end growth was identified in the *futsch*^{N94} null and heterozygous larvae relative to wild type (wild type= 4.66 μm/min ± 0.10, n=377. *futsch*^{N94}/+= 5.03 μm/min ± 0.09, n=404. *futsch*^{N94}= 5.51 μm/min ± 0.11, n=451) (Figure 1-10I). One explanation for the increased rate of plus end advance in the absence of Futsch may the loss of a subset of dynamic microtubules that would otherwise be stabilized and incorporated into the bundled core. This would be consistent with the role of Futsch, which is known to bundle and stabilize microtubules at the synapse (Hummel et al., 2000, Roos et al., 2000). Interestingly this

activity was not required in the axon, suggesting the activity may be uniquely important at the synapse. Taken together the above data reveal that changes in the organization of the bundled microtubule core cannot be always be interpreted to reflect changes in the underlying dynamic behavior of microtubules at the synapse. Instead these data support the hypothesis that two independent populations of microtubules exist within the NMJ, an exploratory and dynamic pioneer population and a structurally stable core population.

Discussion

Recently, increasing attention has been focused on the regulation of the neuronal microtubule cytoskeleton during development and disease (Lucas et al., 1998; Hall et al., 2000; Roos et al., 2000; Zhang et al., 2001; Eaton et al., 2002; Pennetta et al., 2002; Rolls et al., 2007; Pielage et al., 2008). However, while there is a wealth of developmental and disease related data implicating regulation of microtubule dynamics in disease progression, the analysis of axonal and synaptic microtubules *in vivo* has largely been restricted to the analysis of fixed tissue. Together, two recent studies have identified a population of dynamic microtubules that are suitable for live imaging within the axons and synapses of Drosophila neurons (Rolls et al., 2007; Yan and Broadie, 2007). Despite this work however, very little is known about the basic orientation, regulation and behavior of this population within the synapse. Here quantitative live imaging of synaptic microtubules was combined with genetic analysis in *Drosophila* to examine the mechanisms and modulation of microtubule plus-end growth *in vivo*.

EB1-GFP as a Quantitative Tool for the Analysis of Axonal and Synaptic Microtubules *in vivo*.

Several lines of evidence demonstrate that the expression of EB1-GFP in *Drosophila* selectively marks microtubule plus-ends *in vivo* and can be used as a quantitative tool for the analysis of dynamic microtubule behavior. First, EB1-GFP puncta are lost following treatment with agents that either stabilization or destabilize

microtubules, consistent with the requirement of a dynamic plus-end for EB1-GFP (Morrison et al., 1998; Mimori-Kiyosue et al., 2000; Schuyler and Pellman, 2001). Within axons and synapses, EB1-GFP takes on a characteristic comet pattern indicative of EB1-GFP gradually being released from the microtubule as the GTP cap is gradually hydrolyzed (Schuyler and Pellman, 2001; Tirnauer et al., 2002). In addition, a quantitative comparison of EB1-GFP puncta movement and synaptobrevin-GFP labeled transport vesicles supports the conclusion that EB1-GFP marked the microtubule plus-end and not transport vesicles. Finally, the demonstration that EB1-GFP puncta movement is not strongly altered by GAL4 expression levels suggests that EB1-GFP does not significantly affect microtubule plus-end polymerization over the range of expression tested and used in this study. This is consistent with studies in other *in vitro* systems that characterize EB1 as an anti-pausing/anti-catastrophe factor with little or no function to directly modulate the rate of microtubule polymerization (Rogers et al., 2002; Tirnauer et al., 2002).

Cell Type and Compartment Specific Modulation of Microtubule Behavior.

It is quite surprising that the rate of EB1-GFP movement is dramatically slower in sensory as compared to motor axons. Since the polymerization rates as measured by EB1-GFP movement in these cell types remains significantly different following disruption of dynein/dynactin function, it is clear that this motor complex is involved in regulating dynamics in both lineages. These data highlight a fundamental difference in the regulation of the dynamic microtubule cytoskeleton in these two cell types. This is particularly interesting given the link between mutations in MAPs and

axonal transport proteins, and the cause of neurodegenerative diseases that selectively target motoneurons versus sensory neurons (Pennetta et al., 2002; Puls et al., 2003).

Qualitative and quantitative changes in EB1-GFP movement can also be observed within the presynaptic nerve terminal compared to the axon. In the synapse, the rate of EB1-GFP movement is slightly but significantly increased. Although the underlying reason for this increase is not clear, it may be due to a combination of synapse specific MAPs. These data highlight the synapse as a unique compartment for the regulation of the microtubule cytoskeleton. Identification of the signaling systems responsible for the synapse-specific modulation of the dynamic microtubule cytoskeleton will be an important avenue for future investigation with implications for the control of synaptic growth, plasticity and stabilization.

Synaptic Pioneer Microtubules Represent an Independent Population of Microtubules at the NMJ.

Recently, several studies have proposed that microtubule dynamics are required for synaptic growth at the *Drosophila* NMJ (Roos et al., 2000; Pennetta et al., 2002; Ruiz-Canada et al., 2004). However, these studies are based on the visualization of fixed synaptic microtubules. As a result very little was understood about the relationship between dynamic and Futsch-labeled microtubules at the synapse. Here, a comparison of the movement of EB1-GFP-labeled plus-ends with the fixed pattern of Futsch staining was undertaken to elucidate the relationship between these two populations. Interestingly, EB1-GFP movements did not appear to be constrained to the bounds of the Futsch core. For example, although the levels of Futsch protein

diminish greatly at the distal end of the NMJ, there is no such change in the distribution of EB1-GFP puncta. Instead, EB1-GFP labeled microtubules are frequently found in regions of the synapse lacking Futsch protein, such as distal and nascent boutons. Further, even in regions of the synapse where Futsch levels are high, the movement of EB1-GFP labeled plus ends do not appear to be limited by the organization of the stable core. This is evident from the bidirectional nature of plus-end movement and the observation that plus-ends often traverse across the open center of Futsch loops. Thus, these data suggest the dynamic, EB1-GFP microtubules in the motor neurons may represent a population this is independent of the Futsch labeled core.

In support of this hypothesis the behavior of dynamic microtubules was largely unaltered in the background of loss of Futsch function. Based on genetic evidence it is clear that Futsch is required to bundle and organize the synaptic microtubule core (Roos et al., 2000). Changes in the organization of this core have been interpreted to reflect changes in the dynamic behavior of microtubules (Roos et al., 2000; Pennetta et al., 2002; Ruiz-Canada et al., 2004). In this study however, no significant change in the exploratory nature of EB1-GFP puncta movement was observed. Specifically, there was no change in the distribution or cortical targeting of labeled plus-ends in the *futsch*^{N94} background. However, a small increase in the rate of plus-end advance in the synapse was observed in the absence of *futsch*. This slight increase may indicate that in a wild type synapse a small subset of the dynamic microtubule pool is incorporated into the stable core through the actions of Futsch. This would be consistent with the role of Futsch to bundle and stabilize microtubules. It is noteworthy that this increase

appeared to be synapse- specific, as it was not observed within the axon. Taken together these data present a more complex picture of the relationship between the dynamic, pioneer microtubules and the stable microtubule core at the NMJ.

Dynamic Microtubules and Synapse Growth.

Together, the invasive behavior of synaptic pioneer microtubules as well as the interaction with Futsch, suggest a possible model for their role in synapse growth. The behavior of dynamic, EB1-GFP labeled microtubules within the *Drosophila* NMJ is reminiscent of previously described pioneer microtubule populations in other cellular systems, such as the navigating growth cone (Barth et al., 1997; Waterman-Storer and Salmon, 1997; Fukata et al., 2002; Gundersen, 2002; Schaefer et al, 2002; Gundersen et al., 2004; Suter et al., 2004; Molk and Bloom, 2006). In these systems, a population of independent and dynamic pioneer microtubules has been demonstrated to constantly sample the cell periphery. It has been hypothesized that this exploration of the cell periphery is required to link transient signaling events at the cell surface to the interior of the cell (Kirschner and Mitchison, 1986). For example, the invasion of the peripheral region of the growth cone by dynamic microtubules is required for normal turning in response to guidance cues (Schaefer et al., 2002; Suter et al., 2004; Schaefer et al., 2008). Similarly, dynamic microtubules at the NMJ may contribute to the growth of the NMJ by identifying trophic or other signals permissive of growth (Aberle et al., 2002; McCabe et al., 2003). This hypothesis is supported by the observation of EB1-GFP labeled plus-ends probing the cortex of newly forming boutons, as well as nascent bouton buds throughout the synapse. The ability of plus-ends to identify trophic signals and new sites

of growth would require receptors at the cell surface capable of microtubule plus-end capture as has been observed in budding yeast. In *Drosophila* there are two prominent candidates for such a function, APC and Vap33 (Pennetta et al., 2002). Future studies will attempt to establish molecular linkages at the synaptic plasma membrane responsible for the dynamic behavior of microtubules within the synapse.

A common cellular effect of signal acquisition by pioneer microtubules is a change in cytoskeletal organization and dynamics, a role which could also be important in synapse development (Kabir et al., 2001; Schaefer et al., 2002; Rodriguez et al., 2003; Suter et al., 2004). For example, both in the growth cone and in migrating fibroblasts pioneer microtubules are captured and become stabilized following signal acquisition (Tanaka et al., 1995; Dent and Kalil, 1999; Schaeffer et al., 2002; Suter et al., 2004). This selective stabilization of pioneer microtubules may also play a role in synaptic development. For example, the identification of an active growth site or trophic receptor at the NMJ may result in an increase in microtubule stability. In this study it was found that Futsch activity is required to regulate the rate of plus end advance within the NMJ. These data raise the possibility that Futsch is required to incorporate a subset of pioneer microtubules into the stable core. Thus, the role of pioneer microtubules in synapse growth may be to initiate the formation of new boutons downstream of activated trophic receptors. The acquisition of a growth signal in turn leads to membrane protrusion and ultimately, bouton formation. The lack of Futsch core in these newly formed boutons suggests the stable core may not be required for the initial outgrowth. As a new bouton is formed, a Futsch stabilized microtubule core begins to develop in the new growth, possibly incorporating a subset

of pioneer microtubules. The development of the Futsch core likely provides both structural and trafficking support to the newly formed bouton and is required for its stabilization and maintenance. Consistent with this idea, it is well known that mutations affecting Futsch function result in decreased synapse growth. Further work will be required to establish whether the presynaptic pioneer microtubule population is needed to regulate synapse growth.

Microtubule Dynamics and Neuromuscular Degenerative Disease.

Causal links have been established between mutations in microtubule associated proteins and neuromuscular neurodegenerative disease. In humans, mutations in dynactin are linked to familial ALS (Puls et al., 2003; Munch et al., 2004). In mice, disruption of dynein/dynactin function leads to progressive ataxia and neurodegenerative phenotypes identical to that observed in other mouse models of this disease (LaMonte et al., 2002). In *Drosophila*, it was previously shown that disruption of dynein/dynactin function leads to retraction of the NMJ (Eaton et al., 2002). Importantly, the retraction of the synaptic microtubule core (identified by anti-Futsch staining) was one of the earliest markers of synapse retraction. This lead to speculation that local destabilization of the microtubule cytoskeleton could be a precipitating event in synapse retraction. In the current analysis, microtubule plus-end growth was found to be demonstrably and significantly slower in mutations that disrupt dynein/dynactin function compared to wild type. In addition, the nature of polymerization appeared altered as pause events were frequently seen in the dynein/dynactin mutant backgrounds. In contrast, no obvious changes in the invasive

behavior of EB1-GFP puncta were observed in these backgrounds. In particular, EB1-GFP puncta still associate with the synaptic bouton cortex suggesting that a failure to link microtubules to the cell cortex is not a cause of synapse retraction in these animals (Eaton et al., 2002). It remains an open question whether slowed polymerization of microtubules in the NMJ could be a contributing cause to the synapse retraction observed in *Drosophila* and, by extension, relevant to the cause or progression of neurodegenerative disease in humans.

Figure 1-1: EB1-GFP labels microtubule plus-ends in S2 cells.

(**A**) Single time point image of S2 cell expressing EB1-GFP. The characteristic EB1 comet-tail can be clearly visualized (inset). (**B**) Quantification of the rate of EB1-GFP advance throughout S2 cell, n=344.

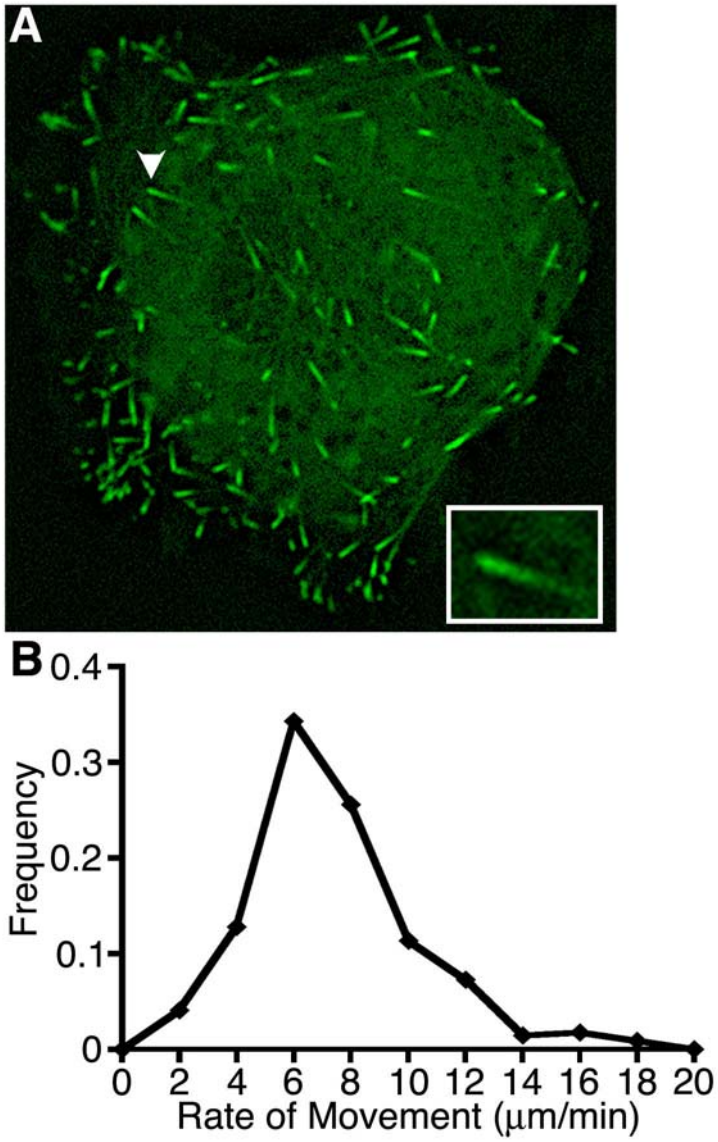
A
B
0.4
0.3
0.2
0.1
0
Frequency
0 2 4 6 8 10 12 14 16 18 20
Rate of Movement (μm/min)

Figure 1-2: Rate of advance of EB1-GFP labeled plus-ends within axons of different neural types.

(**A**) Single time point image of a fasciculated axon bundle from a third instar larvae expressing UAS-EB1-GFP under the control of *elaV-Gal4*^{C155}. Arrowheads mark individual EB1-GFP comets. Scale bar=5μm (**B**) Histogram of the rates of EB1-GFP in sensory and motor axons. Motor neuron specific expression of UAS-EB1-GFP was under control of *OK6-Gal4* (diamonds). Sensory neuron specific expression of UAS-EB1-GFP was under control of *ppk-Gal4* (squares). Movement from motor axons (circles) and sensory axons (triangles) in the background of *elaV-Gal4*^{C155} mediated expression of UAS-EB1-GFP. The rate of EB1-GFP puncta advance is significantly slower in sensory axons versus motoneuron axons (*OK6-GAL4/+*= 4.10 μm/min ± 0.086, n=247. *PPK-GAL4/+*= 3.02 μm/min ± 0.12, n=128. *ElaV-Gal4*^{c155} sensory = 3.09 μm/min ± 0.091, n=159. *ElaV-Gal4*^{c155} motor neuron = 4.12 μm/min ± 0.038, n=1121.). (**C**) Histogram distributions of EB1-GFP puncta velocities as a function of expression levels using different Gal4 drivers *OK6-GAL4* (squares), *D42-GAL4* (diamonds), *elav-GAL4*^{C155} (triangles). Note that the velocity of EB1-GFP puncta does not change with changes in expression level (*elaV-GAL4*^{C155}*/Y*=4.12 μm/min ± 0.038, n=1121. *D42-GAL4/+*= 4.46 μm/min ± 0.022, n=140. *OK6-GAL4/+*= 4.10 μm/min ± 0.086, n=247).

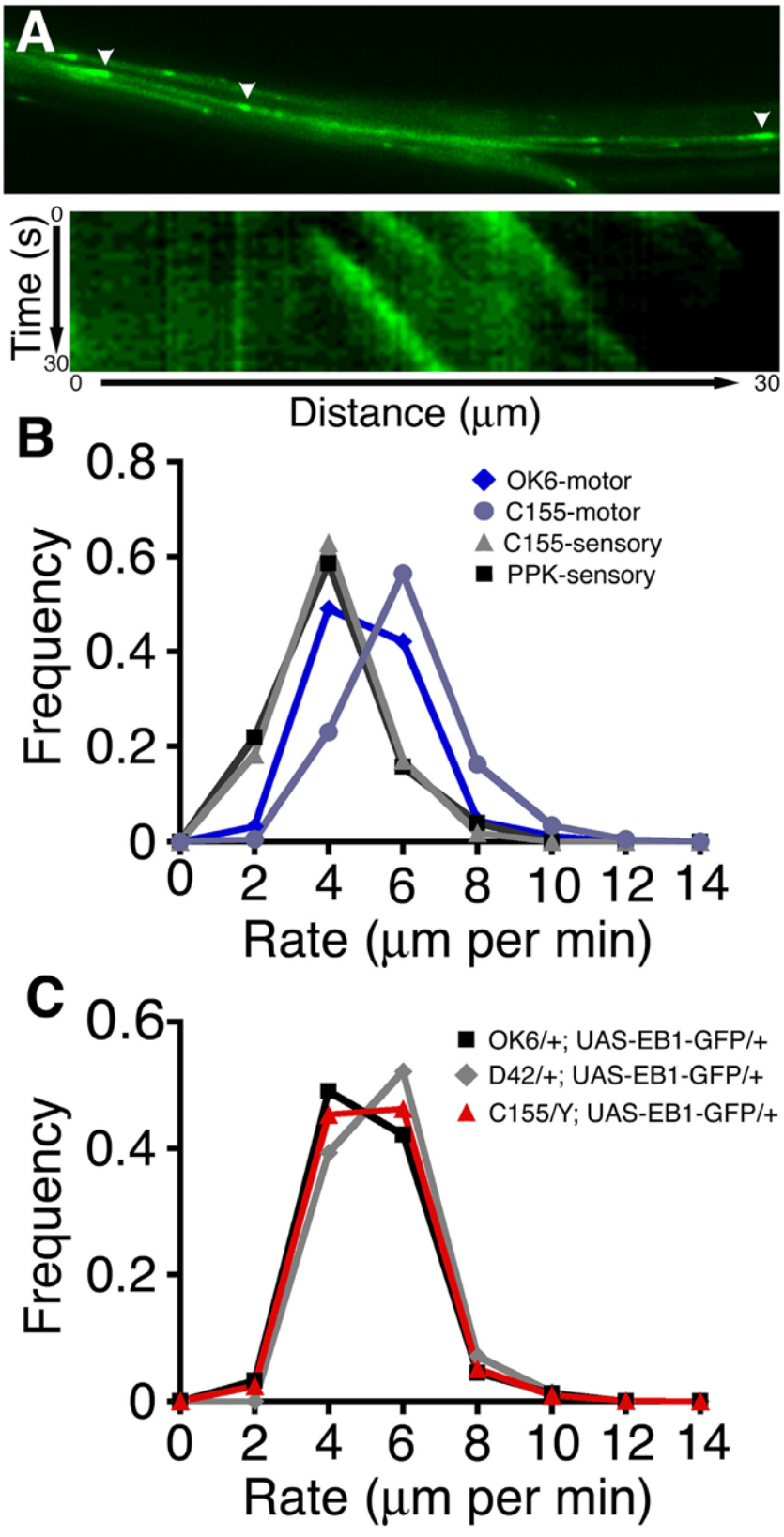
A
Time (s)
0
30
0
30
Distance (μm)
B
Frequency
0.8
0.6
0.4
0.2
0
OK6-motor
C155-motor
C155-sensory
PPK-sensory
0 2 4 6 8 10 12 14
Rate (μm per min)
C
Frequency
0.6
0.4
0.2
0
OK6/+; UAS-EB1-GFP/+
D42/+; UAS-EB1-GFP/+
C155/Y; UAS-EB1-GFP/+
0 2 4 6 8 10 12 14
Rate (μm per min)

Figure 1-3: EB1-GFP puncta are sensitive to drugs that target the stability of microtubules.

(**A,A'**) Images of axons expressing EB1-GFP following incubation with DMSO (**A**) or nocodazol (**A'**). Note presence of EB1-GFP puncta within axons incubated in vehicle alone (arrowhead in A) but not in nocodazole. (**B, B'**) Kymographs generated from time lapse imaging of axons incubated in DMSO (**B**) and nocodazole (**B'**). (**C, C'**) Images of axons expressing EB1-GFP following incubation with DMSO (**C**) or taxol (**C'**). Note EB1-GFP puncta are clearly visible in the presence of DMSO (arrowheads in C) and not taxol. (**D, D'**) Kymographs generated from time-lapse imaging of axons incubated in DMSO (**D**) and taxol (**D'**).

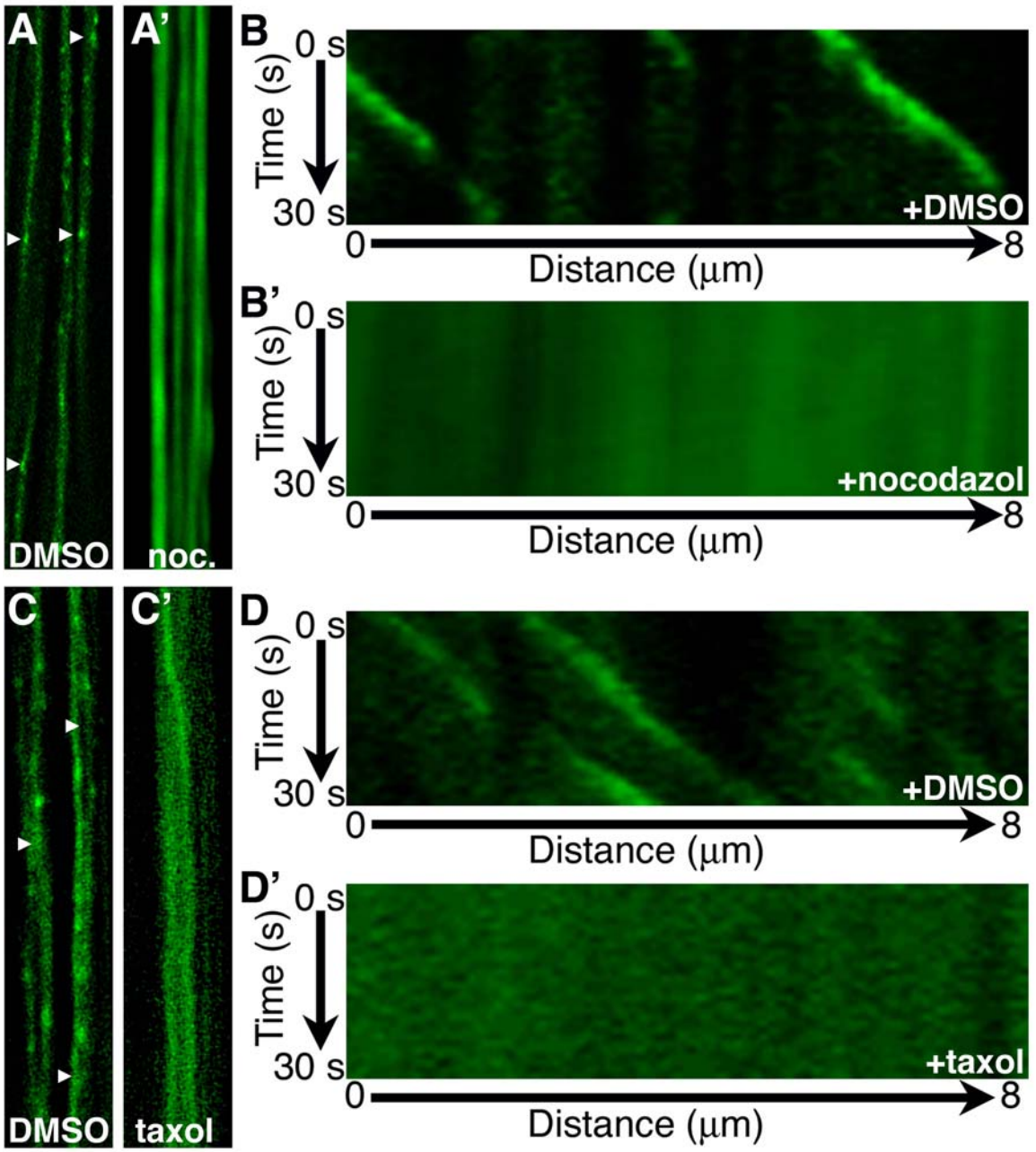
A
A'
B
0 s
Time (s)
30 s
+DMSO
0
8
Distance (μm)
B'
0 s
Time (s)
30 s
+nocodazol
0
8
Distance (μm)
DMSO
noc.
C
C'
D
0 s
Time (s)
30 s
+DMSO
0
8
Distance (μm)
D'
0 s
Time (s)
30 s
+taxol
0
8
Distance (μm)
DMSO
taxol

Figure 1-4: Movement of synaptobrevin-GFP is qualitatively and quantitatively different from EB1-GFP.

Representative projection images were generated from time-lapse series from axons expressing either EB1-GFP (**A**) or syb-GFP (**B**). Scale bar=5μm. Single plane images highlight the different morphology of syb-GFP (**C**) and EB1-GFP (**D**) puncta within the axon. Note the spherical nature of syb-GFP (arrowhead in C) compared to the comet-tail of EB1-GFP (arrowhead in D). Representative kymograph image from an animal expressing UAS-synaptobrevin-GFP using *elaV*-Gal4 generated from time-lapse imaging of the axon. Puncta are frequently observed to undergo reversals in the direction of the paths followed (**E**, arrowheads). Representative kymograph image from an animal expressing UAS-EB1-GFP using *elaV*-Gal4 generated from time-lapse imaging of the axon (**F**). In this background puncta are not observed changing direction. Quantification of reversals measured for both UAS-synaptobrevin-GFP (0.3 reversals/s ± 0.017, n=52) and EB1-GFP puncta (no reversals observed) expressed using the $elaV^{c155}$-Gal4 driver (**G**).

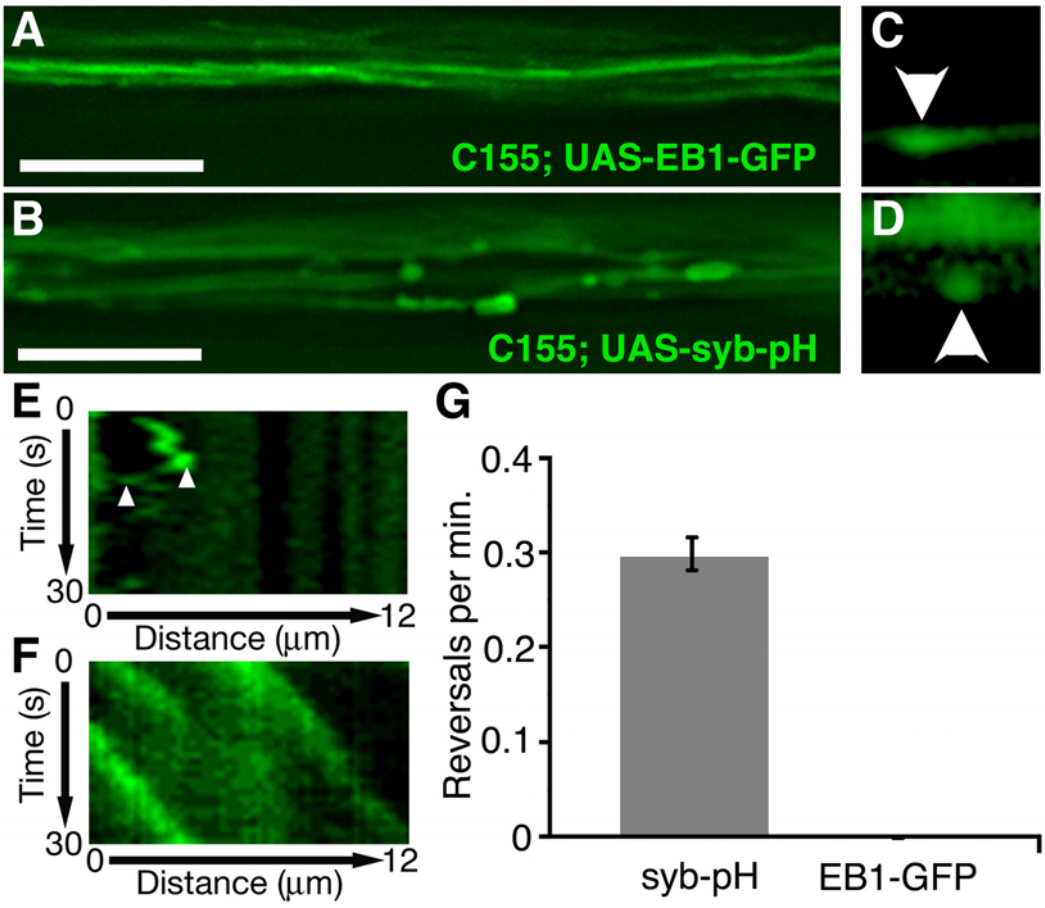
A
C155; UAS-EB1-GFP
C
B
C155; UAS-syb-pH
D
E
Time (s)
0
30
0
12
Distance (µm)
F
Time (s)
0
30
0
12
Distance (µm)
G
Reversals per min.
0.4
0.3
0.2
0.1
0
syb-pH
EB1-GFP

Figure 1-5: Expression of EB1-GFP does not alter synaptic development.

(**A**) Quantification of bouton number in wild type and EB1-GFP expressing synapses. (**B**) Quantification of bouton diameter in wild type and EB1-GFP expressing synapses. There is no significant difference comparing these genotypes. (**C,C',D,D'**) Synapse development is normal comparing wild type (left) to animals expressing EB1-GFP (right). The wild type and EB1-GFP expressing synapses are co-stained with anti-Dap160 (green), a marker of the peri-active zone, and anti-Brp (red), a marker of the active zone. Expression of EB1-GFP does not significantly alter the expression level or distribution of these markers at the NMJ.

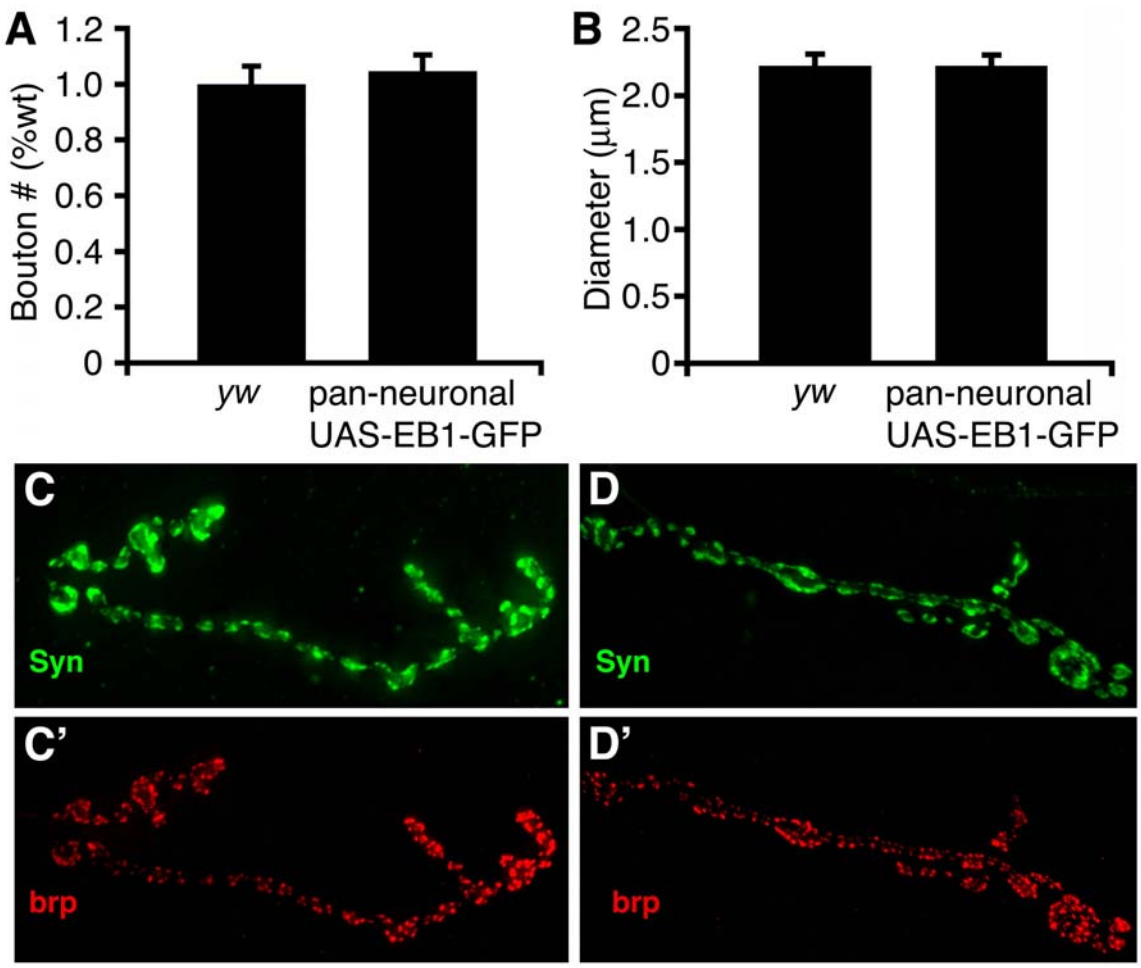
A
Bouton # (%wt)
1.2
1.0
0.8
0.6
0.4
0.2
0
yw
pan-neuronal
UAS-EB1-GFP
B
Diameter (µm)
2.5
2.0
1.5
1.0
0.5
0
yw
pan-neuronal
UAS-EB1-GFP
C
Syn
D
Syn
C'
brp
D'
brp

Figure 1-6: EB1-GFP movement is increased in the synapse relative to the axon.

(**A**) Representative image of synaptic EB1-GFP puncta (arrowheads) at the NMJ on muscle 4. The segmental nerve (axon) courses above the muscle. A single MN leaves the axon bundle to synapse upon the muscle. Note EB1-GFP puncta can be observed throughout the synapse (arrowheads). Scale bar=5μm. (**B**) Representative kymographs depicting movement of EB1-GFP puncta within the synapse at muscle 4. (**C**) Histogram of EB1-GFP puncta velocities in axons (diamonds) and synapses (squares) from wild type animals showing a small but significant difference in velocities (wild type axon = 4.12 μm/min ± 0.038 n=1121. Wild type synapse = 4.66 μm/min ± 0.10, n=337). Statistical significance was determined by Kolmogorov-Smirnov and Student's T-tests to a 99% confidence interval. Kolmogorov-Smirnov $p<0.01$, Student's T-test $p=5.44x10^{-6}$). (**D**) EB1-GFP comet tails lengths were measured in axons and synapses. Comet tails lengths were significantly increased in synapse relative to the axon (wild type= 0.37 μm ± 0.008, *DN-Glued*= 0.35 μm ± 0.007). Statistical significance was determine by Student's T-test to a 99% confidence level, p=0.20. For measurement of comet tails, EB1-GFP expression was under the control of $elaV\text{-}GAL4^{C155}$.

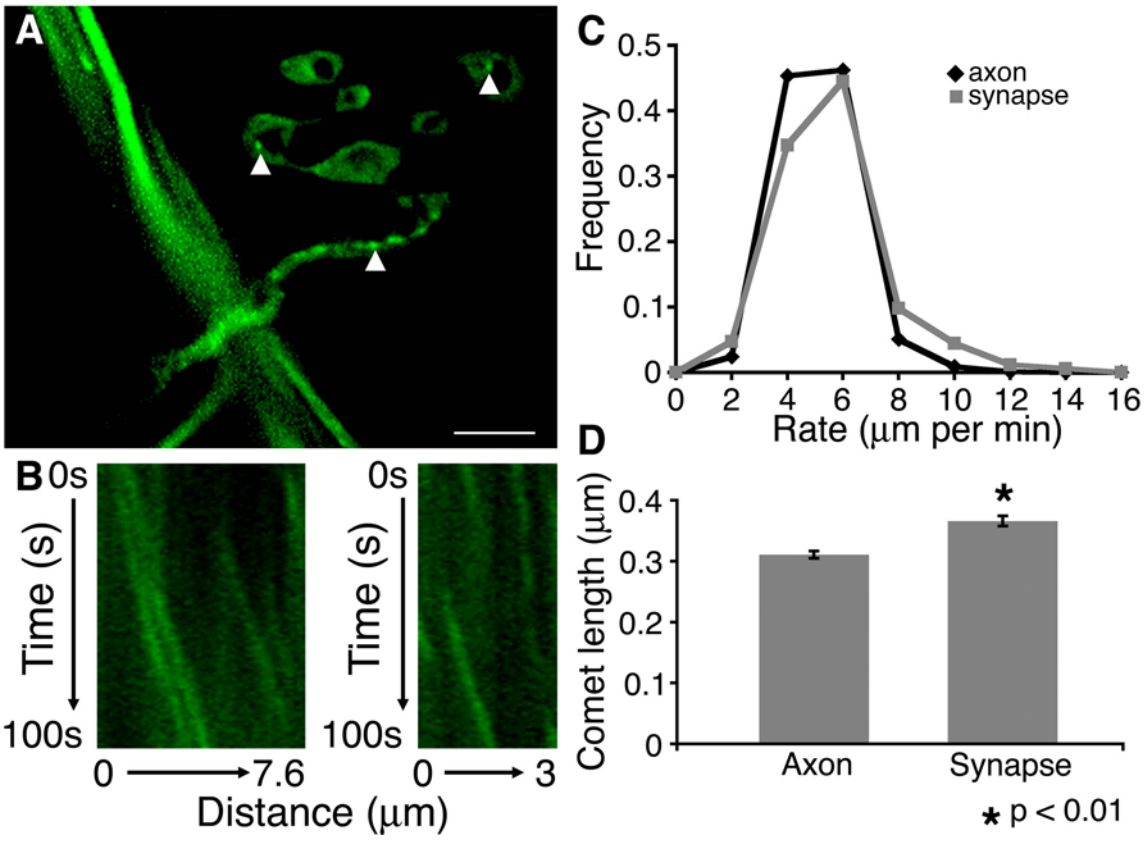
A
B
0s
Time (s)
100s
0
7.6
0
3
Distance (μm)
C
Frequency
axon
synapse
Rate (μm per min)
D
Comet length (μm)
Axon
Synapse
* p < 0.01

Figure 1-7: Inhibition of dynein/dynactin slows the velocity of EB1-GFP puncta within axons and synapses.

(A-C) Projection images generated from time-lapse images of axons from wild type (**A**), C155/Y; *DN-glued*/UAS-EB1 (**B**), and C155/Y; *dhc*/UAS-EB1-GFP backgrounds (**C**). Representative kymographs depicting movement of EB1-GFP puncta within the synapse at muscle 4. (**D**) Histograms of EB1-GFP velocity at axons in wild type (diamonds), *DN-Glued* (squares), and *dhc/+* (triangles). Note that velocity of EB1-GFP puncta is slower in experimental animals with impaired dynein/dynactin function (wild type= 4.12μm/min ± 0.038, n=1121; *DN-Glued*= 2.89 μm/min ± 0.03, n= 1249; *dhc/+*= 2.90 μm/min ± 0.031, n=1091). Statistical significance was determined by Kolmogorov-Smirnov and Student's T-tests to a 99% confidence interval. Wild type compared with *DN-Glued* Kolmogorov-Smirnov $p<0.01$, Student's T-test $p= 3.27x10^{-127}$. Wild type compared with *dhc/+* Kolmogorov-Smirnov $p<0.01$, Student's T-test $p= 1.10x10^{-53}$. (**E-G**) Projections images generated form time-lapse images of m4 synapses from wild type (**E**), C155/Y; DN-glued/UAS-EB1-GFP (**F**) and C155/Y; dhc/UAS-EB1-GFP (**G**) backgrounds. (**H**) Histograms of EB1-GFP velocity at synapses in wild type (diamonds), *DN-glued* (squares), and *dhc/+* (triangles). Note that velocity of EB1-GFP puncta is slower in experimental animals with impaired dynein/dynactin function (wild type= 4.66μm/min ± 0.10, n=337; *DN-Glued*= 2.69 μm/min ± 0.070, n=381; *Dhc/+*= 2.68 μm/min ± 0.067, n=377). Statistical significance was determined by Kolmogorov-Smirnov and Student's T-tests to a 99% confidence interval. Wild type compared with *DN-Glued* Kolmogorov-Smirnov

$p<0.01$, Student's T-test $p=1.92x10^{-44}$. Wild type compared with *Dhc/+*, Kolmogorov-Smirnov $p<0.01$, Student's T-test $p=1.75x10^{-45}$. (**I**) Representative kymographs of EB1-GFP puncta movement in animals neuronally expressing *DN-Glued.* In some axonal regions, multiple puncta move slowly with uniform processivity (top left). In other regions clear pausing events can be observed where the normally rapid rate of movement slows (top right and bottom panels, arrowhead). (**J**) Histogram of EB1-GFP velocities in the PNS of wild type (diamonds), neurally expressed *DN-glued* (squares), and *dhc/+* (triangles) animals. Note that both experimental conditions have significantly slower EB1-GFP puncta velocities compared to wild type (wild type = 3.02μm/min ± 0.12, n=128; *DN-Glued*=2.19μm/min ± 0.071, n=159; *dhc/+* = 2.35 μm/min ± 0.88, n = 173). Statistical significance was determined by Kolmogorov-Smirnov and Student's T-tests to a 99% confidence interval. Wild type compared with *DN-Glued* Kolmogorov-Smirnov $p<0.01$, Student's T-test $p = 2.12x10^{-9}$. Wild type compared with *dhc/+* Kolmogorov-Smirnov $p<0.01$, Student's T-test $p = 3.24x10^{-6}$.

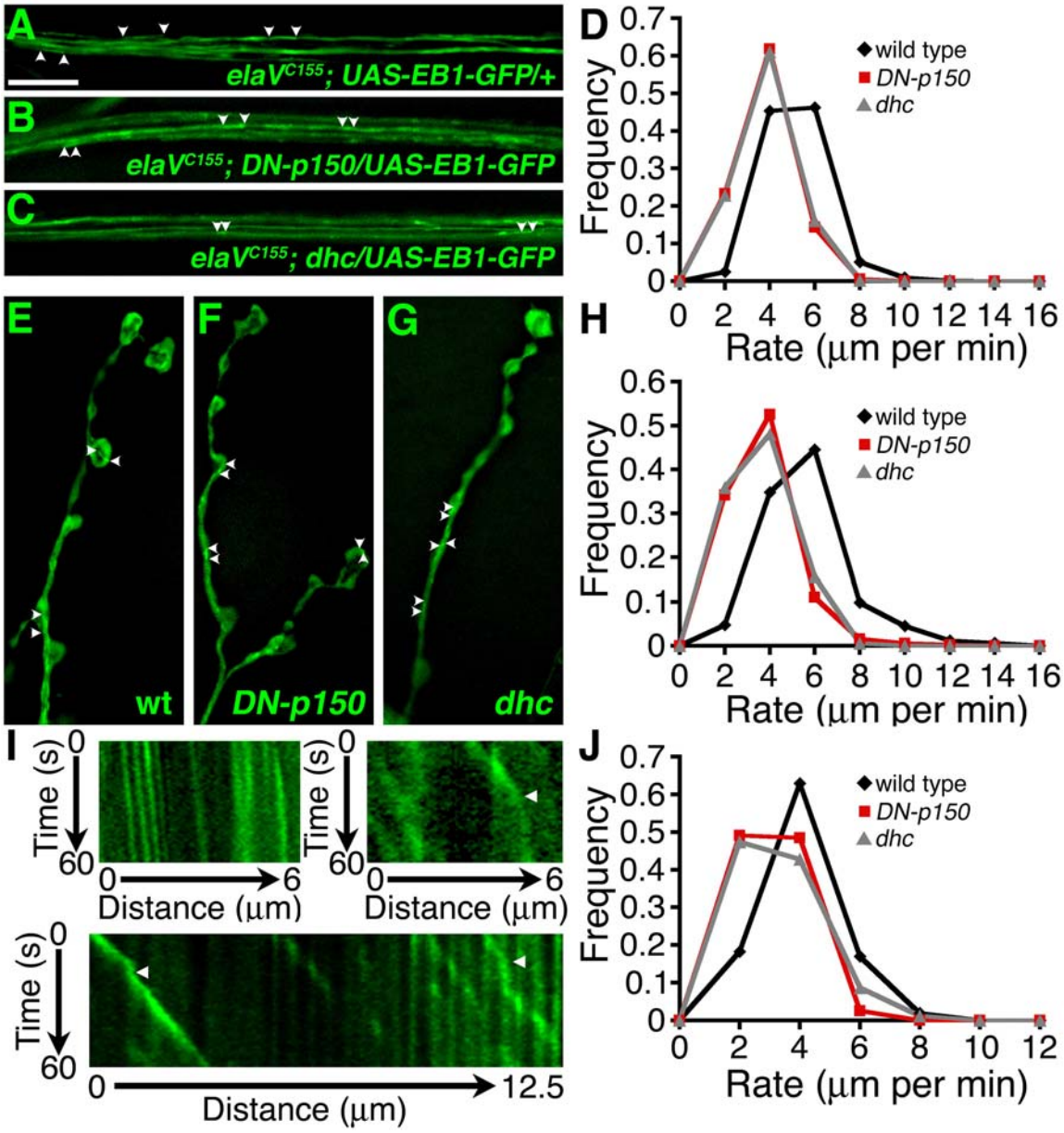
A
elaV^C155; UAS-EB1-GFP/+
B
elaV^C155; DN-p150/UAS-EB1-GFP
C
elaV^C155; dhc/UAS-EB1-GFP
D
Frequency
wild type
DN-p150
dhc
Rate (µm per min)
E
F
G
wt
DN-p150
dhc
H
Frequency
wild type
DN-p150
dhc
Rate (µm per min)
I
Time (s)
Distance (µm)
J
Frequency
wild type
DN-p150
dhc
Rate (µm per min)

Figure 1-8: Path analysis of EB1-GFP puncta at the synapse.

(A) A fixed image of a synapse at muscle 4 showing the distribution of Futsch immunoreactivity. EB1-GFP was imaged at this synapse prior to fixation. The dotted outline indicates the boundary of the perimiter of the most distal boutons that are not stained with futsch (feathered arrow). The arrowhead indicates the presence of a Futsch loop structure within the synapse. (**B**) A time-lapse series shows the movement of EB1-GFP puncta along the cortical surface of the terminal bouton (feathered arrows). The solid arrow (t=48.1 s) indicates the starting position of the EB1-GFP puncta in this series. In subsequent images of this series the hollow arrow demarcates the start position (for reference) and the solid white arrow follows the movement of the EB1-GFP puncta along the bouton cortex. EB1-GFP puncta are also observed to travel simultaneously around both sides of a microtubule loop structure identified by anti-Futsch staining (arrowheads). Time is shown at the lower right in seconds.

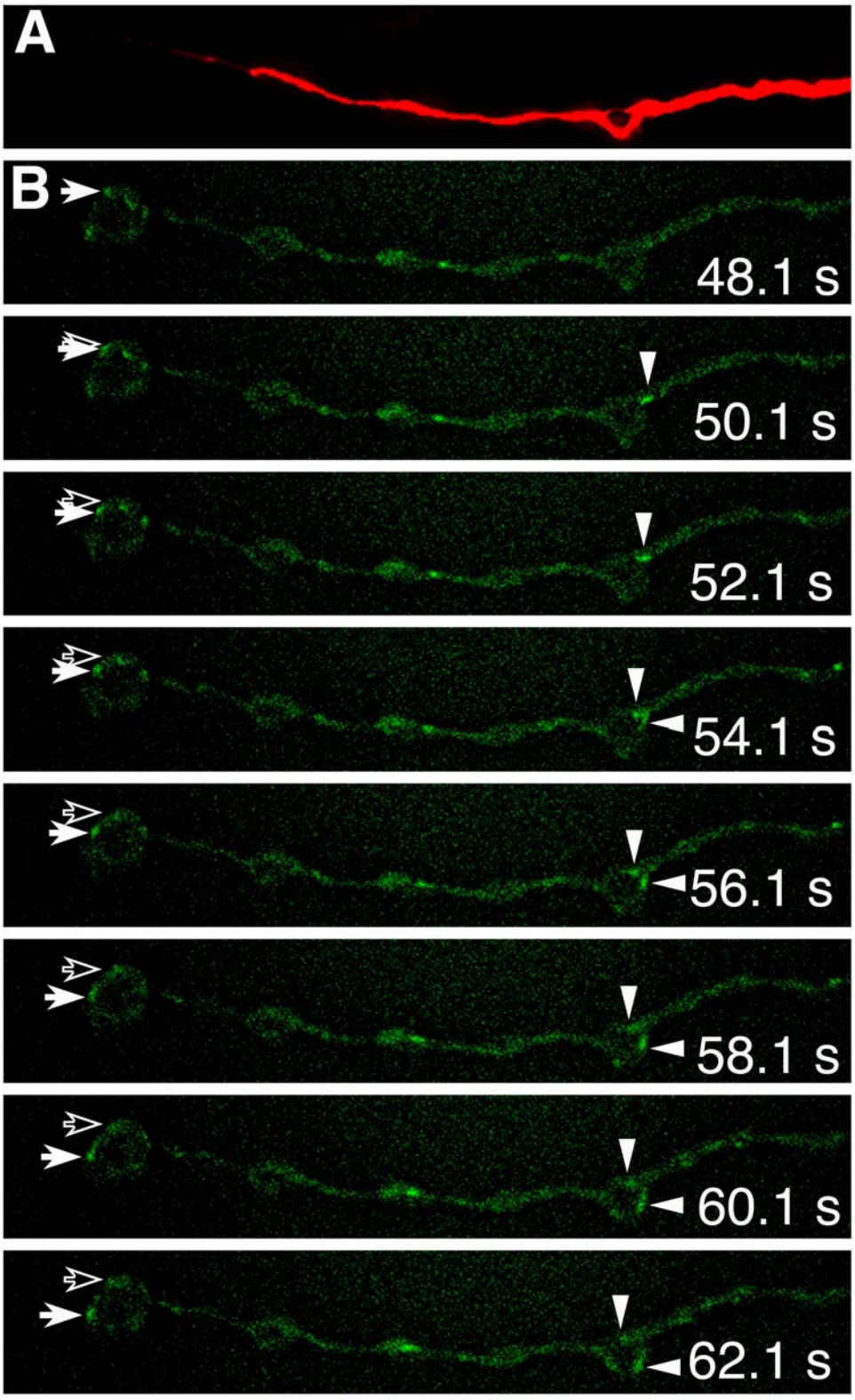
A
B
48.1 s
50.1 s
52.1 s
54.1 s
56.1 s
58.1 s
60.1 s
62.1 s

Figure 1-9: Mixed orientation of EB1-GFP puncta movement at the synapse.

(A, panel i**)** An image of the synapse at muscle 4 that was fixed and stained with anti-Futsch to reveal the Futsch-positive microtubule cytoskeleton. The arrow and box indicate the region of synapse shown at higher magnification in panel Aii showing a clear microtubule loop structure within a synaptic bouton. (**A**, panel ii) The portion of the synapse highlighted in Ai shown at higher magnification. (**A**, panel iii) Prior to fixation, this synapse was imaged for EB1-GFP puncta movement. EB1-GFP fluorescence is shown within the same region of the synapse highlighted in panels Ai and Aii, but prior to fixation. The dotted line demarcates the approximate position of the Futsch positive microtubules based on comparison with the panels Ai and Aii. (**B**) A series of time-lapse images is shown from the highlighted region of the synapse in A. The time-lapse series shows the movement of two individual puncta traveling in opposite directions within this bouton. The white arrow indicates a puncta traveling to the left and the red arrow indicates puncta traveling to the right. The dotted line in first image of this series indicates the approximate distribution of anti-Futsch immunoreactivity within the synapse as shown in Aiii. (**C**) A different time-lapse series from the same region of the synapse as in A and B. In this series an EB1-GFP puncta moves into a region of the synapse that is devoid of anti-Futsch immunoreactivity. The solid arrow (t=106.2) indicates the starting position of the EB1-GFP puncta in this series. In subsequent images of this series the hollow arrow demarcates the start position (for reference) and the solid white arrow follows the

movement of the EB1-GFP puncta. The dotted line in the first image of this series indicates the distribution Futsch immunoreactivity within the synapse.

A
5µm
i
ii
iii
B
32 s
34 s
36 s
38 s
40 s
42 s
44 s
C
106.2 s
108.2 s
110.2 s
112.2 s
114.2 s
116.2 s
118.2 s

Figure 1-10: Dynamic microtubules do not rely on Futsch for normal behavior at the synapse.

Representative images of the wild type (**A**) and *futsch*^{N94} muscle 4 synapse. The presynaptic membrane is labeled with HRP in red while the microtubule core is labeled by 22C10 in green. Note the absence of 22C10 staining in (**B**). Scale bar =5μm. (**C-E**) Projection images generated from time-lapse images of axons from wild type (**C**), *futsch*^{N94}/+; UAS-EB1/D42 (**D**), and *futsch*^{N94}/Y; UAS-EB1-GFP/D42 (**E**) backgrounds. Scale bar=10 m. (**F**) Histogram of the EB1-GFP puncta velocities within the axons in wild type (diamonds), *futsch*^{N94}/+ (squares) and *futsch*^{N94} (triangles), animals. There is no significant change in velocity of EB1-GFP puncta in *futsch*^{N94} compared to wild type axons (wild type=4.46 μm/min ± 0.022, n=140. *futsch*^{N94}/+=4.44μm/min ± 0.09, n=221. *futsch*^{N94}= 4.81 μm/min ± 0.02, n=139). Statistical significance was determined by Kolmogorov-Smirnov and Student's T-tests to a 99% confidence level. Wild type compared to *futsch*^{N94}/+ Kolmogorov-Smirnov p=0.545, Student's T-test p=0.885. D42/+ compared to *futsch*^{N94} Kolmogorov-Smirnov p=0.120 and Student's T-test p=0.043. In these experiments the wild type animals are *D42-GAL4/+,* which controls for the use of *D42-GAL4* to drive expression of EB1-GFP in these experiments (*elaV-GAL4* is not used since it is on the same chromosome as the *futsch* mutation). (**G, H**) Projection images generated from time-lapse images of synapses from wild type (**G**), and *futsch*^{N94}/Y; UAS-EB1-GFP/D42 (**H**) backgrounds. Scale bar=10μm. (**I**) Histogram of the EB1-GFP puncta velocities within the synapse at muscle 4 for wild type (diamonds), *futsch*^{N94}/+ (squares) and

futsch^{N94} (triangles). There is a small but significant increase in the velocities of puncta in *futsch*^{N94} and the heterozygous sibling control compared to wild type synapses (wild type= 4.66 μm/min ± 0.10, n=377. *futsch*^{N94}/+= 5.03 μm/min ± 0.09, n=404. *futsch*^{N94}= 5.51 μm/min ± 0.11, n=451). Statistical significance was determined by Kolmogorov-Smirnov and Student's T-tests to a 99% confidence level.

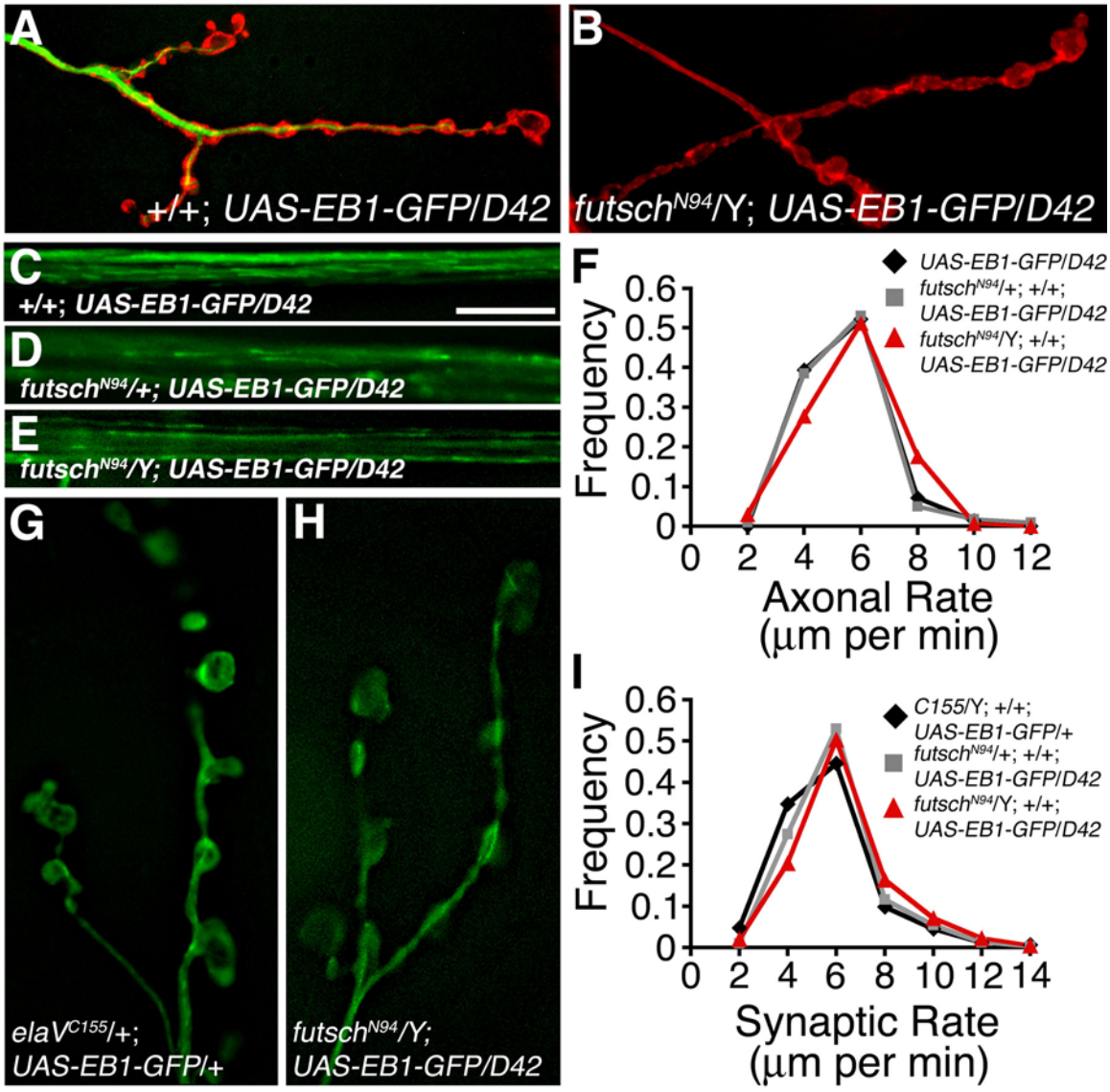
A
+/+; UAS-EB1-GFP/D42
B
futschN94/Y; UAS-EB1-GFP/D42
C
+/+; UAS-EB1-GFP/D42
D
futschN94/+; UAS-EB1-GFP/D42
E
futschN94/Y; UAS-EB1-GFP/D42
F
UAS-EB1-GFP/D42
futschN94/+; +/+; UAS-EB1-GFP/D42
futschN94/Y; +/+; UAS-EB1-GFP/D42
Frequency
0.6
0.5
0.4
0.3
0.2
0.1
0
0 2 4 6 8 10 12
Axonal Rate (µm per min)
G
elaVC155/+; UAS-EB1-GFP/+
H
futschN94/Y; UAS-EB1-GFP/D42
I
C155/Y; +/+; UAS-EB1-GFP/+
futschN94/+; +/+; UAS-EB1-GFP/D42
futschN94/Y; +/+; UAS-EB1-GFP/D42
Frequency
0.6
0.5
0.4
0.3
0.2
0.1
0
0 2 4 6 8 10 12 14
Synaptic Rate (µm per min)

Figure 1-11: Model for the role pioneer microtubules in the growth of the NMJ.

(**A**) Within a stable synapse pioneer microtubules are observed to invade and explore all regions of the NMJ. Within proximal boutons these movements may follow a pattern similar to the pattern of Futsch staining. In the distal most bouton that lacks any significant Futsch-core, pioneer microtubules track the membrane cortex possibly searching for sites permissive of new growth. (**B**) Trophic signaling results in the activation of membrane bound receptors. Invading microtubules interact with this activated trophic receptors, relaying the signal to the interior. This in turn may result in membrane protrusion and the initiation of bud formation. (**C**) Pioneer microtubules continue to invade and explore this new bud as it grows and becomes a bouton. As this occurs, Futsch bundles microtubules in the penultimate bouton, likely stabilizing this structure and allowing further growth of the NMJ. As the Futsch-labeled core advances, a small subset of pioneer microtubules may become stabilized and incorporated into core. (**D**) As the bud matures into a fully functional bouton low levels of Futsch begin to be observed, acting to stabilize the new addition. Pioneer microtubules continue to explore all regions of the synapse for sites permissive of new growth.

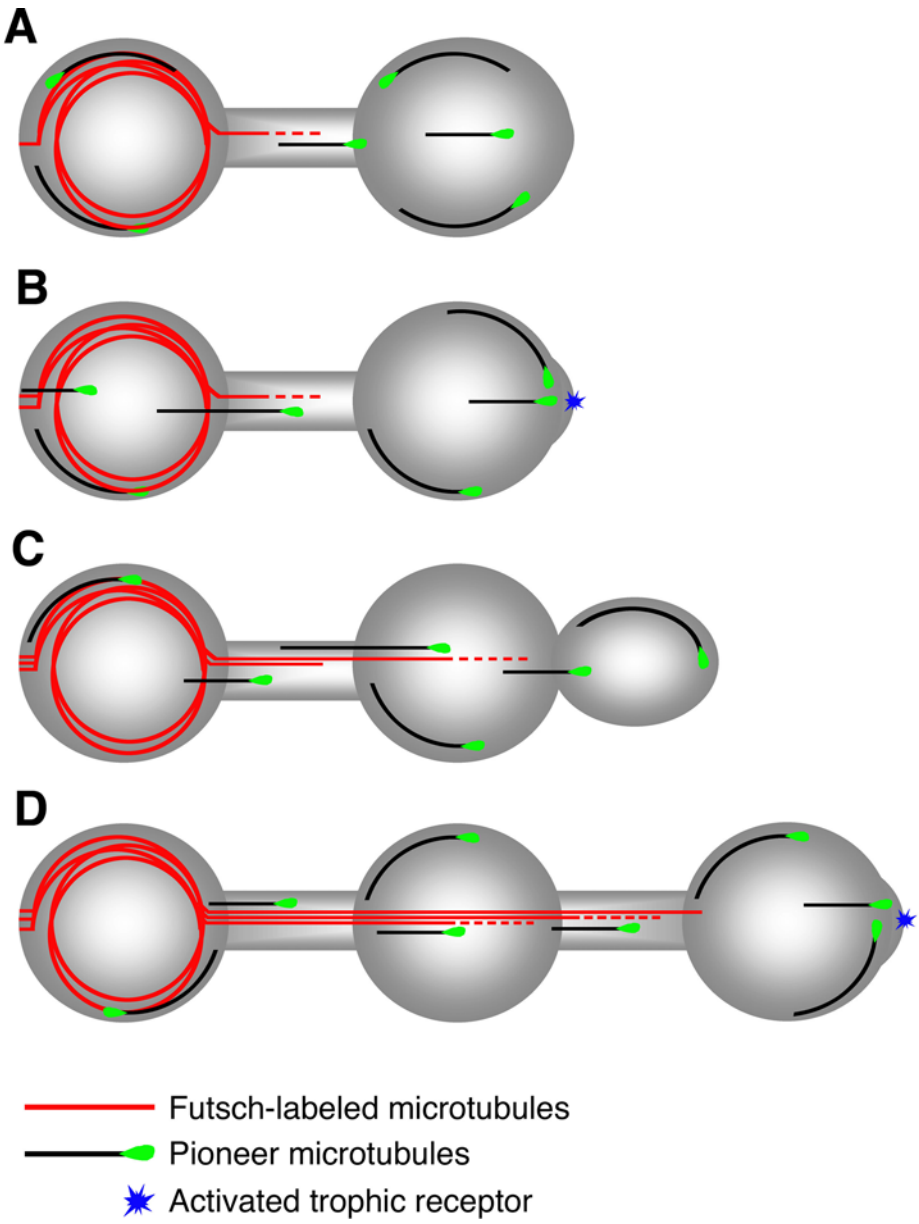
A
B
C
D
Futsch-labeled microtubules
Pioneer microtubules
Activated trophic receptor

Supplemental Movie 1-1: EB1-GFP movement within a Drosophila S2 cell.

This movie accompanies Figure 1-1. Note EB1-GFP labeled plus-ends move uni-directionally towards the periphery.

Supplemental Movie 1-2: EB1-GFP movement within axons of the segmental nerve.

EB1-GFP is expressed using the pan-neuronal GAL4 driver *elaV*-Gal4. Individual EB1-GFP puncta can be visualized moving apparently bi-directionally within the axons contained in the segmental nerve. This movie accompanies Figure 1-2.

Supplemental Movie 1-3: EB1-GFP movement within the neuromuscular synapse at muscle 4.

This movie accompanies Figure 1-6. EB1-GFP puncta move within the axons that traverse above muscle 4 and are observed to move throughout the synaptic boutons.

Supplemental Movie 1-4: EB1-GFP movement at the NMJ and within the terminal synaptic bouton.

This movie accompanies Figure 1-8. The synapse at muscle 4 is shown with EB1-GFP movement. Note the prominent movement of EB1-GFP puncta at the cortex of the terminal synaptic bouton (far left).

Supplemental Movie 1-5: EB1-GFP movement at the NMJ and within a nascent bouton.

This movie accompanies Figure 1-9. The synapse at muscle 4 is shown with EB1-GFP movement corresponding to the fixed image of the synapse stained with anti-Futsch in Figure 1-9. Note the targeting of the nascent bouton bud shown in Figure 1-9C by the dynamic microtubule plus ends.

Formin-Dependent Synaptic Growth; Evidence that Dlar Signals via Diaphanous to Modulate Synaptic Actin and Dynamic Pioneer Microtubules.

ABSTRACT

The *diaphanous* gene is the founding member of a family of Diaphanous Related Formin proteins (DRF). We identified *diaphanous* in a screen for genes that are necessary for the normal growth and stabilization of the Drosophila neuromuscular junction (NMJ). Here we demonstrate that *diaphanous* mutations perturb synaptic growth at the NMJ. Diaphanous protein is present both pre- and postsynaptically. However, genetic rescue experiments in combination with additional genetic interaction experiments support the conclusion that *dia* is necessary presynaptically for normal NMJ growth. We then document defects in both the actin and microtubule cytoskeletons in *dia* mutant nerve terminals. Defects in both synaptic actin and dynamic pioneer microtubules are correlated with impaired synaptic growth in *dia* mutants. Finally, we present genetic evidence that Dia functions downstream of the presynaptic receptor tyrosine phosphatase Dlar and the Rho-type GEF *trio* to control NMJ growth. Based upon the established function of DRFs as Rho-GTPase dependent regulators of the cell cytoskeleton, we propose a model in which Diaphanous links receptor tyrosine phosphatase signaling at the plasma membrane to growth-dependent modulation of the synaptic actin and microtubule cytoskeletons.

INTRODUCTION

Individual neurons acquire stereotyped morphologies during development. It is well established that signaling molecules including the neurotrophins, growth factors and morphogens can profoundly influence the global growth and survival of individual nerve cells (Aberle et al., 2002; Marques, 2005; Zweifel et al., 2005; Bamji et al., 2006; Reichardt, 2006). There is also evidence that local, intercellular signaling systems participate in defining synaptic and dendritic arborizations (Luo and O'Leary, 2005). Although considerable progress has been made, the identity of the intercellular signaling systems, and how these signals are coupled to the modulation of the underlying neuronal cytoskeleton, remain to be elaborated.

The importance of the presynaptic actin and microtubule cytoskeletons during synapse morphogenesis and growth of the Drosophila neuromuscular junction has been established through the analysis of mutations in essential cytoskeletal regulatory proteins. For example, perturbation of the presynaptic Spectrin-Actin skeleton profoundly disrupts NMJ growth and stability (Pielage et al., 2005, 2006). Additional actin regulatory proteins implicated in synaptic growth in Drosophila include the NWASP interacting protein *nervous wreck* (*Nwk*), the dynamin-associated protein *Dap160/Intersectin*, and NSF (Stewart et al., 2002; Coyle et al., 2004; Marie et al., 2004; Stewart et al., 2005). The integrity of a stable population of bundled presynaptic microtubules at the Drosophila NMJ is also required for normal synaptic growth (Roos et al., 2000). Presynaptic bundled microtubules are labeled by the MAP1b-like protein Futsch and *futsch* mutations disrupt both NMJ growth and synaptic microtubule organization (Roos

et al., 2000). Several additional signaling systems have been shown to be required for the normal integrity of presynaptic microtubules including Vap33A (Pennetta et al., 2002), aPKC (Ruiz-Canada et al., 2004), spastin (Sherwood et al., 2004; Trotta et al., 2004), sec8 (Liebl et al., 2005) and protein phosphatase 2A (Viquez et al., 2006).

Despite this progress, there is not a clear picture for how the synaptic microtubule and actin cytoskeletons are regulated by inter-cellular, synaptic growth related signaling at the Drosophila NMJ. The formins are a highly conserved family of proteins with well-established functions during the assembly and organization of the actin and microtubule cytoskeletons (Palazzo et al., 2001; Wallar and Alberts, 2003; Eng et al., 2006). Although the formins have been implicated in diverse cellular processes, little is known about formin protein function within the nervous system. Here we provide evidence that a Drosophila formin encoded by *diaphanous* is an essential molecular effector that conveys signaling from a presynaptic receptor protein tyrosine phosphatase (Dlar) to the underlying actin and microtubule cytoskeletons. We also show that this signaling is necessary for normal synaptic growth. Finally, in so doing, we also characterize a population of dynamic, pioneer synaptic microtubules and provide evidence for Diaphanous-dependent regulation of these pioneer microtubules.

RESULTS

Formins have been shown to participate in the nucleation of unbranched actin filaments by association with the barbed end of actin filaments (Pruyne et al., 2002; Zigmond et al., 2003; Romero et al., 2004). In this capacity, the formins have been implicated in the formation and modulation of actin cables, stress fibers and actin-rich cell adhesions (Watanabe et al., 1999; Ishizaki et al., 2001; Kovar et al., 2003; Kobielak et al., 2004; Zigmond, 2004). A sub-family of formins, the Diaphanous related formins (DRFs), have also been shown to bind microtubule plus ends and function with APC to control microtubule stabilization (Palazzo et al., 2004; Wen et al., 2004). In *Drosophila, diaphanous* encodes a prototypical DRF protein.

We identified mutations in the *diaphanous* gene in a large-scale screen for genes that are required for the normal growth and/or stability of the *Drosophila* NMJ. The basis of this forward genetic screen is direct visualization of the *Drosophila* NMJ in dissected third instar larvae. For each independent mutant or gene-specific RNAi, we directly visualize juxtaposed pre- and postsynaptic compartments at the third instar NMJ. The presynaptic nerve terminal is stained with either anti-synapsin (vesicle associated protein) or anti-Brp (labeling the presynaptic active zone) in combination with anti-Dlg to label the postsynaptic muscle membrane folds. We examine 30-50 NMJ from at least three independent animals per mutant or gene-specific RNAi and score each for a change in bouton number (an assay for synapse growth) or the increased presence of synaptic retraction events (an assay for synapse stability as defined in previous publications; Eaton et al., 2002; Eaton and Davis, 2005; Pielage et al., 2005). The *diaphanous* gene was

identified as being required for normal NMJ growth without an effect on synapse stability.

Diaphanous is present both pre and postsynaptically at the NMJ.

Diaphanous is a classical formin with two formin homology domains (FH1 and FH2) (Figure 2-1B). The FH1 domain is a proline rich domain that binds SH3 and WW containing proteins such as profilin (Sagot et al., 2002; Higgs, 2005). The C-terminal FH2 domain is known to make contacts with actin and is required for protein dimerization (Higgs, 2005). Together, the FH1 and FH2 domains mediate the actin regulatory abilities common to formin proteins (Sagot et al., 2002; Kovar and Pollard, 2004; Romero et al., 2004; Higgs, 2005; Pellegrin and Mellor, 2005). In addition to the classical formin domains, Diaphanous also contains an N-terminal Rho-type GTPase binding domain (GBD) and a C-terminal autohibitory domain (Alberts, 2001; Higgs, 2005; Wallar et al., 2006). These domains are typical of the DRF subfamily of formin proteins. The C-terminal auto-inhibitory domain binds to a sequence within the N-terminal GBD and is thought to prevent the interaction of profilin and g-actin with the FH1 and FH2 domains. Binding of active Rho-GTPases to the GBD is thought to relieve the association of the autoinhibitory domain with the N-terminus, allowing the DRF to become active (Alberts, 2001; Wallar et al., 2006).

Previous genetic studies of *diaphanous* in Drosophila have identified mutations in the *dia* gene including the dia^2 and dia^9 alleles (Figure 2-1A). The dia^2 mutation lacks the entire first exon and deletes half of the second coding exon. Previously published genetic data are consistent with the conclusion that dia^2 is a null mutation (Castrillon and

Wasserman, 1994). The *dia*^{2} homozygous animals are early larval lethal, although some larvae survive to third instar stage allowing analysis of synaptic growth and function. The *dia*^{9} allele lacks a portion of the first exon and is considered to be a hypomorphic mutation (Castrillon and Wasserman, 1994). These animals survive to late third instar stages.

We first addressed whether Dia protein is present at the third instar larval NMJ. In wild type third instar larvae anti-Dia staining was observed to concentrate at the NMJ (Figure 2-1C). Some staining is clearly post-synaptic, localizing to punctate structures in the muscle that may represent endosomes based upon their size and distribution (Figure 2-1C arrow). Additional staining overlaps the presynaptic nerve terminal. The synaptic and putative endosomal staining are both eliminated in the *dia*^{2} null mutant background, demonstrating that this staining pattern represents the distribution of Dia protein at the NMJ (Figure 2-1C). We pursued additional experiments to investigate whether Dia protein might reside within the presynaptic nerve terminal. To do so, we co-stained the NMJ for Dia and the presynaptic-specific microtubule associated protein Futsch (Roos et al., 2000). Three-dimensional reconstruction of the nerve terminal demonstrates that a portion of the Dia immunoreactive puncta reside in close association with bundled presynaptic microtubules (Figure 2-1D). A similar conclusion was made after analysis of the NMJ that was co-stained with Dia and the presynaptic membrane marker anti-HRP (not shown). Thus, we conclude that Dia is present both pre- and postsynaptically at the Drosophila NMJ.

Presynaptic Dia is necessary for normal synaptic growth.

We identified *dia* mutations in a screen based on a decrease in synaptic bouton number at muscles 6/7 (Figure 2-2A, B). This decrease in bouton number is also observed at muscle 4 (Figure 2-2C, D) demonstrating a general requirement of *dia* during NMJ growth. We have focused our analysis on muscle 4 because this NMJ is typically positioned in the central, flattest region of the muscle and is, therefore, ideally suited for live imaging studies of the synaptic actin and microtubule cytoskeletons (see below). Quantification of bouton numbers at muscle 4 confirms a significant decrease in bouton number at the *dia* null and hypomorphic NMJs compared to wild type (dia^2/Df = 65.64888 ± 2.256%; dia^2/dia^2 = 64.744 ± 2.4956%; dia^2/dia^9 = 69.8213 ± 2.86946%; data are percent wild type bouton number, Figure 2-2F). It has been shown that muscle growth is coupled to growth of the presynaptic nerve terminal at the Drosophila NMJ (Aberle et al., 2002). To determine whether the decrease in bouton number observed in the *dia* mutants was due to a decrease in muscle size, we measured muscle size in each mutant background. There is no significant decrease in muscle size in any of the tested mutations compared to wild type (data not shown). However, we observe a significant 15% increase in muscle size in the dia mutant, which would cause us to under-estimate the bouton to muscle surface ratio. Thus, we conclude that the observed changes in bouton number reflect impaired presynaptic nerve terminal growth. Finally, we measured bouton areas in the *dia* mutant background since impaired bouton numbers are often associated with a change in bouton morphology. We find a highly significant increase in average bouton area in the *dia* mutant background (wild type = 4.96 ± 0.15 μm^2, n=725; dia^2 = 12.6+/-0.49 μm^2, $p<0.001$, n=334), consistent with observed changes in NMJ morphology in other mutations such as the receptor tyrosine phosphatase *dlar*.

Since Diaphanous protein is present both pre- and postsynaptically, we next addressed whether Diaphanous is required in the presynaptic neuron or postsynaptic muscle cell for normal synaptic growth. To do so, we expressed a *diaphanous* rescue transgene (*UAS-dia^{act}*) in the background of the *dia^{2}* null mutant background. The *UAS-dia^{act}* transgene lacks both the N-terminal GBD and the C-terminal DAD domains. Based upon work in other systems, this transgene is predicted to behave as a constitutively active Diaphanous molecule, allowing us to increase Dia function independent of the signaling systems necessary for activation of the Dia protein (Watanabe et al., 1999; Tominaga et al., 2000; Somogyi and Rørth, 2004; Williams et al., 2007). We find that overexpression of *UAS-dia^{act}* in either the nerve or the muscle in a wild-type background has no effect on synaptic growth (data not shown). However, neuronal expression of *UAS-dia^{act}* is sufficient to rescue synaptic growth in the *dia^{2}* null mutant background (Figure 2-2E, F). It is possible that non-specific actions of the activated dia transgene contribute to genetic rescue. However, we believe that the specificity of the observed rescue, restoring the NMJ to wild type size without causing a neomorphic alteration in NMJ morphology, makes this possibility unlikely. Therefore, we conclude that Diaphanous is required presynaptically for normal NMJ growth.

A second, prototypical formin is encoded by the *cappuccino* gene in Drosophila (Emmons et al., 1995). We also examined mutations in *capp* to determine if synaptic growth might be generally perturbed by altered formin signaling. However, quantification of synaptic bouton numbers demonstrates that *capp* is not required for NMJ growth (Figure 2-2F). Additionally, synapse morphology is normal in *capp* (data

not shown). These data highlight the fact that *dia* mutations were identified randomly in a forward screen for mutations that disrupt synaptic growth.

Dia is necessary for the maintenance of the presynaptic actin cytoskeleton.

Dia and other formin proteins have been shown to influence actin polymerization. Therefore, we asked whether impaired synaptic growth observed in the *dia* mutant background is correlated with a change in the presynaptic actin cytoskeleton. To visualize the presynaptic actin cytoskeleton we expressed a *UAS-actin-GFP* transgene presynaptically in the dia^2 mutant background. Consistent with a recent study (Nunes et al., 2006) we find that presynaptic actin at the Drosophila NMJ is organized into discreet foci that are distributed throughout the NMJ (Figure 2-3A,C,E). Post-fixation staining of the presynaptic nerve terminal membrane allowed us to quantify the distribution of these presynaptic actin puncta within individual synaptic boutons (Figure 2-3B,D, F). Quantification of the number of actin foci per bouton reveals an approximate 50% decrease in the number of organized actin foci at the *dia* NMJ compared to wild type (wt = 5.51+/-0.2 foci/bouton, n=325; dia^2/dia^2=2.64+/-0.1 foci/bouton, n=369, $p < 0.001$) (Figure 2-3G). We also visualized presynaptic actin foci by expressing a GFP-tagged actin binding protein (Edwards et al., 1997). This transgene controlled for possible artifacts arising from actin overexpression. When the NMJs of larvae expressing this transgene were imaged, the GFP pattern was indistinguishable from that observed using the *UAS-actin-GFP* (data not shown). These data suggest that loss of Dia within the presynaptic nerve terminal leads to impaired actin polymerization or stabilization and, as a consequence, a decrease in the steady-state levels of polymerized actin. This defect

could reasonably account for impaired synaptic growth. To investigate this possibility further, we pursued genetic epistasis experiments with genes known to participate in the regulation of neuronal actin.

Genetic evidence that Dia functions downstream of Dlar and Trio during NMJ growth.

The *dia* mutant phenotype is manifest as a decrease in synaptic bouton number with a corresponding increase in bouton area. A similar phenotype has been documented at the NMJ of the *dlar* mutant animals. The *dlar* gene encodes a receptor tyrosine phosphatase that has been shown to signal via an associated Rho-GEF encoded by *trio* to control motor axon guidance (Krueger et al., 1996; Bateman et al., 2000; Kaufmann et al., 2002). By contrast, loss of other putative actin-regulatory proteins present at the Drosophila NMJ such as NSF (Stewart et al., 2002, 2005), Nervous-wreck (Coyle et al., 2004), Dap160/Intersectin (Marie et al., 2004) and Profilin (unpublished data) cause a dramatic change in synapse morphology including an increase in the formation of small, highly branched synaptic boutons termed satellite boutons. Thus, the phenotypic similarity of the *dlar* and *dia* mutations suggested that these genes might function together to control synaptic growth. Furthermore, by analysis with DRF function in other systems, it is reasonable to hypothesize that *trio* could signal via a GTPase that subsequently activates Dia to mediate a change in the underlying synaptic cytoskeleton necessary for synaptic growth (Watanabe et al., 1999; Li and Higgs, 2003, 2005; Ridley, 2006; Wallar et al., 2006). Therefore, we tested this hypothesis genetically by analyzing double mutant combinations of *dia* with *dlar* and *trio*.

First, we demonstrate that heterozygous null mutations in *dia* as well as *dlar* and *trio* do not significantly impair synaptic growth at the NMJ. Indeed, the *dlar* heterozygous animals show a small, but statistically significant, increase in bouton number (Figure 2-4 A, B, G). We also confirmed prior results demonstrating that homozygous *dlar* mutant NMJ have significantly fewer synaptic boutons compared to wild type (data not shown) (Kaufmann et al., 2002). Next, we analyzed bouton number in animals that harbor double heterozygous mutations by combining dia^{2}/+ with either $dlar^{5.5}$/+ (Figure 2-4E, G) or $trio^{1}$/+ (Figure 2-4D, G). In both cases, the double heterozygous mutant combinations result in a statistically significant decrease in synaptic bouton number (Figure 2-4 G; $p<0.01$). Finally, we asked whether the genetic interaction between *trio* and *dlar*, first identified in the context of Drosophila axon guidance, also occurs when NMJ growth is assayed (Krueger et al., 1996; Bateman et al., 2000). We find that the double heterozygous mutant combination of $dlar^{5.5}$/+; $trio^{1}$/+ resulted in a significant decrease in NMJ size, similar to that seen for the *dia* genetic combinations (Figure 2-4 F, G). Together, these genetic data indicate that *dia*, *dlar* and *trio* all function in the process of NMJ growth and could function as a single signaling pathway. To further explore this possibility, we generated animals that are double homozygous mutations of *dia* and *dlar*. If these genes function in the same pathway, then we expect that the double mutant will be no more severe than the dia^{2} null mutation alone. Analysis of the dia^{2}-$dlar^{5.5}$ double mutants reveals a decrease in synaptic bouton number that is not significantly different from either single mutation alone (Figure 2-4C, G). Furthermore, when we image actin-GFP at the NMJ of the $dla^{5.5}$ mutants we find a defect that is quantitatively identical to that observed in the *dia* mutant background (Figure 2-3).

These same experiments could not be repeated with *trio* since it is a homozygous lethal mutation. Together, these data lend support to the conclusion that Diaphanous functions with Dlar and Trio to control synaptic growth. Since Dia is a Rho-GTPase effector protein, we propose that Dia functions downstream of Trio to control NMJ growth. Finally, since Dlar and Trio are expressed only presynaptically at the NMJ (Newsome et al., 2000; Kaufmann et al., 2002), these genetic data also provide further evidence that Dia functions presynaptically to specify NMJ growth.

If Dia functions downstream of Dlar and is primarily responsible for mediating the growth related function of the Dlar receptor, then we might expect that expression of the activated Dia transgene (*UAS-dia^{act}*) would be able to rescue the NMJ growth defects observed in the *Dlar* mutant. Remarkably, neuronal expression of *UAS-dia^{act}* not only rescues boutons numbers in the *Dlar* mutant (Supplemental Figure 2-1), but also significantly improves several measures of adult health and viability. In this experiment, bouton numbers were, once again, statistically significantly decreased in *dlar* mutant compared to wild type at muscle 4 (56.9$\pm$2.8% of wild type, n=22, $p<0.001$) and expression of *UAS-dia^{act}* in the *dlar* mutant significantly increased bouton numbers toward wild type values (86.29$\pm$3.27% of wild type, n=22; the rescue of bouton number is significant compared to *dlar* alone, $p<0.001$). This experiment was repeated with quantitatively identical results at muscles 6/7 (*dlar$^{5.5}$/ dlar$^{13.2}$* = 41.0$\pm$3.98% of wild type, n=18, and expression of *UAS-dia^{act}* in *dlar$^{5.5}$/ dlar$^{13.2}$* = 85.77$\pm$5.04% of wild type, n=18; the rescue of bouton number is significant compared to *dlar* alone, $p<0.001$). There is no change in statistical significance if the bouton counts are corrected for muscle size. In addition, *dlar* mutants eclose into adults at a lower rate compared with genetic controls

and those *dlar* mutants that do eclose, do so with severely impaired health and fail to inflate their wings (Table 1). By contrast, expression of *UAS-dia*^{act} in the *dlar* mutant increases the percentage of animals that eclose to adults. Furthermore, a much higher percentage of these animals inflate their wings. Together, these data provide additional genetic evidence that Dia functions downstream of Dlar during neural development and during NMJ growth.

Evidence in other systems indicates that Diaphanous can function together with additional components of the cellular machinery necessary for actin polymerization including profilin. Therefore, we also tested for genetic interactions between *dia*^{2} and *profilin* and the tyrosine kinase *abl*. However, we did not uncover evidence of a trans-heterozygous interaction between *dia* and either *profilin/+* or *abl/+*. The early lethality of both genes prevented us from assaying synaptic growth in double homozygous mutations. These data are inconclusive regarding how Dia might interact with the actin regulatory machinery. However, these data serve to highlight the significance of the observed trans-heterozygous interaction between *dia* and both *dlar* and *trio*.

Diaphanous modulates the behavior of dynamic pioneer microtubules within the presynaptic nerve terminal.

In addition to their role in regulating the actin cytoskeleton, Diaphanous related formin proteins have recently been shown to modulate the dynamic behavior of microtubules. For example, activated mDia1 and mDia2 lead to the formation of a stable population of microtubules labeled by glu-tubulin whereas inhibition of mDia activity prevents the generation of this population of microtubules in cell-wounding and

migration assays (Palazzo et al., 2001; Palazzo et al., 2004; Wen et al., 2004; Eng et al., 2006). In mammalian cell culture studies, these effects on microtubules are independent of the Dia-dependent modulation of actin polymerization. Therefore, we sought to investigate the function of Dia on the synaptic microtubule cytoskeleton.

As highlighted earlier, it is clear from several studies that disruption of a stable core of bundled microtubules at the NMJ is correlated with a defect in synaptic growth (Roos et al., 2000). Recent work however, has demonstrated that a second dynamic population of microtubules exists at the NMJ (Yan and Broadie, 2007). In contrast however, previous work on Dia has been shown to primarily influence dynamic microtubules through signaling at the microtubule plus ends. Recent work has made use of a fluorescently labeled microtubule plus-end marker to monitor and characterize a population of dynamic microtubules within *Drosophila* neurons (Rolls et al., 2007). Here we make use of this technique to examine the role of Diaphanous in regulating the dynamic population of presynaptic microtubules at the Drosophila NMJ.

We began the analysis of Dia's effect on dynamic microtubules by imaging axons in wild type and dia^2/dia^2 larvae. Time-lapse series were projected to reveal the extent of microtubule plus-end displacement over an identical period of imaging for both genetic backgrounds. We find that the path lengths of EB1-GFP are longer in the dia^2/dia^2 background than in wild type (Figure 2-7 A, B arrowheads), suggesting that microtubule plus-ends are able to move farther in a *dia* loss of function background than in a wild type background over the same time period. To quantify this result, the rate of EB1-GFP puncta movement was measured in both dia^2/dia^2 and wild type larvae. There is a

statistically significant shift in the distribution of puncta movement in the *dia* mutant toward faster rates compared to wild type (Figure 2-7C).

We repeated this analysis for EB1-GFP puncta within the presynaptic nerve terminal. As within axons, the path lengths observed in projection images from the dia^2/dia^2 synapses are longer than those observed in the wild type synapses (Figure 2-7 D, E arrowheads). Quantification of the rate of EB1-GFP puncta movement again shows a statistically significant shift toward faster rates in the dia^2/dia^2 animals compared to wild type (Figure 2-7F). Taken together the increased rate of movement seen in axon and the synapse implies that loss of Diaphanous leads to an increase in the rate of microtubule polymerization. The length of EB1-comet tails has been used in other studies as a means of measuring differences in rates of polymerization. As the comet-tail is thought to arise from the release of EB1 molecules as the GTP-cap is hydrolyzed, a longer comet-tail represents an increase in polymerization. We measured and compared the length of the EB1-GFP comet-tails in dia^2/dia^2 and wild type axons. Consistent with the increased rate of movement, the comet-tails in the dia^2/dia^2 larvae are two-fold longer than those in wild type (wt=0.31 $\pm$ 0.006μm, $dia^{2/2}$=0.565 $\pm$ 0.006μm, p=$9.7E^{-129}$).

Finally, we asked whether the regulation of dynamic microtubules by Diaphanous could be generalized to other Drosophila cell types. To do so, we used gene-specific RNAi to *dia* to deplete Dia protein from S2 cells. Western blots revealed that Diaphanous protein level was absent after five days of dsRNA treatment (data not shown). Previous studies in which Dia has been knocked down with RNAi have shown that S2 cell size increases and the cells become multinucleate due to a failure to undergo cytokinesis. In our study we noted that cells treated with dsRNA against *diaphanous* showed these same

phenotypes. Following Dia RNAi, EB1-GFP puncta have longer path lengths relative to the control cells, consistent with the results from the axon and synapse (Figure 2-7G, H). A histogram of the rate of EB1-GFP puncta movement in both the RNAi treated and control cells reveals a statistically significant shift toward faster puncta movement in *diaphanous* RNAi cells (Figure 2-7I).

One possibility is that the Dia-dependent change in synaptic actin leads to a change in the rate of microtubule plus end movement. To test this possibility, we pharmacologically depolymerized synaptic actin and assayed microtubule plus end movement within the presynaptic nerve terminal. We find that synaptic actin foci were completely eliminated by incubation in 7.5μM latrunculin A (Figure 2-8A, B). We then imaged microtubule plus end movement following this treatment. We find that loss of actin foci has no direct effect on microtubule plus end movement compared to controls (Figure 2-8C, D, E). Therefore, taken together with our *in vivo* and *in vitro* imaging data, our results are consistent with the conclusion that Diaphanous participates in the regulation of microtubule plus end polymerization within the axon and the presynaptic nerve terminal. These data are consistent with results from other systems indicating that Dia has a stabilizing activity at microtubule plus ends.

It is possible that the change in microtubule plus end behavior has a direct effect on synaptic growth. Microtubule dynamic instability is essential for growth cone and cell motility (Rodriguez et al., 2003; Lee et al., 2004; Suter et al., 2004) and has been proposed to be involved in the detection or relay of signaling events at the cell plasma membrane (Kalil and Dent, 2005). Another possibility is that the change in microtubule plus end behavior results in a defect in the assembly or organization of the underlying

stable microtubule population identified by anti-Futsch staining. Therefore, we quantified Futsch staining and compared wild type and *dia* mutants. We find that Futch-positive microtubules remain well organized in the *dia* mutant background (Figure 2-9A, B, C). However, closer examination reveals a modest, though statistically significant, decrease in the abundance of Futsch positive microtubules at the distal most regions of the NMJ. In wild type animals, the caliber of the Futsch-positive microtubule filament decreases along the length of the NMJ until it becomes a very fine filament in the most distal bouton. In *dia* mutant NMJ, the Futsch positive microtubles taper more rapidly within the NMJ (Figure 2-9B, C). As a consequence, the distal regions of the *dia* mutant NMJ appear to lack a clear core of bundled microtubules. Quantitatively identical results were obtained imaging Futsch-positive microtubules in the *dlar* mutant and the *dlar; dia* double mutant ($p<0.01$, data not shown). This effect in the *dia* mutant is not caused by decreased numbers of pioneer microtubules in distal regions of the NMJ (Figure 2-9D-E). When we quantify the number of EB1-GFP plus ends in the distal 50µm of the NMJ there is no statistically significant difference comparing wild type and dia^2/dia^2 (plus ends in distal 50µm of NMJ; $elaV^{C155}$*; UAS-EB1-GFP/+* = 20±2.5 compared to $elaV^{C155}$;dia^2*; UAS-EB1-GFP/+* = 22.8±2.0; $p>0.3$). Therefore, we speculate that altered behavior of these pioneer microtubules could be related to the impaired incorporation/stabilization of new microtubules into the bundled, MAP-positive core of microtubules. Live imaging studies have shown that NMJ growth can be achieved, in part, through the addition of new synaptic boutons at the distal end of the NMJ (Zito et al., 1999). Since the integrity of the Futsch-positive microtubules is necessary for

synaptic growth, it is possible that this defect observed in the *dia* and *dlar* mutants contributes to defective synaptic growth.

DISCUSSION

Here we advance our understanding of synaptic growth and development in several fundamental ways. In a forward genetic screen, we identified Diaphanous as an important regulator of synaptic growth. Immunohistochemical data as well as several independent genetic experiments demonstrate that Dia functions presynaptically to influence synaptic growth. We then provide evidence that Dia is necessary for the normal regulation of both the presynaptic actin and microtubule cytoskeletons, including a population of newly characterized dynamic pioneer microtubules. Finally, we provide genetic evidence that Dia functions downstream of the receptor tyrosine phosphatase Dlar. Based upon our data we propose that Dia functions downstream of Dlar and Trio to influence either the formation or maintenance of the synaptic actin and microtubule cytoskeletons. In this way, Dia represents an essential effector that could couple inter-cellular growth related signaling at the synaptic membrane to the regulation of synaptic actin and a dynamic population of synaptic microtubules. It has been proposed that formin proteins such as Dia may be able to coordinate the regulation of the actin and microtubule cytoskeletons. Although our data do not directly address this topic, it is interesting to speculate that synaptic growth might require both actin-mediated membrane extension and a coordinate microtubule-dependent stabilization of newly formed synaptic boutons.

Evidence that Dia functions downstream of Dlar and Trio to control synaptic growth.

A genetic epistasis analysis provides evidence that Dia functions in the same genetic pathway as Dlar and Trio to control synaptic growth. There are strong trans-heterozygous interactions of the *dia* null mutation with mutations in both *dlar* and *trio*. In addition, synaptic growth defects in the *dia; dlar* double mutant are no more severe that that observed in either single mutation alone. The placement of Dia downstream of Dlar is supported by the demonstration that neuronal expression of an activated *diaphanous* transgene rescues NMJ morphology and animal health in the *dlar* mutant background. Furthermore, the placement of Dia downstream of Trio is consistent with the proposed function of Diaphanous related formin proteins as Rho-type GTPase effectors that link signaling at the plasma membrane to the regulated modulation of the underlying cytoskeleton (Palazzo et al., 2004; Wen et al., 2004; Pellegrin and Mellor, 2005). Dlar has been implicated in the mechanisms of synaptic growth in organisms ranging from C. elegans to Drosophila and mammals (Kaufmann et al., 2002; Wyszynski et al., 2002; Dunah et al., 2005). For example, disruption of mammalian Lar signaling has been shown significantly alter synapse and spine morphogenesis in the vertebrate central nervous system (Wyszynski et al., 2002; Dunah et al., 2005; Hoogenraad et al., 2007). However, the means by which Lar might influence the synaptic cytoskeleton were not addressed in these studies. By providing a molecular link between Dlar and the underlying cytoskeleton, Dia may provide an important advance in dissecting the complex function of Lar signaling, and formin signaling, in the nervous system.

Current evidence indicates that Dlar-dependent control of neural development is complex. In systems ranging from C. elegans to mammals, Dlar has been shown to interact both biochemically and genetically with the cytoplasmic protein Liprin-alpha (Zhen and Jin, 1999; Kaufmann et al., 2002; Wyszynski et al., 2002; Dunah et al., 2005; Hoogenraad et al., 2007). Liprin-alpha may be responsible for the regulated trafficking of Dlar to specific sites within the cell (Shin et al., 2003) and thereby influence synapse development. However, genetic analyses demonstrate that Liprin-alpha dependent signaling mediates effects that are more extensive than can be accounted for by loss of *dlar* alone. For example, liprin-alpha mutations strongly perturb active zone architecture and neurotransmission, whereas *dlar* mutations have milder effects on active zone organization and function (Kaufmann et al., 2002). It seems, based on current evidence from diverse systems, that Liprin-alpha function extends to influence the synaptic particle web in a manner that is independent of DLar function (Zhen and Jin, 1999; Kaufmann et al., 2002; Wyszynski et al., 2002; Dunah et al., 2005).

Recently, two studies independently identified ligands for the Dlar receptor in Drosophila (Fox and Zinn, 2005; Johnson et al., 2006). At the Drosophila NMJ, Dlar binds to the heparin sulfate proteoglycans (HSPGs) Dally-like (Dlp) and Syndecan (Sdc) (Johnson et al., 2006). Current analysis indicates that Dlp inhibits Dlar function while Sdc activates Dlar. Interestingly, mutation of Sdc phenocopies the defect in synaptic growth observed in the Dlar mutant, but *sdc* mutants do not have a defect in synaptic transmission, active zone structure or the distribution of synaptic markers (Johnson et al., 2006). Thus, while the regulation of Dlar-mediated signaling may be quite complex, it is possible that the Dlar-dependent synaptic growth is mediated by a specific set of

signaling interactions that include the ligand Sdc and downstream signaling mediated by Trio and Diaphanous.

In Drosophila, unlike mammalian systems, Dlar is specifically presynaptic. Consistently, Dia functions presynaptically to specify NMJ growth and regulation of the presynaptic cytoskeleton. Thus, the Dia-Dlar genetic interaction presumably reflects the action of this signaling pathway in the presynaptic nerve terminal. In other systems, such as mammalian central synapses, LAR is present on both sides of the synaptic terminal and defects in both AMPA receptor clustering and synapse morphogenesis are observed (Wyszynski et al., 2002). It is interesting to speculate that Dia may be involved in synapse morphogenesis downstream of LAR while liprin-alpha related signaling is involved in the control of AMPA receptor abundance and active zone integrity.

Synaptic Pioneer Microtubules and the Control of Synapse Morphology.

The importance of the synaptic microtubule cytoskeleton during synaptic development and neurological disease has been highlighted by many studies (Zhang and Broadie, 2005; Ruiz-Canada and Budnik, 2006). In particular, essential microtubule regulatory proteins are linked to diverse neurological disease including spastic paraplegia and Fragile-X syndrome (Sherwood et al., 2004; Roll-Mecak and Vale, 2005; Zhang and Broadie, 2005). Although defects in the MAP-stabilized microtubules have been interpreted to reflect changes in microtubule dynamics (Roos et al., 2000; Ruiz-Canada et al., 2004), there is no evidence that the Futsch stabilized microtubules represent a dynamic population of microtubules. By labeling microtubule plus ends with EB1-GFP we are able to visualize a population of dynamic pioneer microtubules at the Drosophila

NMJ, allowing us to investigate Diaphanous-mediated regulation of this population during synapse development.

There are two possible models for how Dia-dependent modulation of pioneer microtubules could influence synaptic growth. Dia and other formins have been implicated in microtubule stabilization through plus end binding (Palazzo et al., 2004). We have previously found that pioneer microtubules are evenly distributed throughout the NMJ and probe the cortex of the presynaptic membrane (see previous chapter). One possibility is that Dia-dependent stabilization of the pioneer microtubule plus ends is involved in relaying signaling from the plasma membrane to the microtubule cytoskeleton. Consistent with this hypothesis is the observation that microtubule plus end movement is more rapid in *dia* mutants, potentially disrupting the signaling relay between plasma membrane signaling complexes and the dynamic microtubule plus end. Alternatively, Dia-dependent modulation of pioneer microtubule behavior could influence the consolidation of dynamic microtubules into the MAP-stabilized, Futsch-positive core. Impairment of this process could disrupt NMJ growth. This model is similar to the consolidation of dynamic peripheral microtubules into a MAP-stabilized central domain of the growth cone, a process necessary for growth cone advance (Rodriguez et al., 2003). In either case, our data open up a new avenue of investigation for synaptic development at the Drosophila NMJ.

MATERIALS AND METHODS

Generation of UAS-EB1-GFP Transgenic *Drosophila*:

C-terminal fusion of green fluorescent protein with *Drosophila* EB1 (EB1-GFP) was obtained from Drs. Steve Rogers and Ron Vale (UCSF, unpublished data) and cloned into the pUAST vector using standard methodology. Transgenic *Drosophila* lines were obtained with homozygous viable *UAS-EB1-GFP* transgenes inserted on the second and third chromosomes.

Cell Culture:

All *Drosophila* S2 cell protocols were performed as described in the *Drosophila* Expression System Manual (Stratagene; La Jolla, CA). Briefly, *Drosophila* S2 cells, stably expressing the GAL4 transcription factor, were cultured in Schneider's Medium supplemented with 10% fetal calf serum at 25°C. For RNA mediated knockdown of Diaphanous, cells were incubated in serum free media with 19µg dsRNA against Dia. Cells were incubated in RNA for 5 days prior to transfection with the pUAST-EB1-GFP plasmid using a standard calcium phosphate transfection protocol. Cells were incubated for 48 hrs prior to plating on ConA (0.5 mg/ml stock; Sigma) coated coverslips for live imaging and subsequent analysis (Rogers et al., 2002).

Genetics:

Drosophila were maintained at 25ºC on normal food. The following strains were used in this study: 1) dia^{2}/*CyO-GFP* 2) *Df(2L)TW2/CyO-GFP* 3) $dlar^{5.5}$/*Cyo-GFP* 4) *UAS-HA-*

Dia[ΔNΔC]/TM6 (gift of Purnilla Rørth), 5) *dlar*$^{13.2}$*/CyO-GFP*, 6) *trio*^{1}*/TM6*, 7) *abl*^{1}*/TM6*, 8) *chic*^{221}*/CyO-GFP* 9) *UAS-EB1-GFP* 10) *UAS-GFP-actin*. For CNS expression of *UAS-EB1-GFP,* or *UAS-GFP-actin,* flies were crossed to one of three GAL4 lines: 1) *elaV*^{c155}*-GAL4* (pan neuronal), 2) *OK6-GAL4* (motor neuron specific; Aberle et al., 2002) and 3) *D42-GAL4* (CNS specific; Parkes et al., 1998).

Live imaging and kymograph analysis

Wandering third instar larvae were dissected in HL3 saline (0.5mM Ca^{++}) and stably positioned on glass coverslip using pressure pins held in place using a magnetic surface surrounding the glass slide. EB1-GFP labeled microtubules were imaged using a GFP filter set (Chroma) with a 100x Plan-Apochromat (0.97 NA) oil immersion objective (Zeiss). Images were acquired with a Photometrics CoolSnap HQ cooled CCD camera (Roper Scientific) and Kodak EEV57 back thinned chip (Roper Scientific) mounted on an inverted microscope (Zeiss Axiovert 200). The sample was illuminated using a 100W Xenon light source (Sutter Instruments) and liquid light guide (Sutter Instruments). Images were acquired with a 500ms exposure and 750 ms frame rate. Images were collected at room temperature (18ºC) for a maximum of one hour per preparation. Imaging was controlled by Slidebook software (Intelligent Imaging Innovations).

To generate kymographs for rate analysis, axons in the segmental nerve overlaying muscle four were imaged and the images were deconvolved to remove background fluorescence. A one pixel wide mask was drawn over a length of axon in the first time point this mask was copied to all subsequent frames. The smooth curve analysis function of SlideBook 4 was applied to these masks to generate the kymographs. This function aligns the masked regions from each time point. Any movement that occurs in

the masked region over the time imaged appears as a diagonal line through the kymograph. The slope of this line was measured using Slidebook software to determine the rate of movement. The synapse on muscle four was selected for imaging and analysis as it was possible to image several boutons in the same plane of focus. Puncta in the synapse often took a curved path in a bouton. To generate kymographs for the synapse a mask was created over the specific path of an individual puncta, resulting in a curved line for many of the masks. These masks were then converted to kymographs using the smooth curve analysis function of Slidebook software. For a given segment of axon or synapse, all puncta that remained in the plane of focus for at least 5 frames were analyzed.

Pharmacology

Latrunculin A was dissolved in DMSO to a concentration of 1mM to create a stock. The latrunculin A stock solution was diluted to a range of concentrations in HL3 saline (0.5mM Ca^{++}). Wandering third instar larvae were dissected in HL3 (0.5mM Ca^{++}) and incubated for 15 minutes at room temperature in either DMSO (control) or latrunculin A (experimental). Larvae were then imaged for GFP-actin or EB1-GFP.

Antibody staining:

Primary antibodies used in this study include mAb 22C10 (1:50; obtained from the Developmental Studies Hybridoma Bank, University of Iowa), Cy3 and FITC conjugated HRP (1:200; obtained from ICN/Cappel), anti-brp and mAb3C11 (1:10; obtained form the Developmental Studies Hybridoma Bank). Secondary antibodies used were FITC

labeled anti-mouse (1:200), and Cy3 conjugated anti-mouse (1:200). All secondary antibodies were obtained from ICN/Cappel.

Figure 2-1. Diaphanous is present pre and post-synaptically.

(**A**) Diagram of the *Diaphanous* locus with protein coding sequences (CDS) and untranslated sequences (UTR) indicated. Small deletions associated with the dia^2 and dia^9 mutants are shown (Castrillon and Wasserman, 1994). (**B**) Diagram of Dia protein including the GTP-binding domain (GBD), the coiled-coil region (CC), and the formin homology domains 1 and 2 (FH1 and FH2, respectively). The % a.a. sequence identity between Drosophila Dia protein and the mouse Dia2 protein (mDia2) is indicated. (**C**) Immuno-fluorescent image of a 3rd instar NMJ from wild type (left two panels) and a dia^2 larva (right two panels) stained with anti-Dia (top) and anti-HRP (bottom). The arrow indicates Dia staining of putative endosomes post-synaptically. Note that staining is nearly absent at the dia^2 mutant NMJ. (**D**) Three-dimensional imaging demonstrates colocalization of Dia protein (left panel) and the Futsch protein (center panel) within a single presynaptic bouton. Right panel represents a merged image of the staining of the Dia and Futsch proteins. Arrow indicates Dia protein closely associated with presynaptic Futsch bound microtubules. Insets above represent the z-axis cut as a horizontal line through the indicated Dia puncta (arrow). Insets to the left represent the z-axis cut as a vertical line through the same puncta.

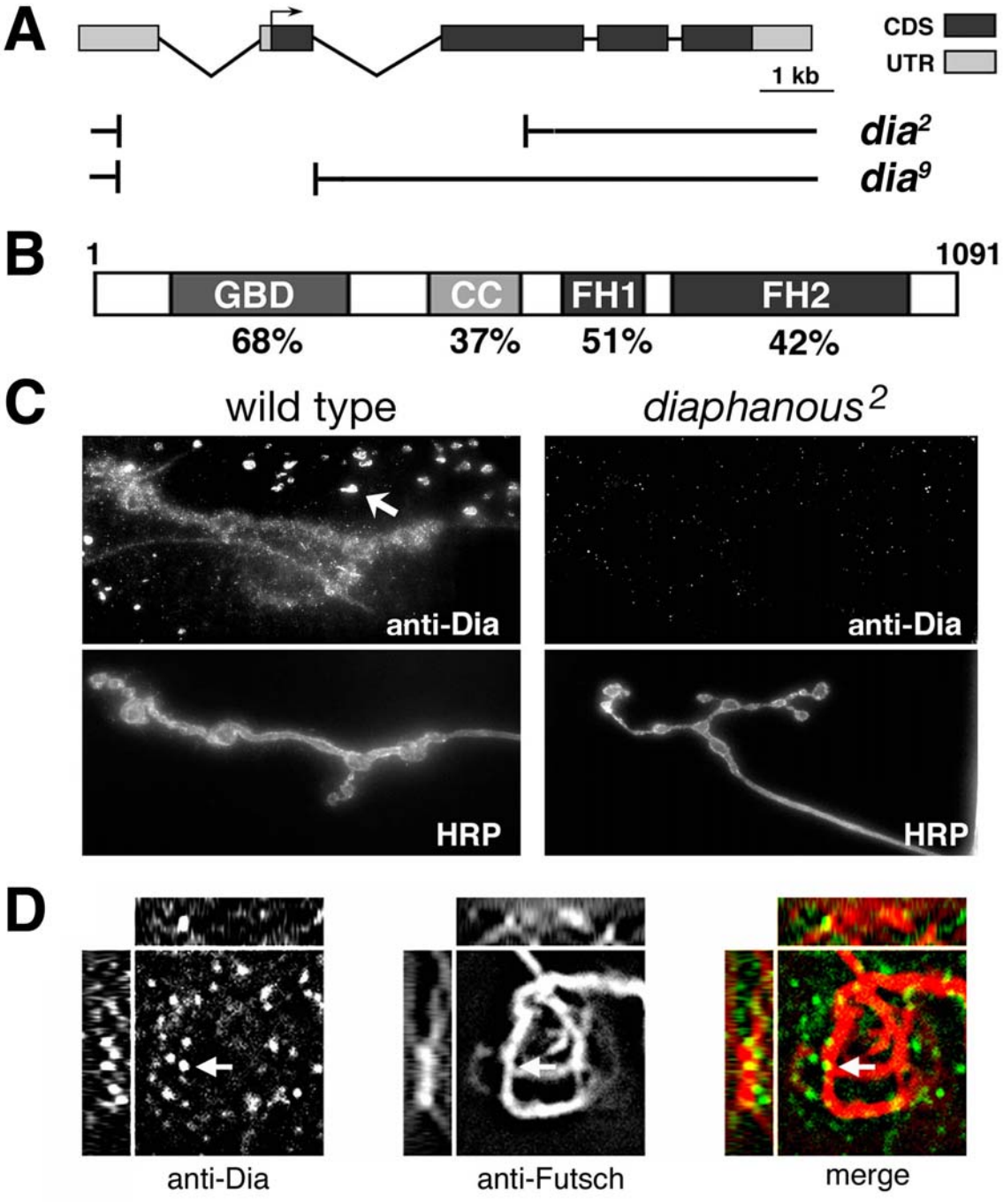
A
CDS
UTR
1 kb
dia2
dia9
B
1
1091
GBD
CC
FH1
FH2
68%
37%
51%
42%
C
wild type
diaphanous2
anti-Dia
anti-Dia
HRP
HRP
D
anti-Dia
anti-Futsch
merge

Figure 2-2. *Diaphanous* is required presynaptically for normal synaptic growth.

(A-E) Immuno-fluorescent images of 3rd instar NMJs on muscles 6/7 (**A, B**) or muscle 4 (**C, D, E**) from wild type (**A, C**), $dia^{2/2}$ mutants (**B, D**), or presynaptic *dia* rescue animals (**E**). The $dia^{2/2}$ mutant phenotypes are rescued by presynaptic expression of $UAS\text{-}Dia^{Act}$ in the $dia^{2/2}$ background using a neuronal (*elaV-GAL4*) driver (**E**). Synapses were stained using the anti-HRP antibody. Scale bar=20μm. (**F**) Quantification of number of boutons per NMJ normalized to wild type synapses. Error bars represent SEM.

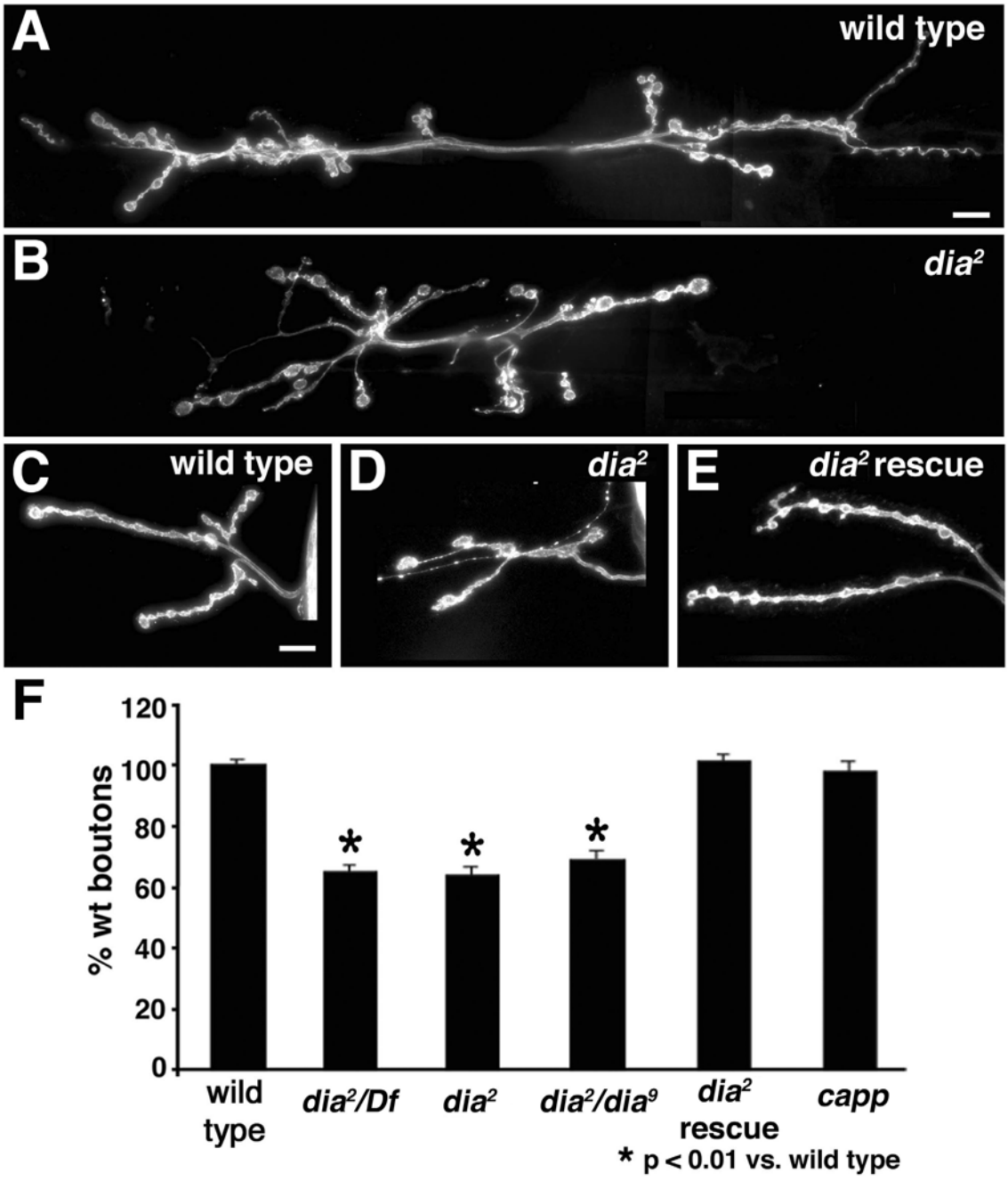
A
wild type
B
dia2
C
wild type
D
dia2
E
dia2 rescue
F
% wt boutons
120
100
80
60
40
20
0
*
*
*
wild type
dia2/Df
dia2
dia2/dia9
dia2 rescue
capp
* p < 0.01 vs. wild type

Figure 2-3. Diaphanous regulates the presynaptic actin cytoskeleton.

Representative projections from larval NMJs expressing an actin-GFP transgene in either a wild type (**A, B**), a *dia*$^{2/2}$ mutant animal (**C, D**), and a *dlar*$^{5.5}$ mutant animal (**E, F**). Images show either a live image of actin-GFP or the same NMJ following fixation and staining with anti-HRP to reveal the presynaptic membrane, as indicated. (**G)** Graph represents the number of synaptic actin foci divided by the number of boutons. Error bars represent SEM. Scale bar = 10 μm, panel B.

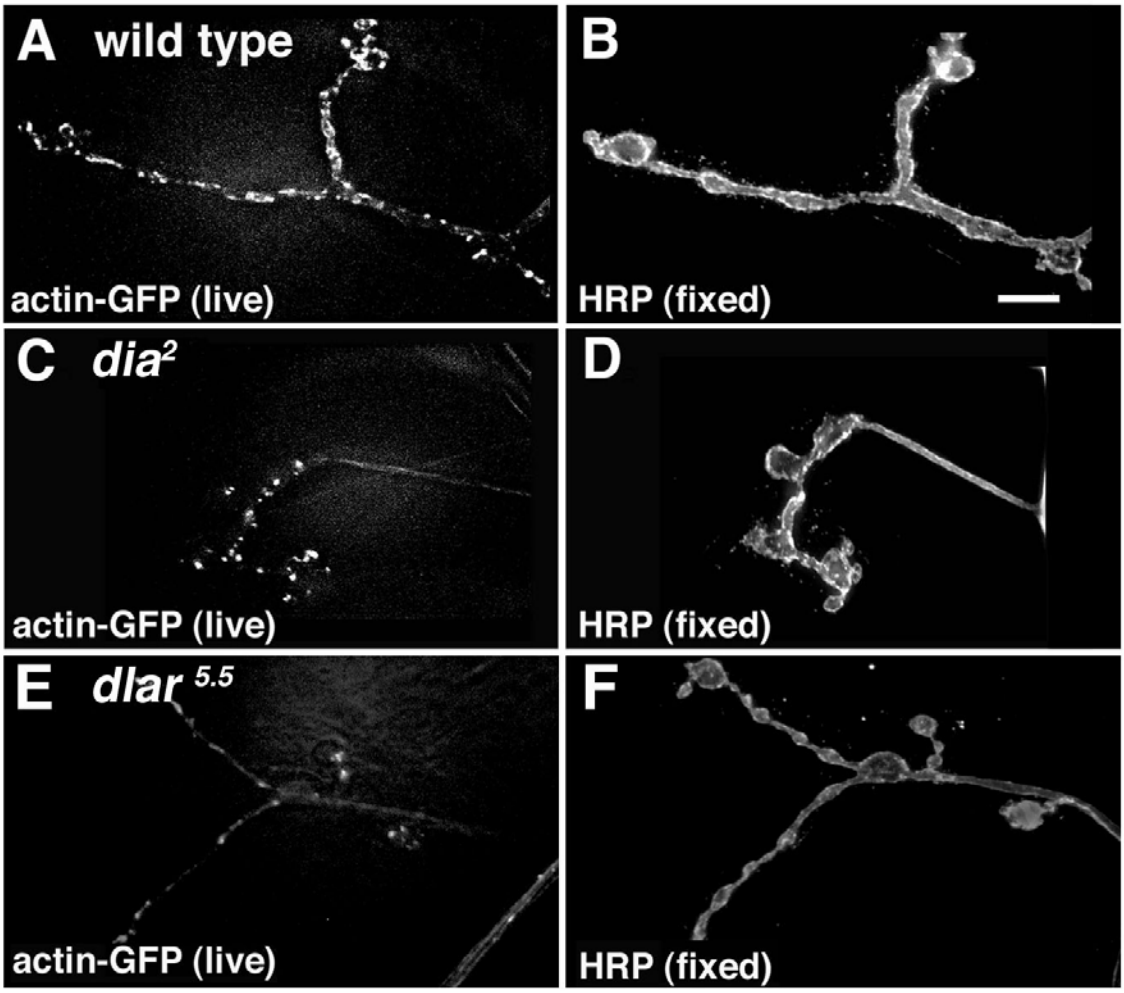
A wild type
actin-GFP (live)
B
HRP (fixed)
C dia2
actin-GFP (live)
D
HRP (fixed)
E dlar 5.5
actin-GFP (live)
F
HRP (fixed)

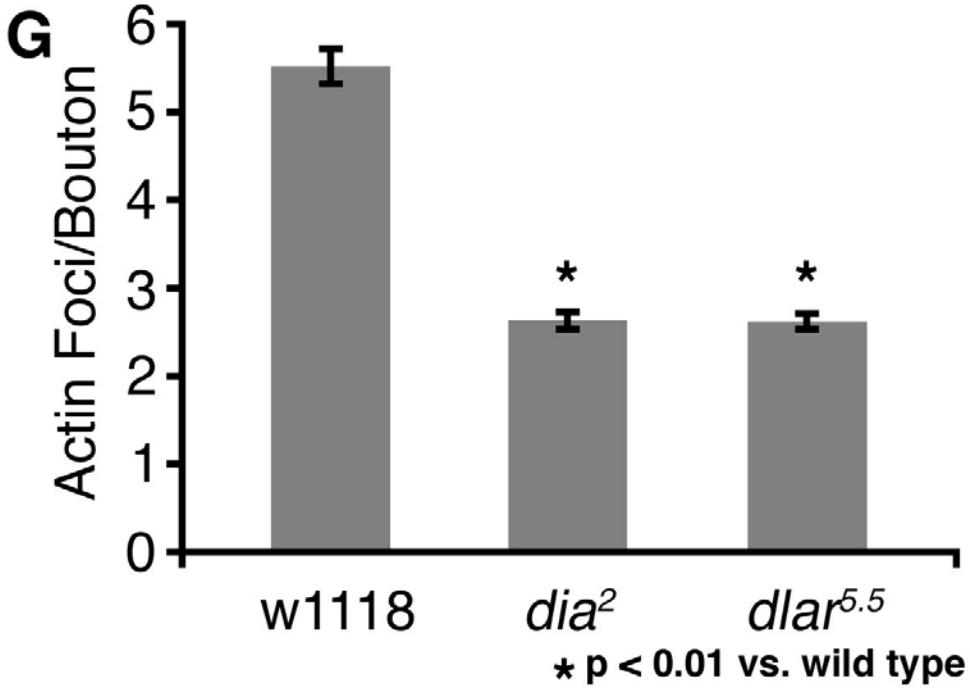
G
Actin Foci/Bouton
0
1
2
3
4
5
6
*
*
w1118
dia2
dlar5.5
* p < 0.01 vs. wild type

Figure 2-4. Genetic Epistasis analysis of *dia* with *dlar* and *trio*.

(**A-F**) Immuno-fluorescent images of 3rd instar m4 NMJs from wild type (**A**), $dlar^{5.5}$/+ (**B**), $dlar^{5.5}$-dia^{2}/$dlar^{5.5}$-dia^{2} (**C**), dia^{2}/+; *trio*/+ (**D**), $dlar^{5.5}$/dia^{2} (**E**), $dlar^{5.5}$/+; $trio^{1}$/+ (**F**). Synapses were stained with the neuronal membrane marker HRP (green) and synaptic vesicle marker synapsin (red). Scale bar, 10μm. (**G**) Quantification of bouton number in control, transheterozygous and recombinant synapses. Wild type and heterozygous control genotypes are shown in dark gray bars, genetic combinations that showed an interaction with *dia* are shown in red, genetic combinations that showed no interaction with *dia* are shown in light gray. In all genotypes, bouton number was normalized to wild type.

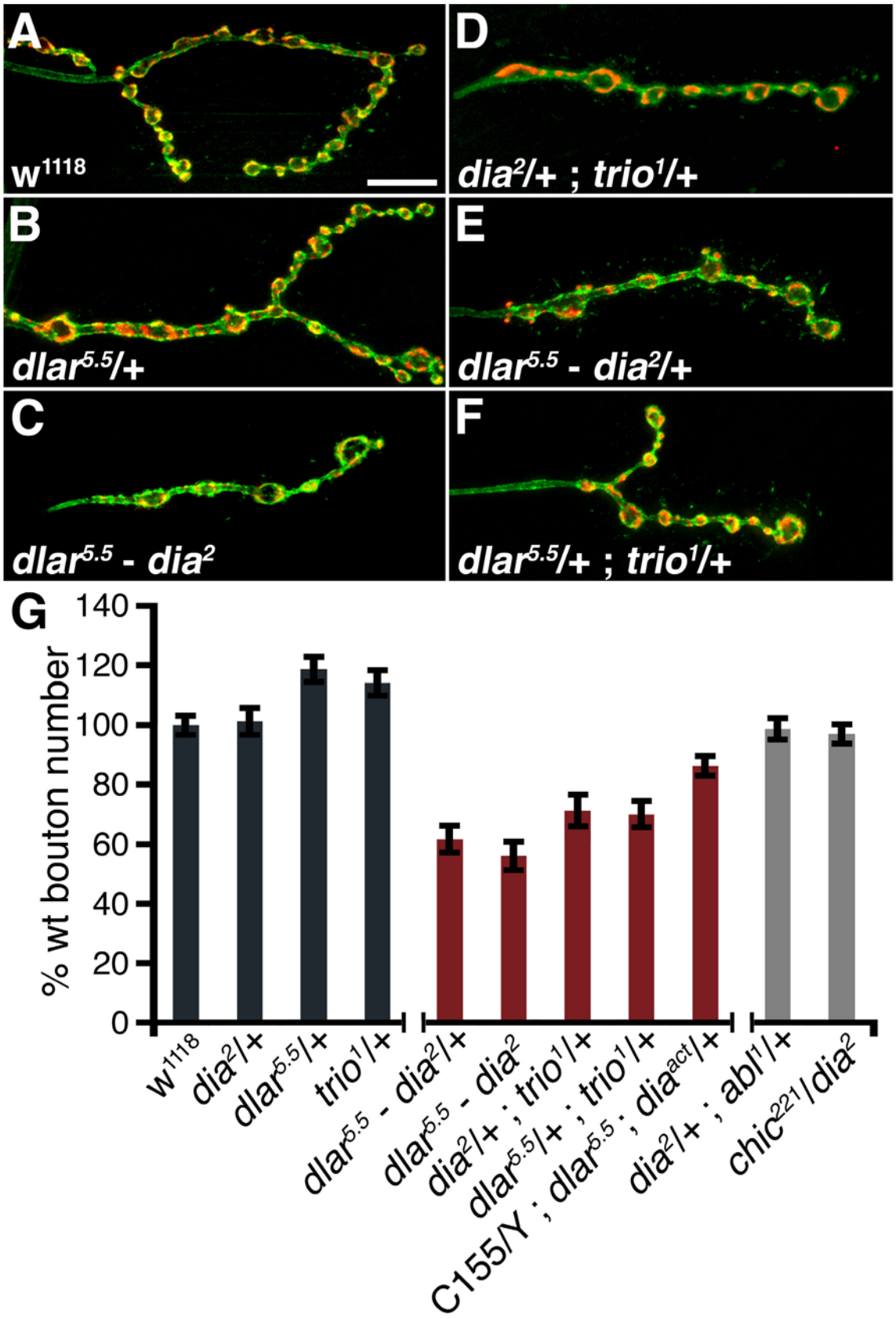
A
w1118
D
dia2/+ ; trio1/+
B
dlar5.5/+
E
dlar5.5 - dia2/+
C
dlar5.5 - dia2
F
dlar5.5/+ ; trio1/+
G
% wt bouton number
0
20
40
60
80
100
120
140
w1118
dia2/+
dlar5.5/+
trio1/+
dlar5.5 - dia2/+
dlar5.5 - dia2
dia2/+ ; trio1/+
dlar5.5/+ ; trio1/+
C155/Y ; dlar5.5 ; diaact/+
dia2/+ ; abl1/+
chic221/dia2

Figure 2-5. Activated *diaphanous* rescues synaptic growth in *dlar* mutant larvae.

(**A-C**) Immuno-stained images of the NMJ at muscle 4 from mutant $dlar^{5.5}/dlar^{13.2}$ (**A**), $C155/+; dlar^{5.5}/dlar^{13.2}; dia^{act}/+$ (**B**), and wild type (**C**). NMJ were stained with the α-DV-glut antibody to visualize the presynaptic nerve terminal. Scale bar=10μm. (**D**) Quantification of bouton number at muscle 4, normalized to wild type ($dlar^{5.5}/dlar^{13.2}$ = 56.94±2.85% of wild type, n=22; $C155/+; dlar^{5.5}/dlar^{13.2}; dia^{act}/+$ = 86.29±3.27% of wild type, n=22). (**E**) Quantification of number of boutons per m6/7 NMJ normalized to wild type synapses. $dlar^{5.5}/dlar^{13.2}$ = 41.0±3.98% of wild type, n=18. $dlar^{5.5}/dlar^{13.2}$ rescue=85.77±5.04% of wild type, n=18. Error bars represent SEM.

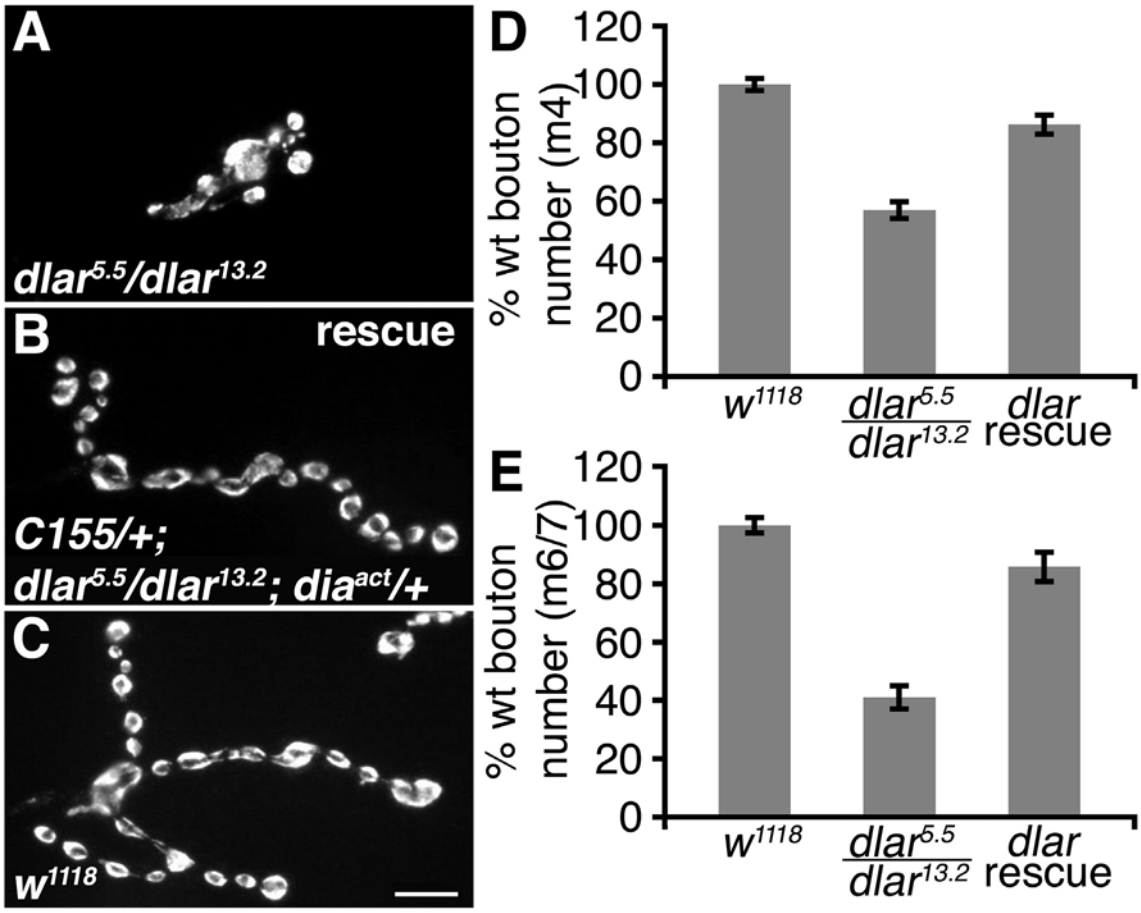
A
dlar5.5/dlar13.2
B
rescue
C155/+;
dlar5.5/dlar13.2; diaact/+
C
w1118
D
% wt bouton number (m4)
120
100
80
60
40
20
0
w1118
dlar5.5/dlar13.2
dlar rescue
E
% wt bouton number (m6/7)
120
100
80
60
40
20
0
w1118
dlar5.5/dlar13.2
dlar rescue

Figure 2-6: Microtubule plus end movement rates are altered in *diaphanous*.

(**A, B**) Projections of time-lapse series illustrate the displacement of EB1-GFP labeled microtubule plus-ends for axons in wild type (**A**) and dia^2/dia^2 (**B**) over 30s. Arrowheads mark the start and end of displacement over the period of imaging. Scale bar=5μm. (**C**) Histogram of the EB1-GFP puncta velocities within the axons in wild type (diamonds) and dia^2/dia^2 (squares). There is a significant increase in the EB1-GFP puncta velocities in the dia^2/dia^2 compared to wild type (wild type = 4.12μm/min $\pm$ 0.038, n=1121; dia^2/dia^2 =5.62μm/min $\pm$0.09, n=687). Statistical significance was determined by Kolmogorov-Smirnov and Student's T-tests to a 99% confidence interval. (**D** and **E**) Projections of time-lapse series illustrate the displacement of the EB1-GFP labeled plus-ends at the NMJ of wild type (**D**) and dia^2/dia^2 (**E**) over a 30s interval. Arrowheads mark the start and end of displacement over the period of imaging. Scale bar=5μm. (**F**) Histogram of the EB1-GFP puncta velocities within the synapses as in (**C**). There is a significant increase in the EB1-GFP puncta velocities in the dia^2/dia^2 compared to wild type (wild type = 4.66μm $\pm$ .11, n=337; dia^2/dia^2 = 6.71μm/min $\pm$ 0.13, n=539). (**G**) Representative projection images of time-lapse images acquired in a wild type S2 cell transfected with EB1-GFP. (**H**) Image as in (**G**) for an S2 cell treated with dsRNA against *diaphanous*. Scale bars=10μm. (**I**) Histogram of the EB1-GFP puncta velocities in control S2 cells (diamonds) and *dia* dsRNA treated S2 cells (squares). There is a significant increase in the velocities of puncta in the dsRNA compared to the control cells (control= 6.9μm/min $\pm$ 0.25, n=189; Dia dsRNA knockdown= 10.9μm/min $\pm$ 0.31, n=256).

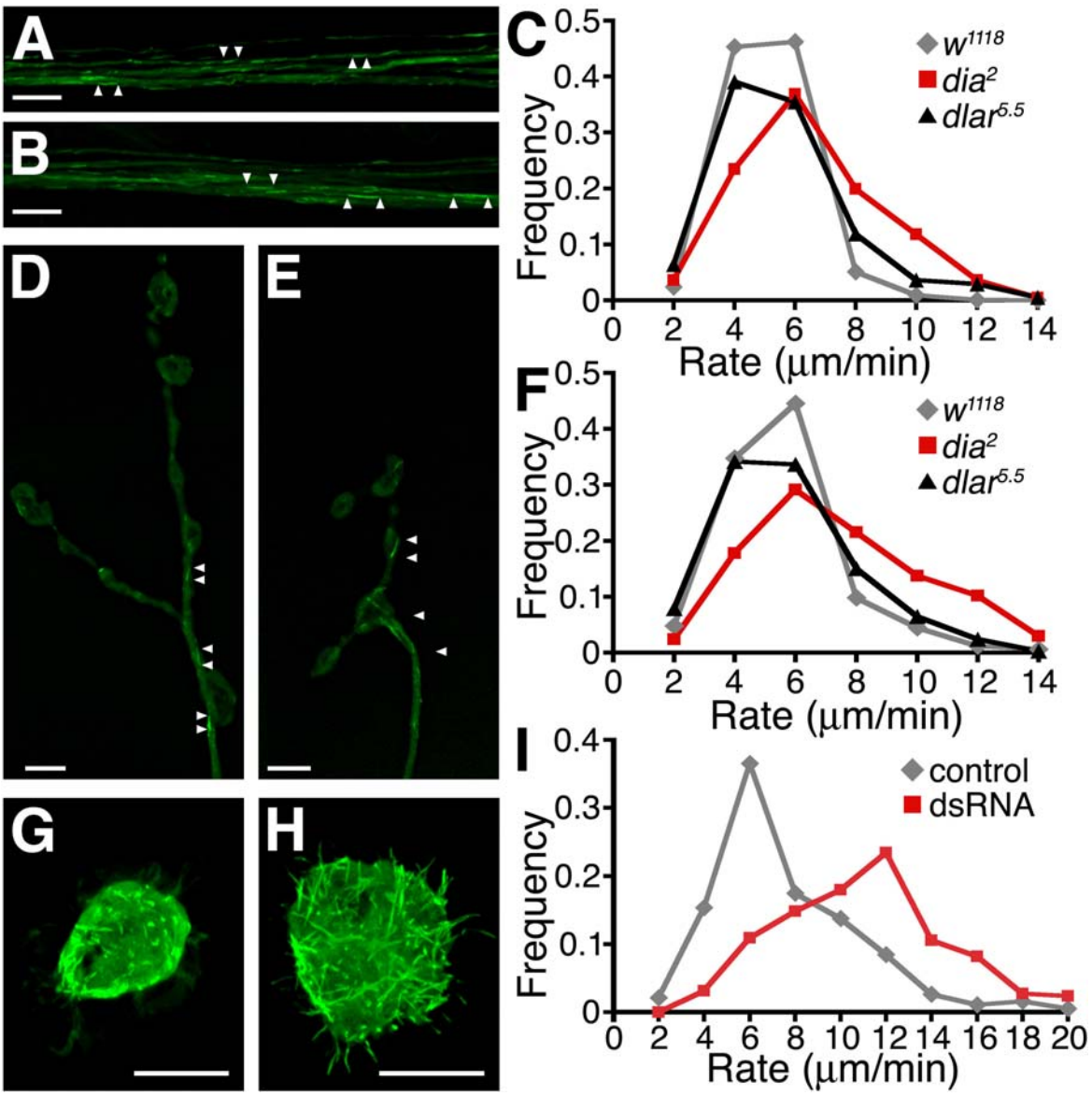
A
B
C
D
E
F
G
H
I
Frequency
Rate (µm/min)
w1118
dia2
dlar5.5
control
dsRNA

Figure 2-7: Behavior of synaptic microtubule plus-ends is not altered by disruption of synaptic actin.

(**A,B**) Representative images of 3rd instar m4 NMJs in animals expressing UAS-GFP-actin driven by *elavGAL4^{C155}* incubated in vehicle (DMSO) alone (**A**) or in 7.5μM latrunculinA (B). (**C**,**D**) Representative projections of time-lapse images at m4 in animals expressing *UAS-EB1-GFP* driven by *elavGAL4^{C155}* incubated in vehicle alone (**C**) or in 7.5μM latrunculinA (**D**)**.** Arrowheads highlight the paths of individual EB1-GFP puncta over the same time frame. Scale bars=5μm**.** (**E**) Average EB1-GFP puncta velocities in DMSO (gray bars) and latrunculin A (red bars) treated animals for the concentrations tested (2.5μM: DMSO=3.18±0.08 μm/min, n=194. LatA=3.34±0.1 μm/min, n=136, p-value=0.23. 5μM: DMSO=3.3±0.05 μm/min, n=351. LatA=3.44±0.06 μm/min, n=340, p-value=0.07. 7.5μM: DMSO=3.04±0.05 μm/min, n=368. LatA=2.99±0.05 μm/min, n=291, p-value=0.57. 10μM: DMSO=2.92±0.05 μm/min, n=254. LatA=2.62±0.05 μm/min, n=217, p-value=$3.6x10^{-5}$). There is no significant difference in the average puncta velocity at most of the concentrations tested. At 10μM latrunculinA, EB1-GFP movement is slightly but significantly (*) slower than vehicle alone. Statistical significance was determined by Student's T-test.

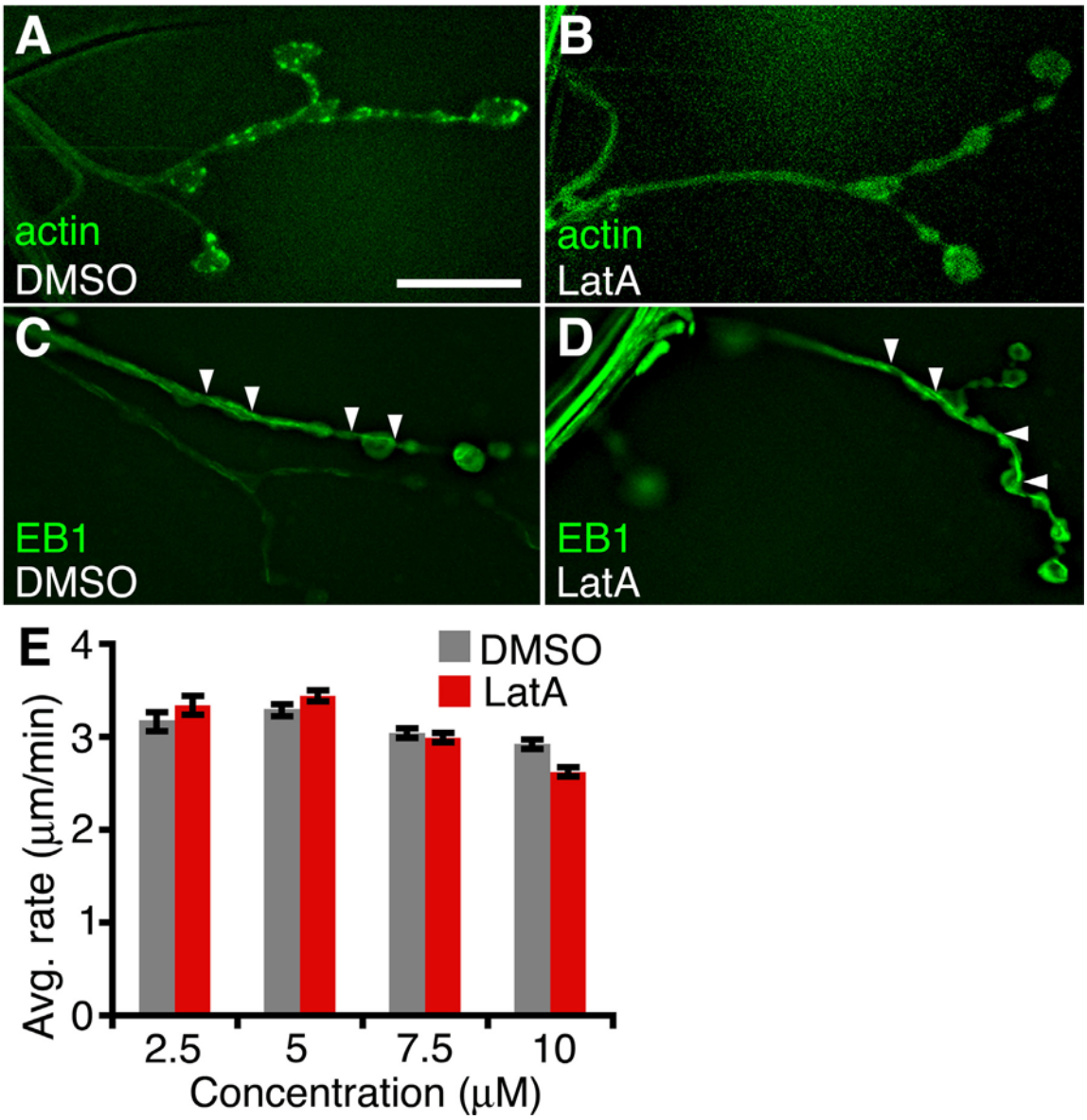
A
actin
DMSO
B
actin
LatA
C
EB1
DMSO
D
EB1
LatA
E
DMSO
LatA
Avg. rate (µm/min)
0
1
2
3
4
2.5
5
7.5
10
Concentration (µM)

Figure 2-8: The density of stable microtubules is disrupted at *dia* mutant synapses.

(**A** and **B**) Immuno-fluorescent image of 3rd instar NMJ at muscle 4 from wild type (**A**) and dia^2/dia^2 (**B**) larvae. Stable microtubules labeled by the 22C10 antibody are shown in red, presynaptic membrane is labeled with the HRP antibody shown in green. Scale bar=10μm. Shown next to each panel is the magnified and isolated 22C10 staining from the distal 50μm of each NMJ (rotated 90º counterclockwise). The region shown in inset is highlighted by brackets in the image at left. (**C**) Quantification of 22C10 average staining intensity in wild type and dia^2/dia^2 m4 synapses. (**D-E**) EB1-GFP puncta are shown in a projected image of wild type (**D**) and dia^2/dia^2 (**E**) over a 30 s interval.

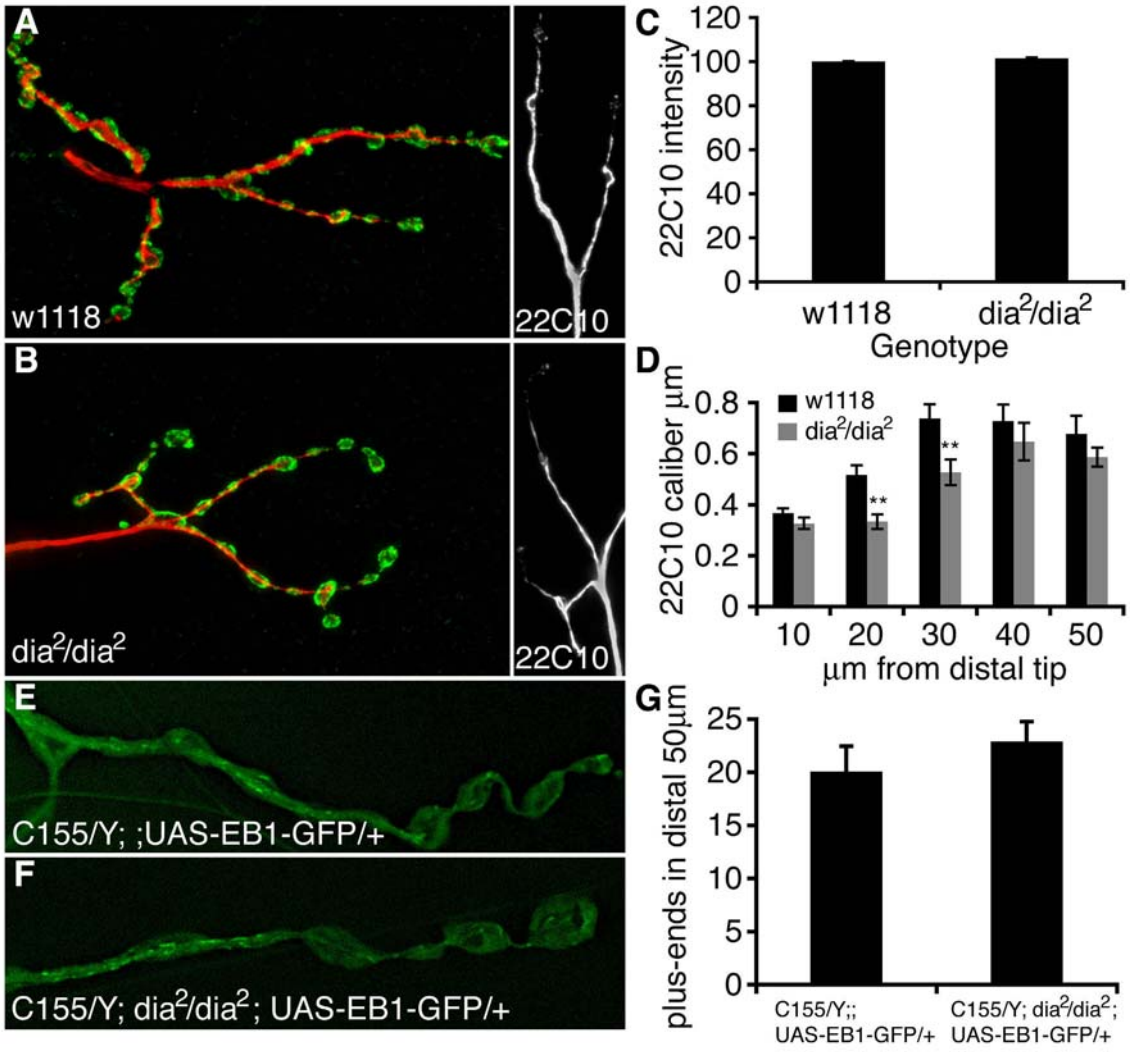
A
w1118
22C10
B
dia2/dia2
22C10
C
22C10 intensity
120
100
80
60
40
20
0
w1118
dia2/dia2
Genotype
D
22C10 caliber µm
0.8
0.6
0.4
0.2
0
w1118
dia2/dia2
**
**
10
20
30
40
50
µm from distal tip
E
C155/Y; ;UAS-EB1-GFP/+
F
C155/Y; dia2/dia2; UAS-EB1-GFP/+
G
plus-ends in distal 50µm
25
20
15
10
5
0
C155/Y;;
UAS-EB1-GFP/+
C155/Y; dia2/dia2;
UAS-EB1-GFP/+

Table 2-1: Pupation, eclosion, and wing inflation defects in *Lar* mutant backgrounds

Genotype[a]	larvae seeded[b]	# pupae	# adults	wing defects[c]	% pupation[d]	% eclosed[e]	% wing defective[f]
C155/+; $Lar^{13.2}$/+	116	115	115	0	99.1	100	0
C155/+; $Lar^{5.5/13.2}$	96	79	25	25	82.3	31.6	100
C155/+; $Lar^{5.5/13.2}$; UAS-Dia^{act}/+	113	110	99	7	97.4	90	6.1

[a]Strains generated by crossing virgin *C155-elavGal4; $Lar^{13.2}$/ Cyo-GFP* flies to either w^{1118}, *$Lar^{5.5}$/ Cyo-GFP,* or *$Lar^{5.5}$/Cyo-GFP; UAS-Dia^{act}*. Desired *Lar* mutant backgrounds were selected from the progeny based on the lack of GFP expression.
[b]1st and 2nd Instar larvae of the indicated genotypes were isolated and raised on apple plates seeded with yeast paste at 25°C.
[c]Represents the number of adults with uninflated wings, determined by inspection of adults 24h post-eclosion for wing inflation defects.
[d]Determined by dividing the number of pupae formed by the number of larvae selected.
[e]Determined by dividing the number of eclosed adults by the number of pupae formed. It should be noted that pharate pupae accounted for 95.5% of the observed pupal lethality.
[f]Determined by dividing the number of adults with uninflated wings by the total number of eclosed adults.

Kin-DAD: A formin-activating construct that disrupts the microtubule cytoskeleton and NMJ growth.

INTRODUCTION

The normal development and remodeling of synaptic connections requires the precise regulation of both the microtubule and actin cytoskeletons. Despite the clear importance of both cytoskeletal elements, few proteins have been identified that are capable of coordinating the regulation of both actin and microtubules during synapse development.

The proteins from the formin family are well known regulators of the cytoskeleton (Palazzo et al., 2001; Wallar and Alberts, 2003; Eng et al., 2006). Classical formins are known to regulate actin, generally by promoting nucleation and growth of unbranched actin filaments (Pruyne et al., 2002; Sagot et al., 2002; Evangelista et al., 2003; Kovar and Pollard, 2004; Wallar et al., 2006). Recent work however, has demonstrated that Diaphanous and related formin proteins (DRFs) also have an important role in regulating microtubules (Ishizaki et al., 2001; Palazzo et al., 2001; Eng et al., 2006; Bartolini et al., 2008; DeWard and Alberts, 2008). Specifically, members of this family have been demonstrated to regulate the generation of a subset of stable microtubules in response to signaling through the Rho type GTPases (Ishizaki et al., 2000; Palazzo et al., 2001; Wen et al., 2004). The ability of formin family proteins to regulate both the actin and microtubule cytoskeletons in response to intercellular signaling raises intriguing questions about the potential role of DRF proteins in synaptic development.

Recent work has identified the formin protein Diaphanous as being an important regulator of synapse growth at the *Drosophila* NMJ (See previous chapter). Genetic disruption of either *diaphanous* or its putative upstream regulator *dlar*, results in a

significant decrease in bouton number at the NMJ (See Figure 2-2, 2-4). This defect appears to correlate with disruptions in cytoskeletal regulation. For example, there is a significant reduction in polymerized actin observed at the NMJ in a *diaphanous* null background. In addition, Diaphanous regulates the behavior and organization of synaptic microtubules. Live-imaging of EB1-GFP, a marker of dynamic microtubules, demonstrated that microtubule growth is significantly enhanced in a *diaphanous* null background relative to wild type. Further evidence suggests that Dia may play a role in stabilizing dynamic microtubules at the NMJ. These results clearly demonstrate that Diaphanous mediated regulation of the synaptic cytoskeleton is essential for synapse development.

To further probe the role of Diaphanous and potentially other DRFs at the NMJ a formin activating construct was designed. Expression of this activator, termed Kin-DAD, resulted in disruption of the morphology and growth of the synapse. Interestingly this phenotype is not ameliorated by Kin-DAD expression in a Dia null background, suggesting that there are other formin proteins involved in regulated synapse growth. Further, microtubule organization and behavior are dramatically altered in the presence of Kin-DAD. Surprisingly very little effect was observed on the actin cytoskeleton, suggesting that actin regulation is not the main role of the Kin-DAD target.

Materials and Methods

Genetics:

Drosophila strains were maintained at 25ºC on normal food. The following strains were used in this study: 1) *dia*^{2}*/CyO-GFP* 2) *UAS-Kin-DAD/TM6* 3) *dia*^{2}*/CyO-GFP; UAS-Kin-DAD-UAS-EB1-GFP/TM6* 4) *UAS-actin-GFP; UAS-Kin-DAD/TM6* and 5) *elaV-Gal4*^{C155}.

Generation of pUAS-Kin-DAD construct:

To create the Kin-DAD construct primers containing the DAD sequence fused at the 3' end with the FLAG epitope were generated and are listed below. EcoRI and XhoI half sites were included in the primers, shown in bold below. This allowed direct ligation of the annealed primers into EcoRI-XhoI digested pBS-Kinesin (VanBerkum and Goodman, 1995), a plasmid containing the isolated motor domain of kinesin. The resulting Kin-DAD-Flag fragment was inserted into pUAST according to standard methodology. Transgenic *Drosophila* lines were obtained with *UAS-Kin-DAD* transgenes inserted on the first and third chromosomes and were placed over balancer chromosomes.

DADFLAG1 5':

(phosp)**AATTC**TGGGCGTGATGGACAGTCTGTTGGAGGCGCTGCAAACGGGCT

CAGCCTTTGACTACAAAGACGATGA CGACAAGTAGC

DADFLAG2 3': **TCGAG**CTACTTGTCGTCATCGTCTTTGTAGTCAAAGGCTGAG

CCCGTTTGCAGCGCCTCCAACAGACTGTCCATCACGCCCAG (phosp).

Antibody staining:

Primary antibodies used in this study include mAb 22C10 (1:50; obtained from the Developmental Studies Hybridoma Bank, University of Iowa), Cy3 conjugated HRP (1:200; obtained from ICN/Cappel), anti-Flag (1:50 obtained from Sigma), anti-α-tubulin (1:200 obtained from Sigma). Secondary antibodies used were FITC labeled anti-mouse (1:200), and Cy5 conjugated anti-rabbit (1:200). All secondary antibodies were obtained from ICN/Cappel.

Live imaging and path trace analysis:

Wandering third instar larvae were dissected in HL3 saline (0.5mM Ca^{++}) and stably positioned on glass coverslip using pressure pins held in place using a magnetic surface surrounding the glass slide. EB1-GFP labeled microtubules were imaged using a GFP filter set (Chroma) with a 100x Plan-Apochromat (0.97 NA) oil immersion objective (Zeiss). Images were acquired with a Photometrics CoolSnap HQ cooled CCD camera (Roper Scientific) and Kodak EEV57 back thinned chip (Roper Scientific) mounted on an inverted microscope (Zeiss Axiovert 200). The sample was illuminated using a 100W Xenon light source (Sutter Instruments) and liquid light guide (Sutter Instruments). Images were acquired with a 500ms exposure and 750 ms frame rate. Images were collected at room temperature (18ºC) for a maximum of one hour per preparation. Imaging was controlled by Slidebook software (Intelligent Imaging Innovations).

Path traces of individual EB1-GFP puncta were generated using the Multi-Track application of ImageJ. Only puncta present for the majority of the imaging session were selected for this analysis to allow a representative view of the plus end movement.

Cell Culture:

All *Drosophila* S2 cell protocols were performed as described in the *Drosophila* Expression System Manual (Stratagene; La Jolla, CA). Briefly, *Drosophila* S2 cells, stably expressing the GAL4 transcription factor, were cultured in Schneider's Medium supplemented with 10% fetal calf serum at 25°C. Transfection of S2 cells with the pUAST-Kin-DAD plasmid and DS-Red was accomplished using a standard calcium phosphate transfection protocol. Cells were incubated for 24 hrs prior to plating on ConA (0.5 mg/ml stock; Sigma) coated coverslips for staining and subsequent analysis (Rogers et al., 2002).

RESULTS

The defining feature of the Diaphanous related formin family is the presence of a C-terminal autoinhibitory domain and an N-terminal activation domain. Prior to activation of the protein the C-terminal Diaphanous autoinhibitory domain (DAD) is bound to the N-terminal GTPase binding domain (GBD) (Alberts, 2001; Otomo et al., 2005). This interaction blocks the interactions of profilin, actin and other FH1 and FH2 domain binding proteins, with DRFs (Sagot et al., 2002; Higgs, 2005). Upon stimulation, an active Rho-type GTPase binds to the N-terminal GBD. This interaction displaces the intra-molecular GBD-DAD interaction, thereby revealing the FH1 and FH2 domains to their cellular binding partners. Together these domains mediate the actin regulatory abilities common to formin proteins (Sagot et al., 2002; Kovar and Pollard, 2004; Romero et al., 2004; Higgs, 2005; Pellegrin and Mellor, 2005). Thus, manipulation of this intra-molecular interaction provides a possible mechanism by which to activate formin proteins in a given tissue. Indeed, a number of studies in mammalian cell culture have made use of the expression of an isolated DAD peptide to activate Diaphanous homologs mDia1 and mDia2 (Eng et al., 2006). The exogenous DAD peptide acts in place of an activated Rho-GTPase, binding in trans to the GBD of the endogenous Dia protein. The expression of an exogenous DAD peptide therefore acts to constituitively activate the endogenous Diaphanous protein by blocking the intra-molecular inhibitory interaction. However, it is noteworthy that the presence of a GBD and DAD domain are common to all members of the DRF sub-family. It is therefore likely that systemic

expression of an isolated DAD peptide would activate not only Diaphanous, but also any other DRFs present.

To utilize the ability of the isolated DAD domain to activate endogenous DRFs, a transgenic construct was designed and expressed in Drosophila motoneurons. The isolated DAD domain was amplified from a full *diaphanous* cDNA. The resulting fragment was placed under the control of the UAS promoter to allow for tissue specific and temporal regulation of expression (Brand and Perrimon, 1994). Additionally, a Flag epitope was added to the C-terminus of the peptide to allow for visualization of the localization of the peptide, as well as to indirectly monitor the activation of DRFs. Finally, the DAD peptide was fused to the motor domain of the plus-end directed microtubule motor, kinesin, to ensure the protein localized to the synapse. This modification allows for the efficient delivery of the peptide to the synapse, as microtubules within the axon and synapse are highly polarized with their plus-ends directed away from the cell body. To study the role of DRFs in synapse development, this construct was used to create transgenic *Drosophila* lines.

Kin-DAD Expression Alters Microtubule Organization *in vitro.*

The cellular activity of the Kin-DAD construct was first tested by expression in S2 cell culture. As a means of identifying positively transfected cells a DS-red construct was co-transfected into the culture. Cells were collected and stained at various time points following transfection according to the methods of Rogers et al. (2002). Expression of the Kin-DAD construct in S2 cells proved highly cytotoxic as few DS-red and Kin-DAD positive cells could not be identified more than 24 hours post-transfection.

Additionally, at 24 hours post-transfection, many of the Kin-DAD positive cells were unhealthy and failed to form a lamella or adhere to coverslips for imaging (Rogers et al., 2002). The high level of cell death in the presence of the Kin-DAD construct precludes live imaging of these cells.

It was next of interest to examine the effect of DRF activation on the cytoskeleotn of S2 cells. In mammalian cells, activation of mDia has been shown to lead to the generation of a subset of stable microtubules (Ishizaki et al., 2001; Palazzo et al., 2001, 2004; Wen et al., 2004; Eng et al., 2006, Bartolini et al., 2008, DeWard and Alberts 2008). Further, RNAi mediated knockdown of Dia in S2 cells was recently shown to disrupt microtubule regulation (See previous chapter, Figure 2-6). For these reasons it was of particular interest to examine the effects of Kin-DAD on the microtubule cytoskeleton. To this end cells were fixed and stained with α-tubulin antibody after 24 hours of expression. Tubulin staining in non-transfected control cells displayed the mesh-like microtubule array typically observed in S2 cells prepared for imaging (Rogers et al., 2002) (Figure 3-1B). This array was severely disrupted in the presence of the Kin-DAD construct. In these cells individual microtubules were not observed. Rather, microtubules were tightly bundled into structures resembling the spokes of a wheel originating at the cell center, presumably within the microtubule organizing center, and terminating with a tangle or knot at the cell periphery (Figure 3-1C). This morphology was never observed in non-transfected cells. As an additional control, the kinesin motor domain alone was expressed in S2 cells to determine whether the disruption in the microtubules was due to this domain. In these cells the organization of the microtubule array was unaffected (data not shown). These data are consistent with the hypothesis that DRF family proteins play

an important role in regulating the microtubule cytoskeleton within isolated cells. It was next of interest to examine the role of this family within the context of the development of the NMJ.

Kin-DAD Expression Disrupts Synapse Growth.

Presynaptic expression of a UAS-Kin-DAD construct under the control of the *elaV-Gal4*^{C155} driver resulted in changes in the growth and morphology of the synapse. Morphologically the Kin-DAD synapse appeared significantly undergrown compared to wild type (Figure 3-1D, F). Quantification of bouton number at muscle four confirmed that bouton number was significantly decreased in this background (Figure 3-1H). The expression of Kin-DAD also resulted in a dramatic change in the overall morphology of the synapse. Specifically, the uniformity of bouton architecture was disrupted in the presence of Kin-DAD (compare Figure 3-1D with Figure 3-1F). A typical wild type NMJ consists of spherical boutons with largely regular size and shape. Apart from nascent bouton buds, typically found at the distal terminus, little variation in the average area of boutons at a wild type NMJ is observed (Figure 3-1D) (Marie et al., 2004). In contrast the Kin-DAD NMJs are typified by the presence of an enlarged bouton (Figure 3-1F, asterisks) followed by a string of unusually small boutons (Figure 3-1F arrow). Quantification of the variance in bouton size in both backgrounds reveals a significantly wider range of bouton size in larvae expressing Kin-DAD (wild type variance=17.4, n=516: Kin-DAD variance=76.6, n=343. $F<0.001$). Analysis of the distribution of bouton sizes revealed a shift to smaller boutons in Kin-DAD relative to wild type synapses, with approximately half off all the boutons in Kin-DAD synapses falling below

$2\mu m^2$ (Figure 3-1I). Immuno-staining of the NMJ reveals these smaller boutons may be functional as they are positive for brp staining and oppose GluRIIA staining (not shown).

To address the specificity of Kin-DAD activity the construct was expressed in the *dia*^{2} null and wild type backgrounds. If the only synaptic target of the Kin-DAD construct is Diaphanous at the NMJ then expression of the activating construct in a *dia*^{2} null background should ameliorate the Kin-DAD phenotype (Figure 3-1F). However, a comparison of the NMJs from both genotypes revealed that the effect of Kin-DAD expression in the *dia*^{2} background was qualitatively and quantitatively indistinguishable from its expression in a wild type background (Figure 3-1F,G,H). Furthermore, expression of an activated Diaphanous construct, UAS-dia^{act} did not show the same dominant effect on synapse development observed with Kin-DAD expression. This was true even when both constructs were expressed under the control of the same Gal4. These data support the conclusion that the activation of Diaphanous is not responsible for the synaptic phenotype associated with Kin-DAD expression. Thus Kin-DAD does not interact exclusively with Dia, but also appears to target other proteins at the NMJ. While the exact identities of these proteins remain to be determined with certainty, the most likely candidates are other Diaphanous-related formin proteins. A search of the *Drosophila* genome using the conserved GBD domain of *diaphanous* identified two other potential DAD interactors. It is possible that one or both of these proteins are targets of the Kin-DAD construct.

Interestingly, there is a clear proximal to distal distribution of morphological defects in all Kin-DAD synapses imaged, mirroring the chronology of synapse growth (Zito et al., 1999). In some cases the initial growth of the NMJ appears normal with wild

type boutons developing first in the most proximal regions of the synapse. However, at some point in development, one bouton becomes overgrown. This event appears to interfere with normal NMJ expansion as typically only abnormally small boutons, referred to here as boutonlets, are observed distal to this point. Thus, the block of growth in the Kin-DAD synapse appears to correlate with the development of a single, enlarged bouton. It was therefore of interest to determine whether there was a measurable disruption of the cytoskeleton in the overgrown boutons.

Kin-DAD Expression does not Alter the Organization of Synaptic Actin.

As formins are known regulators of the actin cytoskeleton, it is possible that expression of the Kin-DAD alters the organization of synaptic actin. Regulation of actin is essential for normal NMJ growth and it is thus possible that changes in actin organization could underlie the changes in NMJ growth (Stewart et al., 2002; Coyle et al., 2004; Marie et al., 2004; Stewart et al., 2005). To visualize the presynaptic actin cytoskeleton a *UAS-actin-GFP* transgene was expressed presynaptically in the background of Kin-DAD expression. As previously demonstrated (Nunes et al., 2006 and see previous chapter, Figure 2-3), actin is localized throughout the synapse as patches or foci. Loss of Diaphanous activity was shown to result in a significant decrease in the number of actin foci at the NMJ (See previous chapter, Figure 2-3). Although the data indicate that Kin-DAD does not act exclusively on Dia, it is reasonable to think that activation of other DRFs at the synapse may similarly disrupt the regulation of the actin cytoskeleton. Thus it was anticipated that Kin-DAD expression would result in a significant increase in the number of actin foci at the synapse. Surprisingly however,

only a very slight increase in the density of actin foci was observed in the background of Kin-DAD expression relative to a wild type synapse (*C155*/+; *UAS-actin-GFP*/+=2.21±0.08 foci/μm^2; *C155*/+; *UAS-actin-GFP*/+; *UAS-Kin-DAD*/+=2.55±0.08 foci/μm^2. $P<0.01$). While this increase was significant it is likely that is largely attributable to the presence of individual actin foci within the small distal most boutons (Figure 3-2B asterisk) of the Kin-DAD synapse creating an artificially high read out of actin density. Despite the clear importance of Diaphanous and other DRFs in regulating the actin cytoskeleton, the activation of this family of proteins does not significantly disrupt actin polymerization or organization at the *Drosophila* NMJ.

Kin-DAD Expression Alters Microtubule Organization and Behavior at the NMJ.

In addition to their role as actin regulators, some formins have been shown to play an important role in regulating the microtubule cytoskeleton (Wallar and Alberts, 2003; Eng et al., 2006; Bartolini et al., 2008; DeWard and Alberts, 2008). Activation of Diaphanous has been demonstrated in mammalian cell culture to result in cortical microtubule capture and stabilization (Alberts, 2001; Ishizaki et al., 2001; Eng et al., 2006). To determine the effect of Kin-DAD expression on the stable microtubule cytoskeleton at the NMJ larvae were stained with the anti-Futsch antibody. In the proximal most regions of the synapse where the boutons are of wild type size and shape, the organization of the stable core is normal. However, within the characteristic overgrown bouton the microtubule core becomes splayed and in many cases disintegrates completely. Distal to this enlarged bouton, specifically within strings of abnormally small boutons, Futsch staining is typically absent. Additionally, quantification of Futsch

staining reveals no significant change in the level of Futsch in the background of Kin-DAD expression. Taken together these data indicate that unlike the activation mDia1 or mDia2 *in vitro* (Ishizaki et al., 2001; Eng et al., 2006), the *in vivo* activation of DRFs at the synapse does not result in an increase in the stability of microtubules as measured by Futsch staining.

Although it is tempting to speculate that the presence of Kin-DAD results in the disruption of the microtubule cytoskeleton, it is not clear as yet where Kin-DAD is localized within the synapse. Thus, to determine the localization of the Kin-DAD construct and therefore the location of DRF activation, larvae were stained with the anti-Flag antibody. Curiously, despite being fused to the kinesin motor domain, Flag staining reveals the majority of the Kin-DAD construct found at the NMJ does not localize to the microtubule core. Instead the staining fills the volume of the bouton, suggesting a cytosolic distribution. Interestingly the distribution of Flag staining appeared to have a pattern opposite to that of Futsch staining. For example in the proximal most region of the synapse Futsch staining levels were high. In contrast Flag staining levels were correspondingly low in these regions of the NMJ. However, in the enlarged bouton, where Futsch staining was weak or absent, Flag levels were consistently high. This was also true of the string of small distal boutons (Figure 3-3E). Thus in areas of the synapse where Kin-DAD levels, and therefore presumably DRF activity, were high, Futsch staining was low (Figure 3-3 F-I). These observations suggest that the promiscuous activation of the Kin-DAD target or targets interferes with the normal interaction between Futsch and microtubules.

It was next of interest to determine whether dynamic microtubule invasion was altered in the background of Kin-DAD expression. To accomplish this EB1-GFP labeled plus-ends were imaged in wild type and Kin-DAD backgrounds. In wild type synapses EB1-GFP puncta move processively throughout all boutons of the NMJ (see previous chapters, Figure 3-3A). In contrast in the Kin-DAD background the pattern of plus-end advance largely mirrored the pattern of Futsch staining. For example, the behavior of plus-ends was not significantly altered within the normal proximal most boutons. However, a dramatic disruption in this behavior was observed in the enlarged bouton of the Kin-DAD synapse (Figure 3-3B, arrow and asterisk). Time-lapse imaging revealed that in this bouton, dynamic plus-ends make little forward advance. Further, EB1-GFP comets are only rarely observed to exit this bouton and invade the small distal boutons (Movie 3-1). The decreased forward advance is particularly obvious in side-by-side comparisons of projection images generated from time-lapse series of wild type and Kin-DAD muscle four synapses (compare Figure 3-3A, B). To more closely examine the advance of EB1-GFP puncta within the swollen bouton path traces were generated for both wild type and Kin-DAD synapses (Figure 3-3C). In the synapses of wild type larvae, EB1-GFP puncta followed a clear path, sometimes curving around the periphery of a bouton but never changing direction. In contrast, EB1-GFP puncta in the Kin-DAD background frequently change direction and typically fail to advance out of the overgrown bouton. In some cases the plus-ends appear to become trapped at the cortex and oscillate around a single point (See Figure 3-3C, bottom right panel). The total displacement of EB1-GFP over an identical time period was measured in wild type and Kin-DAD synapses to quantify the apparent decrease in forward advance. This analysis

revealed that over an identical period of time there is a significant decrease in the distance covered by EB1-GFP labeled plus-ends in a Kin-DAD synapse compared to wild type (*C155/Y; +/+; UAS-EB1-GFP/+* puncta displacement=1.23$\pm$0.019 μm, n=472 puncta; *C155/Y; +/+; UAS-Kin-DAD/UAS-EB1-GFP* puncta displacement = 0.69$\pm$0.018μm, n=671) (Figure 3-3D). These observations raise the possibility that a defect in the microtubule cytoskeleton, and not actin, underlies the disruption in NMJ growth seen in the Kin-DAD background.

Discussion

In this study, the role of the Diaphanous related formin (DRF) family of proteins in synapse development was examined. To allow activation of endogenous formin proteins at the synapse, the C-terminal Diaphanous auto-inhibitory was fused to the Kinesin motor domain. This construct, referred to as Kin-DAD was then expressed in larval motoneurons. Presynaptic expression of Kin-DAD resulted in a defect in synapse growth and a dramatic change in synapse morphology. Genetic evidence suggested that Kin-DAD was not a specific activator of Diaphanous as neither the synaptic morphology nor growth defects were ameliorated when Kin-DAD was expressed in the background of *dia*^{2} null larvae. This data raised the possibility that Kin-DAD targets other potential DRFs at the synapse. Next a combination of genetics and imaging studies were used to demonstrate that misregulation of Diaphanous and related proteins results in severe disruptions of the organization of the stable microtubule cytoskeleton. Additionally, Kin-DAD expression altered the behavior of the newly described pioneer microtubule population within the synapse. Interestingly, despite the common role of formin proteins as regulators of the actin cytoskeleton (Kovar et al., 2003; Kovar and Pollard, 2004; Higgs, 2005), little change was observed in this population in the background of Kin-DAD expression. In the future genetic experiments to identify all targets of Kin-DAD would be worthwhile. Although the source of the synaptic growth defect is not clear, the data acquired in this study suggest that the regulation of the microtubule cytoskeleton by one or more unknown DRF proteins is required for normal synaptic development. In

future it will be essential to identify the specific target or targets of the Kin-DAD construct to better understand the role of DRFs in synapse development.

Kin-DAD Expression Reveals a Role for Multiple DRFs in Synaptic Development.

In this study a DRF activating construct was designed and expressed in the motoneurons of *Drosophila* third instar larvae. Activation of Diaphanous and DRFs requires the disruption of an inhibitory intra-molecular bond between the N-terminal GBD and C-terminal DAD domains (Alberts, 2001; Li and Higgs, 2003; Li and Higgs, 2005; Otomo et al., 2005; Wallar et al., 2006). In a cellular context this is accomplished by the binding of an active Rho-type GTPase to the GBD, displacing the C-terminal DAD (Higgs, 2005; Otomo et al., 2005; Wallar et al., 2006). This changes the conformation of the DRF and allows other binding partners to interact. In many studies expression of an isolated Diaphanous DAD domain has been shown to mimic this activation by binding the GBD of the endogenous protein. The construct used here was designed to mimic the binding of a Rho-type GTPase to the GBD of Diaphanous. Although this construct was designed using the C-terminal autoinhibitory domain from Diaphanous, this domain shows strong homology between DRF family members. Thus, due to the common mechanism of regulation of DRF activity, it was likely the Kin-DAD construct would activate other DRF family members found at the NMJ.

The use of the Kin-DAD construct provides evidence that multiple DRFs are present at, and may play a role in the development of, the NMJ. Pre-synaptic expression of Kin-DAD resulted in a dramatic change in the growth and morphology

of the NMJ. Specifically, the synapses of Kin-DAD expressing larvae showed a 50% decrease in bouton number compared to wild type (Fig. 3-1F, H). Additionally, the morphology of these synapses was notably altered, showing an increase in the variation of bouton size and the presence of both abnormally small and abnormally large boutons (Fig. 3-1F, I). Interestingly, these phenotypes were not altered when Kin-DAD was expressed in a *diaphanous* null background, suggesting that Kin-DAD activity is not targeted specifically to this formin. This is further supported by evidence from a previous study demonstrating that expression of an activated Diaphanous construct (Δ-GBD) did not result in the same synaptic phenotype (See Fig. 2-2 E,F). Together these data argue that Kin-DAD is able to target other proteins at the synapse. Due to the specificity of the GBD-DAD interaction it is most likely these other proteins are members of the DRF family. A search of the Drosophila genome reveals two additional DRFs potentially expressed at the NMJ, Dishevelled Associated Activator of Morphogenesis (DAAM) and a previously uncharacterized GBD-DAD containing protein, CG32138. Future studies will focus on the role of these proteins in synapse growth.

Kin-DAD Mediated Activation of DRFs has no Effect on the Actin Cytoskeleton.

Formin proteins such as Diaphanous and other DRF proteins are well-characterized regulators of the actin cytoskeleton (Evangelista et al., 2003; Li and Higgs, 2003; Kobielak et al., 2004; Kovar and Pollard, 2004; Higgs, 2005). Specifically, the association of Profilin and g-actin with the FH1 and FH2 domains of the DRF results in the nucleation of new, unbranched actin filaments (Pruyne et al.,

2002; Kovar et al., 2003; Romero et al., 2004; Higgs, 2005). These proteins have also been shown to increase the rates of actin polymerization and induce filopodia formation in a number of systems. At the *Drosophila* NMJ, the loss of Diaphanous results in a significant decrease in the level of actin at the synapse and consequently a reduction in synapse size. Surprisingly however, the presynaptic activation of DRFs using Kin-DAD did not dramatically affect the number of polymerized actin structures or their organization at the NMJ (Fig. 3-2 A,B,C). The effect of DRF expression on the actin polymerization rates was not addressed in this study and awaits future *in vitro* studies. While a small increase in the density of actin structures in the background of Kin-DAD expression (Fig. 3-2 C), this is likely a reflection of the presence of a single actin structure within the boutonlets, rather than a legitimate increase in synaptic actin. It is also possible the relatively minor effect on the actin cytoskeleton is due to a compensatory up-regulation of actin de-polymerizing mechanisms. In future, it will be interesting to examine the effect of Kin-DAD expression in the background of a loss of actin filament severing activity.

DRF Activation Regulates NMJ Growth Through Modification of the Cytoskeleton.

The pre-synaptic expression of the Kin-DAD construct resulted in a dramatic change in the growth and morphology of the synapse. Typically, the proximal most boutons are normally formed. However early in synapse development a characteristic enlarged bouton forms. Distal to this enlarged bouton, synapse development is halted with only a few very small boutonlets forming (see Fig. 3-1F,H). Interestingly, Kin-

DAD expression, and therefore DRF activity, is highest within the characteristic enlarged bouton at the NMJ, and in the distal boutonlets. In contrast, Kin-DAD levels are low within the normal proximal boutons. Therefore constituitively high levels of DRF activity impair bouton formation and thus synapse growth. Examination of the effect of Kin-DAD expression on the cytoskeleton provided insight into the underlying defect in synapse growth.

DRFs are unique among formin proteins in that they have been shown to regulate both the microtubule and actin cytoskeletons in a variety of systems (Ishizaki et al., 2004, Higgs, 2005; Eng et al., 2006; DeWard and Alberts, 2008). The activation of Diaphanous and its homologs leads to the generation of a stable subset of microtubules through the capture and stabilization of pioneer microtubule plus-ends (Eng et al., 2006). In contrast, in this study presynaptic expression of Kin-DAD resulted in a severe disruption of the stable, Futsch-labeled core of microtubules. Specifically the Futsch core was severely fragmented or absent within the characteristic enlarged bouton. Additionally, no Futsch core was observed within the distal boutonlets. These findings raise the possibility that one or more DRFs regulate the formation of the stable microtubule core, possibly by regulating the association of Futsch with synaptic microtubules. Such a role has recently been shown to be important for the development of the NMJ (Ruiz-Canada et al., 2004). A second possibility is that high levels of DRF activity compromise the integrity of the stable microtubule core at the NMJ. In future studies, it will be of interest to identify the DRF responsible for regulating this interaction.

Changes in the behavior of the newly identified synaptic pioneer microtubules may also provide some insight into the possible roles of DRFs in synapse growth. Recent work has demonstrated that pioneer microtubule plus ends advance in a processive manner, often tracking the membrane cortex, throughout the length of a wild type synapse (Fig. 3-3C). This behavior has been proposed to be important for the relay of information from active cell surface receptors to the cytoskeleton, a role filled by pioneer microtubules in other systems (Tanaka et al., 1995; Gundersen, 2002; Suter et al., 2004). Interestingly, in the presence of the high levels of DRF activity found within the enlarged bouton of Kin-DAD the plus-ends of the pioneer microtubule population appear to become trapped at the cortex of the bouton. As a result very few pioneer microtubules are able to advance beyond this bouton. These data raise the possibility that the activation of one or more DRF is required for the capture of pioneer microtubule plus-ends in response to trophic signaling. To test this hypothesis, it will be necessary to identify the DRF or DRFs responsible for the membrane trapping of pioneer microtubules in the background of Kin-DAD expression. Future studies will focus on the role and regulation of microtubule capture downstream of DRF signaling.

Figure 3-1: Expression of a formin activating construct disrupts normal growth *in vitro* and *in vivo*.

(**A**) Schematic diagram of the Kin-DAD construct and its predicted interactions with microtubules and DRFs, using Diaphanous as an example. **(B,C**) Representative images of tubulin staining (green) in control (**B**) and UAS-Kin-DAD transfected (**C**) S2 cells stably expressing Gal4. Note the extensive microtubule bundling and tangles in transfected cells. Kin-DAD expressing cells were identified by co-transfection of DS-Red (**C**, asterisk). (**D-G)** Representative images of third instar muscle 4 NMJs in wild type (**D**), dia^2 (**E**), *C155/+; UAS-Kin-DAD/+* (**F**) and *C155/+;* dia^2*; UAS-Kin-DAD/+* (**G**) backgrounds, stained with the presynaptic membrane marker HRP. Note the characteristic overgrown bouton (**F, G** arrow) and mini-boutons (**F, G** asterisks) are present when Kin-DAD is expressed in both w^{1118} and dia^2 backgrounds. Scale bar=5μm. (**H**) Quantification of number of boutons per NMJ normalized to wild type synapses. Error bars represent SEM. (**I**) Histogram of the distribution of bouton areas in wild type and Kin-DAD expressing larvae. Note the large increase in small boutons the background of Kin-DAD expression.

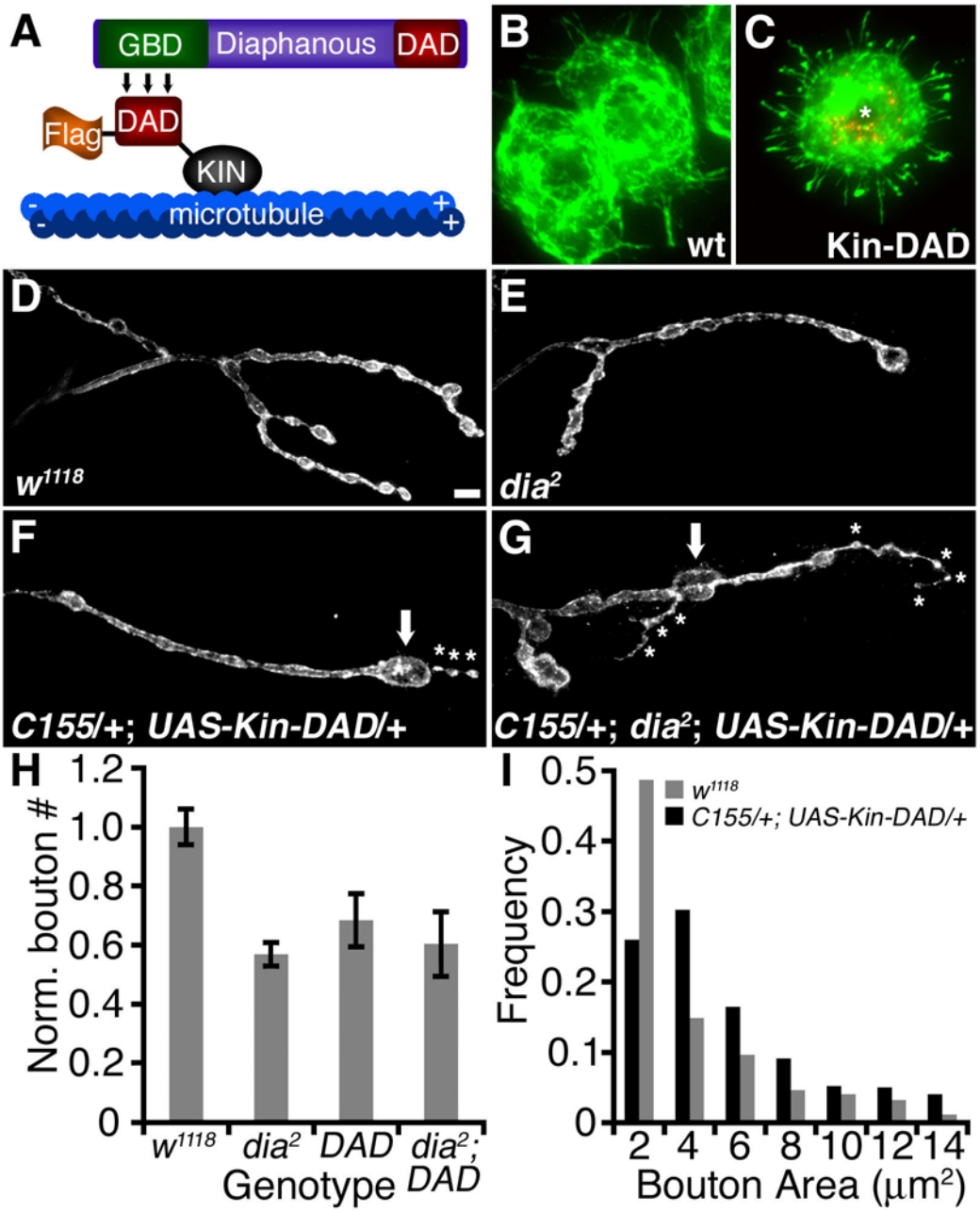
A
GBD
Diaphanous
DAD
Flag
DAD
KIN
microtubule
B
wt
C
Kin-DAD
D
w1118
E
dia2
F
C155/+; UAS-Kin-DAD/+
G
C155/+; dia2; UAS-Kin-DAD/+
H
Norm. bouton #
1.2
1.0
0.8
0.6
0.4
0.2
0
w1118
dia2
DAD
dia2; DAD
Genotype
I
Frequency
0.5
0.4
0.3
0.2
0.1
0
w1118
C155/+; UAS-Kin-DAD/+
2 4 6 8 10 12 14
Bouton Area (µm2)

Figure 3-2: Kin-DAD expression does not alter the organization of the actin cytoskeleton at the NMJ.

(A,B) Representative projection images generated from live imaging of actin-GFP expression at muscle 4 synapses in *C155/+; UAS-actin-GFP/+* (**A**) or *C155/+; UAS-Kin-DAD/UAS-actin-GFP* (**B**) backgrounds. Scale bar=5µm. (**C**) Graph represents the number of synaptic actin foci normalized to synapse area (*C155/+; UAS-actin-GFP* foci/μm^2=2.21$\pm$0.08, n=51 synapses. *C155/+; UAS-Kin-DAD/UAS-actin-GFP* foci/μm^2=2.55$\pm$0.08, n=58 synapses). Error bars represent SEM. (**D,E**) Representative images of third instar muscle 4 NMJ stained with 22C10 (green) and Flag (blue). Kin-DAD expression is under the control of *elaV-Gal4^{C155}*. Note that in the presence of high levels of Flag staining, 22C10 staining is disorganized or absent.

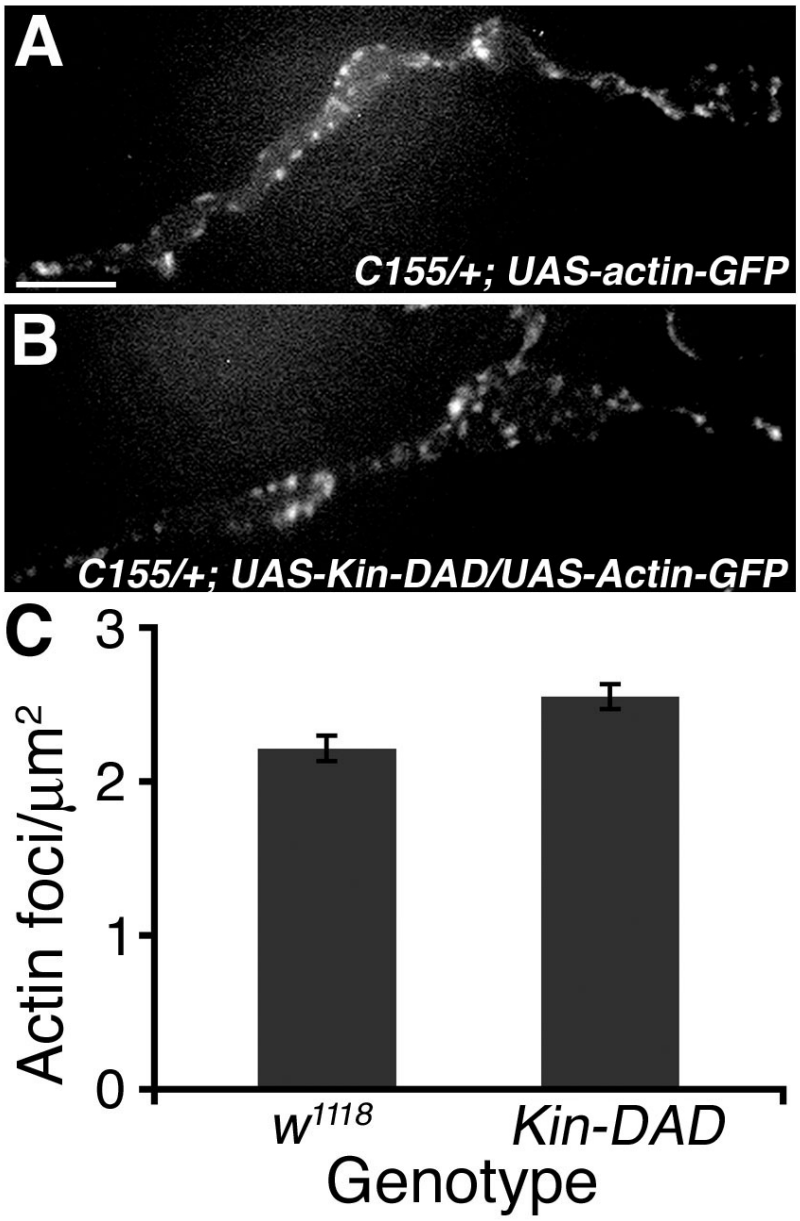
A
C155/+; UAS-actin-GFP
B
C155/+; UAS-Kin-DAD/UAS-Actin-GFP
C
Actin foci/μm²
0
1
2
3
w1118
Kin-DAD
Genotype

Figure 3-3: Expression of Kin-DAD construct dramatically alters the organization and behavior of the microtubule cytoskeleton at the NMJ.

(**A,B**) Representative projection images generated from time-lapse series in the muscle 4 NMJ of EB1-GFP advance in the backgrounds of *elaV-Gal4*^{C155}/+; *EB1-GFP*/+ (**A**) and *elaV-Gal4*^{C155}/+; *UAS-EB1-GFP*/*UAS-Kin-DAD* (**B**). (**C**) Composite path traces of individual plus ends within the muscle 4 synapses of *elaV-Gal4*^{C155}/+; *EB1-GFP*/+ (left column) and *elaV-Gal4*^{C155}/+; *UAS-EB1-GFP*/*UAS-Kin-DAD* (right column) larvae. Each composite trace is composed of a minimum of three individual microtubule plus ends from a single synapse. (**D**) Histogram of the total displacements of EB1-GFP in *elaV-Gal4*^{C155}/+; *UAS-EB1-GFP*/+ (diamonds) and *elaV-Gal4*^{C155}/+; *EB1-GFP*/*UAS-Kin-DAD* (squares). (**E**) Representative image of a muscle 4 NMJ from the *elaV-Gal4*^{C155}/+; *UAS-EB1-GFP/UAS-Kin-DAD* background stained with anti-HRP (red), anti-Futsch (green) and anti-Flag (blue). Below the merged image the individual channels are shown. Note that Futsch staining is severely disrupted upon entering the characteristic overgrown bouton, while in contrast it is in this area that Flag staining intensifies. (**F-I**) Representative images of four of muscle 4 synapses from the *elaV-Gal4*^{C155}/+; *EB1-GFP/UAS-Kin-DAD* background stained with anti-Futsch (green) and anti-Flag (blue) demonstrate a consistent exclusion of Futsch staining in synaptic regions with high levels of Flag.

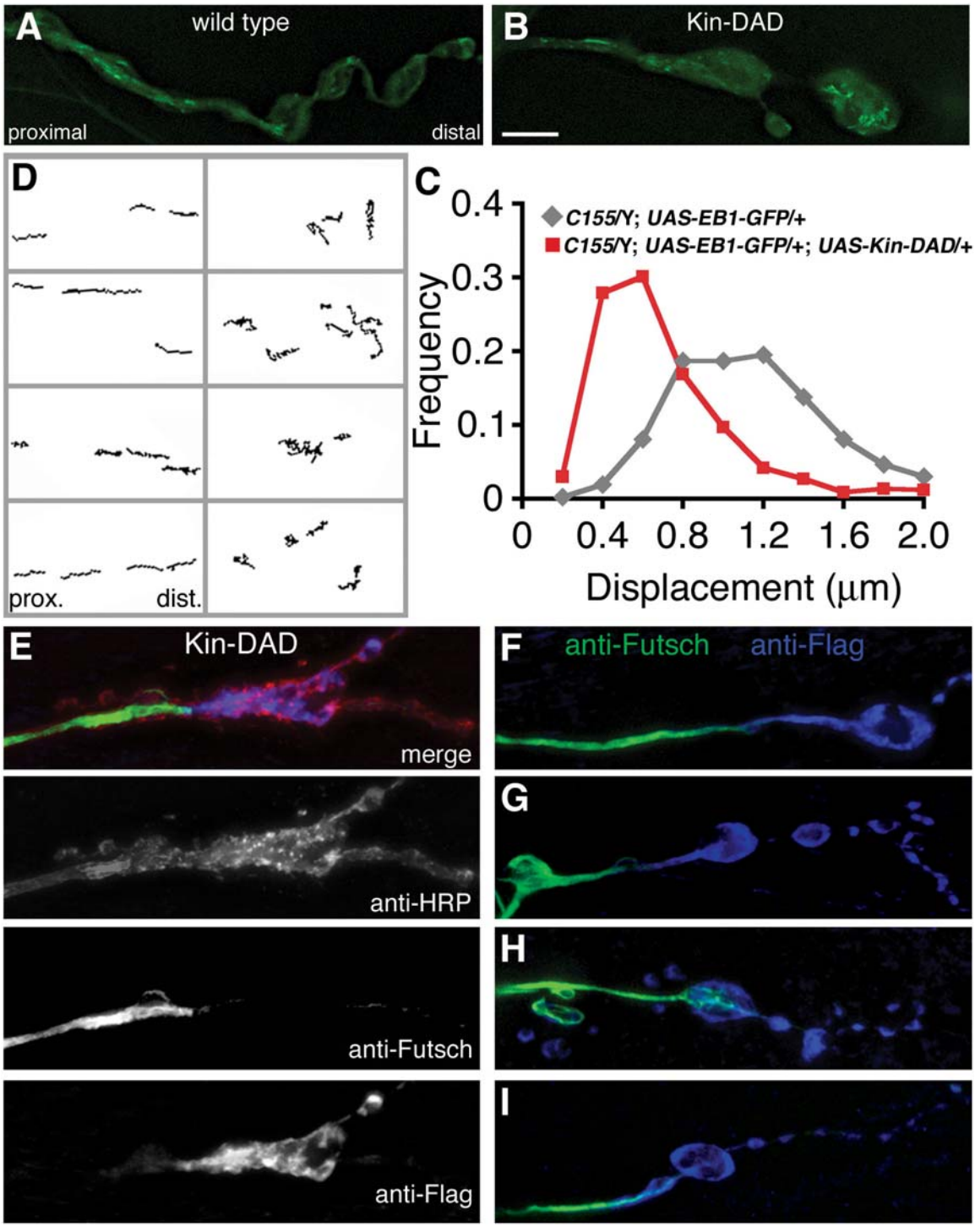
A
wild type
proximal
distal
B
Kin-DAD
D
prox.
dist.
C
C155/Y; UAS-EB1-GFP/+
C155/Y; UAS-EB1-GFP/+; UAS-Kin-DAD/+
Frequency
0.4
0.3
0.2
0.1
0
0
0.4
0.8
1.2
1.6
2.0
Displacement (μm)
E
Kin-DAD
merge
anti-HRP
anti-Futsch
anti-Flag
F
anti-Futsch
anti-Flag
G
H
I

Supplemental Movie 3-1: EB1-GFP movement within the synapse of Kin-DAD expressing larvae. This movie accompanies Figure 3-3. The synapse at muscle 4 is shown with EB1-GFP movement. Note the disruption in processive forward microtubule advance that occurs within the characteristically enlarged Kin-DAD bouton.

DISCUSSION

In the preceding chapters the importance of the dynamic population of microtubules in synapse growth was examined. Previous work has convincingly demonstrated that a population of microtubules bundled and labeled by the MAP, Futsch, is required for normal synaptic growth and stability (Roos et al., 2000; Eaton et al., 2004; Ruiz-Canada et al, 2004; Pielage et al. 2005, 2008). However, the importance of dynamic microtubules in the growth and maintenance of synaptic connections is as yet unclear. Although the dynamic behavior of microtubules has been studied in cell culture, these studies have been limited to the study of microtubules in neurite extension and growth cone advance and have not addressed the behavior or regulation of this population in synapses. Here, a fluorescently tagged microtubule plus-end binding protein was expressed in motoneurons to allow examination of dynamic microtubules at the NMJ (Rolls et al., 2007; Yan and Broadie, 2007). Using this tool, dynamic microtubules were frequently observed to invade regions of the synapse previously thought to be devoid of microtubule infiltration due to a lack of Futsch staining in this region (Roos et al., 2000, Ruiz-Canada et al, 2004). Additionally, the invasive behavior and dynamics of the pioneer microtubule population were largely unaffected by the loss of Futsch. These data suggested that the MAP plays little or no role in the regulation of microtubule dynamics at the NMJ. In a second study, Dia function was found to be required for the regulation of both the actin cytoskeleton and the pioneer microtubule population. These disruptions correlated with a significant reduction in synapse growth in the background of a loss of Dia activity. Interestingly, while the pioneer microtubule population was dramatically altered, there is only a subtle dis-organization of the stable Futsch-labeled core in the background of a loss of Dia. Finally, EB1-GFP was used to probe the role of a sub-

family of formin proteins, the Diaphanous related formins (DRFs) in synapse growth. In this study the expression of a DRF activating construct resulted in a striking defect in synapse growth and morphology. This defect corresponded to dramatic changes in the advance and behavior of EB1-GFP-labeled microtubule plus-ends at the NMJ. Together, the data from these studies strongly suggest that a pioneer population of microtubules plays an important role in the continued growth of synaptic connections throughout development. More studies will be needed to further elucidate the mechanism by which pioneer microtubules support new synaptic growth.

Analysis of Synaptic Pioneer Microtubules Using EB1-GFP.

Many previous studies of synaptic microtubules have focused on the pattern of fixed tissue staining of a stable, microtubule core. These studies revealed a common correlation between disruption of this core and defects in synaptic growth across a variety of systems (Roos et al., 2000; Pennetta et al., 2002; Zhang et al., 2002; Lu et al., 2004; Pannetta et al., 2004). At the *Drosophila* NMJ the microtubule core requires the bundling and stabilizing activity of the MAP, Futsch (Hummel et al., 2000; Roos et al., 2000). In this system, it has been hypothesized that disruption of the organization of Futsch staining reflects changes in the dynamics of the underlying microtubules (Roos et al., 2000; Ruiz-Canada et al., 2004). Due to technical limitations, however, this hypothesis had never been tested. Here it was demonstrated that EB1-GFP could be used to monitor a population of synaptic pioneer microtubules *in vivo*. The findings in these studies largely support an alternate hypothesis that is that the stable microtubule core and microtubule dynamics are regulated independently. It was observed for example, that the

dynamic properties and invasive behavior of pioneer microtubules were largely unaffected by the loss of Futsch, a background with a fragmented and disorganized microtubule core. Additionally, a significant change in microtubule behavior was observed in the NMJs of Diaphanous null larvae, while the stable core was only subtly affected (Fig. 2-8). Thus, to gain a better understanding of the regulation of microtubules at the NMJ, it will be important to re-examine the behavior of pioneer microtubules in other backgrounds known to alter the organization of the stable microtubule core. The use of EB1-GFP will in future allow a more thorough study of the regulation of microtubule cytoskeleton at the NMJ.

Regulation of Synapse Growth by Pioneer Microtubules

Examination of pioneer microtubules in other systems may provide some insight into the mechanisms by which this population may regulate synapse growth. It was demonstrated that pioneer microtubules within the third instar *Drosophila* NMJ invade all regions of the synapse and frequently track the membrane cortex. This behavior is remarkably similar to the behavior of pioneer microtubules in a variety of other systems such as the growth cone, migrating fibroblasts and budding yeast (Tanaka et al., 1995; Dent and Kalil, 1999; Adames et al., 2000: Gundersen, 2002; Salmon et al., 2002; Schaeffer et al., 2002; Gundersen et al., 2004; Suter et al., 2004). In these systems, a population of dynamic plus ends has been shown to constantly explore the cell cortex thereby allowing the identification of rare targets, such as activated signaling receptors or other cell surface proteins. For example, in the growth cone, invasion of filopodia by pioneer microtubules is required for normal and efficient guidance signaling. In the

nervous system, successful transmission of trophic signals is required for the growth and maintenance of synapses (Aberle et al., 2002; Marques, 2005; Zweifel et al., 2005; Bamji et al., 2006; Reichardt, 2006). Thus, a potential role for the pioneer microtubule population at the synapse may be to target and relay trophic signaling at sites permissive of new growth. A number of recent studies have demonstrated that the BMP signaling pathway acts as trophic support for the *Drosophila* NMJ (Aberle et al., 2002, Eaton et al., 2005). In future, it will be of interest to determine whether changes in the behavior of pioneer microtubules alters the efficiency or levels of BMP signaling at the synapse. It will be particularly interesting to address this question under conditions of impaired microtubule advance. For example the pre-synaptic expression of Kin-DAD results in the trapping of dynamic plus-ends at a particular point in the synapse (See Fig.3-3 B). Additionally, it would be worthwhile to examine the effect of expression of an activated BMP receptor, such as Wit, on the behavior of pioneer microtubules. Together these studies will aid in further elucidating the contribution of pioneer microtubules in synapse growth.

The pre-synaptic expression of EB1-GFP may also be of use in dissecting the contribution of dynamic microtubules and actin in synapse growth. The regulation of both actin and microtubules are required for the normal development of the NMJ, although it is likely that each element is required for different aspects of bouton addtion (Roos et al., 2000; Stewart et al., 2002; Pannetta et al., 2002; Marie et al., 2004; Ruiz-Canada et al., 2004; Stewart et al., 2005). Actin is required in many systems for the membrane protrusion required for the formation of new synaptic connections (Stewart et al., 2002; Coyle et al., 2004; Marie et al., 2004; Stewart et al., 2005), while it is

hypothesized that pioneer microtubules are required to identify sites permissive of new bouton addition (see Fig. 1-11). Thus the addition of a new bouton would require the coordinated regulation of both cytoskeletal elements and disruption of either function would be expected to result in synaptic growth defects. Interestingly, in these studies Diaphanous was demonstrated to regulate both actin polymerization and the rate of pioneer plus-end advance (See Fig. 2-3 and Fig. 2-6). As expected, disruption of both of these elements resulted in decreased synapse growth (See Fig. 2-2B,D,F). While it is clear that the mis-regulation of actin contributes to this growth defect, the extent to which defects in pioneer microtubule growth contribute to this phenotype was not examined. To address this question, the expression of a Diaphanous construct lacking the ability to regulate pioneer microtubules, while maintaining actin regulation could be informative. This study will require mapping the tubulin interaction domain of Diaphanous. Thus, in future, the use of EB1-GFP can be used to probe the interplay of microtubule and actin regulation in the development of the synapse.

Regulation of Synapse Stability by Pioneer Microtubules.

The loss of extant synaptic connections underlies the pathology of neurodegenerative diseases. While the mechanisms underlying synapse loss are not clear, there have been a number of hints that the normal regulation of dynamic microtubules may be required for synapse maintenance. For example, loss of p150/Glued activity is correlated with synapse loss in systems from Drosophila to humans (Eaton et al., 2002; LaMonte et al., 2002; Puls et al., 2003; Munch et al., 2004). It is interesting to note that this dynactin complex member is also required for normal pioneer microtubule

advance and growth (Ligon et al., 2003 and Fig1-7B,D,F,G,J). Together these facts raise the possibility that microtubule dynamics play a role in synapse maintenance, perhaps through the efficient relay of trophic signaling. However, the stable microtubule core is also disrupted in a number of retraction backgrounds, suggesting that synapse loss may be the result of loss of protein trafficking and physical support. To further probe the role of dynamic microtubules in synapse retraction, the behavior of pioneer microtubules should be examined in other retraction backgrounds, for example in the background of pre-synaptic disruption of α-spectrin activity (Pielage et al., 2005, Pielage et al., 2008). Live imaging of dynamic plus-ends in a synapse actively undergoing a retraction event could provide some insight into the behavior of pioneer microtubules at sites of synapse loss. However, such a study presents a number of technical challenges. To identify an individual retraction event will require that the pre-synaptic membrane be marked, perhaps using pre-synaptic expression of a fluorescently labeled CD8 molecule or through use of an FM dye, as well as pre-synaptic EB1-GFP. Additionally, this study would require the observation of a single synapse over a period of hours, presenting a challenge to keeping the larval preparation alive for the period of study.

In the preceding studies presynaptic expression of EB1-GFP was used as a tool to characterize the behavior and regulation of a newly described population of pioneer microtubules at the *Drosophila* NMJ. In these studies it was revealed that the behavior and regulation of pioneer microtubules is largely independent from the regulation of the well-studied Futsch-labeled core. In future it will be important to examine the behavior of both the dynamic and stable microtubules when assessing the function of molecule affecting synapse growth. In the above studies the behavior of pioneer microtubules in a

variety of genetic backgrounds has suggested potential roles for this population in the growth of the synapse. Further it is possible that mis-regulation of microtubule dynamics could affect synapse stability. Future studies will be required to continue to probe the role of dynamic microtubules in the growth and maintenance of synaptic connections.

References

Aberle H, Haghighi AP, Fetter RD, McCabe BD, Magalhaes TR, Goodman CS (2002) wishful thinking encodes a BMP type II receptor that regulates synaptic growth in Drosophila. Neuron 33:545-558.

Adames NR, Cooper JA (2000) Microtubule interactions with the cell cortex causing nuclear movements in Saccharomyces cerevisiae. J Cell Biol 149:863-874.

Akhmanova A, Hoogenraad CC (2005) Microtubule plus-end-tracking proteins: mechanisms and functions. Curr Opin Cell Biol 17:47-54.

Akhmanova A, Steinmetz MO (2008) Tracking the ends: a dynamic protein network controls the fate of microtubule tips. Nat Rev Mol Cell Biol 9:309-322.

Akhmanova A, Hoogenraad CC, Drabek K, Stepanova T, Dortland B, Verkerk T, Vermeulen W, Burgering BM, De Zeeuw CI, Grosveld F, Galjart N (2001) Clasps are CLIP-115 and -170 associating proteins involved in the regional regulation of microtubule dynamics in motile fibroblasts. Cell 104:923-935.

Alberts AS (2001) Identification of a carboxyl-terminal diaphanous-related formin homology protein autoregulatory domain. J Biol Chem 276:2824-2830.

Allen MJ, Shan X, Caruccio P, Froggett SJ, Moffat KG, Murphey RK (1999) Targeted expression of truncated glued disrupts giant fiber synapse formation in Drosophila. J Neurosci 19:9374-9384.

Baas PW (2002) Microtubule transport in the axon. Int Rev Cytol 212:41-62.

Baas PW, Brown A (1997) Slow axonal transport: the polymer transport model. Trends Cell Biol 7:380-384.

Baas PW, Black MM, Banker GA (1989) Changes in microtubule polarity orientation during the development of hippocampal neurons in culture. J Cell Biol 109:3085-3094.

Baas PW, Vidya Nadar C, Myers KA (2006) Axonal transport of microtubules: the long and short of it. Traffic 7:490-498.

Bamji SX, Rico B, Kimes N, Reichardt LF (2006) BDNF mobilizes synaptic vesicles and enhances synapse formation by disrupting cadherin-beta-catenin interactions. J Cell Biol 174:289-299.

Banan A, Zhang L, Fields JZ, Farhadi A, Talmage DA, Keshavarzian A (2002) PKC-zeta prevents oxidant-induced iNOS upregulation and protects the microtubules and gut barrier integrity. Am J Physiol Gastrointest Liver Physiol 283:G909-922.

Barth AI, Nathke IS, Nelson WJ (1997) Cadherins, catenins and APC protein: interplay between cytoskeletal complexes and signaling pathways. Curr Opin Cell Biol 9:683-690.

Bartolini F, Moseley JB, Schmoranzer J, Cassimeris L, Goode BL, Gundersen GG (2008) The formin mDia2 stabilizes microtubules independently of its actin nucleation activity. J Cell Biol 181:523-536.

Basu R, Chang F (2007) Shaping the actin cytoskeleton using microtubule tips. Curr Opin Cell Biol 19:88-94.

Bateman J, Shu H, Van Vactor D (2000) The guanine nucleotide exchange factor trio mediates axonal development in the Drosophila embryo. Neuron 26:93-106.

Berrueta L, Tirnauer JS, Schuyler SC, Pellman D, Bierer BE (1999) The APC-associated protein EB1 associates with components of the dynactin complex and cytoplasmic dynein intermediate chain. Curr Biol 9:425-428.

Bettencourt da Cruz A, Schwarzel M, Schulze S, Niyyati M, Heisenberg M, Kretzschmar D (2005) Disruption of the MAP1B-related protein FUTSCH leads to changes in the neuronal cytoskeleton, axonal transport defects, and progressive neurodegeneration in Drosophila. Mol Biol Cell 16:2433-2442.

Black MM, Baas PW (1989) The basis of polarity in neurons. Trends Neurosci 12:211-214.

Brand AH, Manoukian AS, Perrimon N (1994) Ectopic expression in Drosophila. Methods Cell Biol 44:635-654.

Brunner A, O'Kane CJ (1997) The fascination of the Drosophila NMJ. Trends Genet 13(3):85-87

Buck KB, Zheng JQ (2002) Growth cone turning induced by direct local modification of microtubule dynamics. J Neurosci 22:9358-9367.

Burnette DT, Schaefer AW, Ji L, Danuser G, Forscher P (2007) Filopodial actin bundles are not necessary for microtubule advance into the peripheral domain of Aplysia neuronal growth cones. Nat Cell Biol 9:1360-1369.

Carvalho P, Tirnauer JS, Pellman D (2003) Surfing on microtubule ends. Trends Cell Biol 13:229-237.

Cassimeris LU, Walker RA, Pryer NK, Salmon ED (1987) Dynamic instability of microtubules. Bioessays 7(4):149-154

Castrillon DH, Wasserman SA (1994) Diaphanous is required for cytokinesis in

Drosophila and shares domains of similarity with the products of the limb deformity gene. Development 120:3367-3377.

Challacombe JF, Snow DM, Letourneau PC (1997) Dynamic microtubule ends are required for growth cone turning to avoid an inhibitory guidance cue. J Neurosci 17:3085-3095.

Chang S, Svitkina TM, Borisy GG, Popov SV (1999) Speckle microscopic evaluation of microtubule transport in growing nerve processes. Nat Cell Biol 1:399-403.

Comery TA, Harris JB, Willems PJ, Oostra BA, Irwin SA, Weiler IJ, Greenough WT (1997) Abnormal dendritic spines in fragile X knockout mice: maturation and pruning deficits. Proc Natl Acad Sci U S A 94:5401-5404.

Cook TA, Nagasaki T, Gundersen GG (1998) Rho guanosine triphosphatase mediates the selective stabilization of microtubules induced by lysophosphatidic acid. J Cell Biol 141:175-185.

Coyle IP, Koh YH, Lee WC, Slind J, Fergestad T, Littleton JT, Ganetzky B (2004) Nervous wreck, an SH3 adaptor protein that interacts with Wsp, regulates synaptic growth in Drosophila. Neuron 41:521-534.

De Roo M, Klauser P, Garcia PM, Poglia L, Muller D (2008) Spine dynamics and synapse remodeling during LTP and memory processes. Prog Brain Res. 169:199-207
Dehmelt L, Halpain S (2004) Actin and microtubules in neurite initiation: are MAPs the missing link? J Neurobiol 58:18-33.

Dent EW, Kalil K (2001) Axon branching requires interactions between dynamic microtubules and actin filaments. J Neurosci 21:9757-9769.

Dent EW, Gertler FB (2003) Cytoskeletal dynamics and transport in growth cone motility and axon guidance. Neuron 40:209-227.

Dent EW, Callaway JL, Szebenyi G, Baas PW, Kalil K (1999) Reorganization and movement of microtubules in axonal growth cones and developing interstitial branches. J Neurosci 19:8894-8908.

Desai A, Mitchison TJ (1997) Microtubule polymerization dynamics. Annu Rev Cell Dev Biol 13:83-117

DeWard AD, Alberts AS (2008) Microtubule stabilization: formins assert their independence. Curr Biol 18:R605-608.

DiTella MC, Feiguin F, Carri N, Kosik KS, Caceres A (1996) MAP-1B/TAU functional redundancy during laminin-enhanced axonal growth. J Cell Sci 109 (Pt 2):467-477.

Drewes G, Ebneth A, Mandelkow EM (1998) MAPs, MARKs and microtubule dynamics. Trends Biochem Sci 23(8):307-311

Dunah AW, Hueske E, Wyszynski M, Hoogenraad CC, Jaworski J, Pak DT, Simonetta A, Liu G, Sheng M (2005) LAR receptor protein tyrosine phosphatases in the development and maintenance of excitatory synapses. Nat Neurosci 8:458-467.

Eaton BA, Fetter RD, Davis GW (2002) Dynactin is necessary for synapse stabilization. Neuron 34:729-741.

Eaton BA, Davis GW (2005) LIM Kinase1 controls synaptic stability downstream of the type II BMP receptor. Neuron 47:695-708.

Edwards KA, Demsky M, Montague RA, Weymouth N, Kiehart DP (1997) GFP-moesin illuminates actin cytoskeleton dynamics in living tissue and demonstrates cell shape changes during morphogenesis in Drosophila. Dev Biol 191:103-117.

Emmons S, Phan H, Calley J, Chen W, James B, Manseau L (1995) Cappuccino, a Drosophila maternal effect gene required for polarity of the egg and embryo, is related to the vertebrate limb deformity locus. Genes Dev 9:2482-2494.

Eng CH, Huckaba TM, Gundersen GG (2006) The formin mDia regulates GSK3beta through novel PKCs to promote microtubule stabilization but not MTOC reorientation in migrating fibroblasts. Mol Biol Cell 17:5004-5016.

Errico A, Ballabio A, Rugarli EI (2002) Spastin, the protein mutated in autosomal dominant hereditary spastic paraplegia, is involved in microtubule dynamics. Hum Mol Genet 11:153-163.

Evangelista M, Zigmond S, Boone C (2003) Formins: signaling effectors for assembly and polarization of actin filaments. J Cell Sci 116:2603-2611.

Farkasovsky M, Kuntzel H (2001) Cortical Num1p interacts with the dynein intermediate chain Pac11p and cytoplasmic microtubules in budding yeast. J Cell Biol 152:251-262.

Featherstone DE, Broadie K (2000) Surprises from Drosophila: genetic mechanisms of synaptic plasticity. Brain Res Bull 53(5):501-511

Forscher P, Smith SJ (1988) Actions of cytochalasins on the organization of actin filaments and microtubules in a neuronal growth cone. J Cell Biol 107:1505-1516.

Fox AN, Zinn K (2005) The heparan sulfate proteoglycan syndecan is an in vivo ligand for the Drosophila LAR receptor tyrosine phosphatase. Curr Biol 15:1701-1711.

Fukata M, Watanabe T, Noritake J, Nakagawa M, Yamaga M, Kuroda S, Matsuura Y, Iwamatsu A, Perez F, Kaibuchi K (2002) Rac1 and Cdc42 capture microtubules through IQGAP1 and CLIP-170. Cell 109:873-885.

Garcia ML, Cleveland DW (2001) Going new places using an old MAP: tau, microtubules and human neurodegenerative disease. Curr Opin Cell Biol 13:41-48.

Gepner J, Li M, Ludmann S, Kortas C, Boylan K, Iyadurai SJ, McGrail M, Hays TS (1996) Cytoplasmic dynein function is essential in Drosophila melanogaster. Genetics 142:865-878.

Goldstein LS (2003) Do disorders of movement cause movement disorders and dementia? Neuron 40:415-425.

Goode BL, Drubin DG, Barnes G (2000) Functional cooperation between the microtubule and actin cytoskeletons. Curr Opin Cell Biol 12:63-71.

Goold RG, Owen R, Gordon-Weeks PR (1999) Glycogen synthase kinase 3beta phosphorylation of microtubule-associated protein 1B regulates the stability of microtubules in growth cones. J Cell Sci 112 (Pt 19):3373-3384.

Gordon-Weeks PR, Fischer I (2000) MAP1B expression and microtubule stability in growing and regenerating axons. Microsc Res Tech 48:63-74.

Gundersen GG (2002) Evolutionary conservation of microtubule-capture mechanisms. Nat Rev Mol Cell Biol 3:296-304.

Gundersen GG, Bulinski JC (1988) Selective stabilization of microtubules oriented toward the direction of cell migration. Proc Natl Acad Sci U S A 85:5946-5950.

Gundersen GG, Gomes ER, Wen Y (2004) Cortical control of microtubule stability and polarization. Curr Opin Cell Biol 16:106-112.

Gundersen GG, Kreitzer G, Cook T, Liao G (1998) Microtubules as determinants of cellular polarity. Biol Bull 194:358-360.

Hall AC, Lucas FR, Salinas PC (2000) Axonal remodeling and synaptic differentiation in the cerebellum is regulated by WNT-7a signaling. Cell 100:525-535.

Hartman JJ, Mahr J, McNally K, Okawa K, Iwamatsu A, Thomas S, Cheesman S, Heuser J, Vale RD, McNally FJ (1998) Katanin, a microtubule-severing protein, is a novel AAA ATPase that targets to the centrosome using a WD40-containing subunit. Cell 93:277-287.

Hazan J, Fonknechten N, Mavel D, Paternotte C, Samson D, Artiguenave F, Davoine CS, Cruaud C, Durr A, Wincker P, Brottier P, Cattolico L, Barbe V, Burgunder JM,

Prud'homme JF, Brice A, Fontaine B, Heilig B, Weissenbach J (1999) Spastin, a new AAA protein, is altered in the most frequent form of autosomal dominant spastic paraplegia. Nat Genet 23:296-303.

Heidary G, Fortini ME (2001) Identification and characterization of the Drosophila tau homolog. Mech Dev 108:171-178.
Higgs HN (2005) Formin proteins: a domain-based approach. Trends Biochem Sci 30:342-353.

Hirokawa N (1997) The mechanisms of fast and slow transport in neurons: identification and characterization of the new kinesin superfamily motors. Curr Opin Neurobiol 7:605-614.

Hoogenraad CC, Feliu-Mojer MI, Spangler SA, Milstein AD, Dunah AW, Hung AY, Sheng M (2007) Liprinalpha1 degradation by calcium/calmodulin-dependent protein kinase II regulates LAR receptor tyrosine phosphatase distribution and dendrite development. Dev Cell 12:587-602.

Howell BJ, McEwen BF, Canman JC, Hoffman DB, Farrar EM, Rieder CL, Salmon ED (2001) Cytoplasmic dynein/dynactin drives kinetochore protein transport to the spindle poles and has a role in mitotic spindle checkpoint inactivation. J Cell Biol 155:1159-1172.

Hummel T, Krukkert K, Roos J, Davis G, Klambt C (2000) Drosophila Futsch/22C10 is a MAP1B-like protein required for dendritic and axonal development. Neuron 26:357-370.

Ishizaki T, Morishima Y, Okamoto M, Furuyashiki T, Kato T, Narumiya S (2001) Coordination of microtubules and the actin cytoskeleton by the Rho effector mDia1. Nat Cell Biol 3:8-14.

Jan LY, Jan YN (1976) Properties of the larval neuromuscular junction in Drosophila melanogaster. J Physiol 262:189-214.

Janulevicius A, van Pelt J, van Ooyen A (2006) Compartment volume influences microtubule dynamic instability: a model study. Biophys J 90:788-798.

Johnson KG, Tenney AP, Ghose A, Duckworth AM, Higashi ME, Parfitt K, Marcu O, Heslip TR, Marsh JL, Schwarz TL, Flanagan JG, Van Vactor D (2006) The HSPGs Syndecan and Dallylike bind the receptor phosphatase LAR and exert distinct effects on synaptic development. Neuron 49:517-531.

Kabir N, Schaefer AW, Nakhost A, Sossin WS, Forscher P (2001) Protein kinase C activation promotes microtubule advance in neuronal growth cones by increasing average microtubule growth lifetimes. J Cell Biol 152:1033-1044.

Kalil K, Dent EW (2005) Touch and go: guidance cues signal to the growth cone cytoskeleton. Curr Opin Neurobiol 15:521-526.

Karki S, Holzbaur EL (1999) Cytoplasmic dynein and dynactin in cell division and intracellular transport. Curr Opin Cell Biol 11:45-53.

Kaufmann N, DeProto J, Ranjan R, Wan H, Van Vactor D (2002) Drosophila liprin-alpha and the receptor phosphatase Dlar control synapse morphogenesis. Neuron 34:27-38.

Keshishian H, Kim YS (2004) Orchestrating development and function: retrograde BMP signaling in the Drosophila nervous system. Trends Neurosci 27(3):143-147.

Kirschner M, Mitchison T (1986) Beyond self-assembly: from microtubules to morphogenesis. Cell 45:329-342.

Kobielak A, Pasolli HA, Fuchs E (2004) Mammalian formin-1 participates in adherens junctions and polymerization of linear actin cables. Nat Cell Biol 6:21-30.

Kotani N, Sakakibara H, Burgess SA, Kojima H, Oiwa K (2007) Mechanical properties of inner-arm dynein-f (dynein I1) studied with in vitro motility assays. Biophys J 93:886-894.

Kovar DR, Pollard TD (2004) Insertional assembly of actin filament barbed ends in association with formins produces piconewton forces. Proc Natl Acad Sci U S A 101:14725-14730.

Kovar DR, Kuhn JR, Tichy AL, Pollard TD (2003) The fission yeast cytokinesis formin Cdc12p is a barbed end actin filament capping protein gated by profilin. J Cell Biol 161:875-887.

Krueger NX, Van Vactor D, Wan HI, Gelbart WM, Goodman CS, Saito H (1996) The transmembrane tyrosine phosphatase DLAR controls motor axon guidance in Drosophila. Cell 84:611-622.

LaMonte BH, Wallace KE, Holloway BA, Shelly SS, Ascano J, Tokito M, Van Winkle T, Howland DS, Holzbaur EL (2002) Disruption of dynein/dynactin inhibits axonal transport in motor neurons causing late-onset progressive degeneration. Neuron 34:715-727.

Lee H, Engel U, Rusch J, Scherrer S, Sheard K, Van Vactor D (2004) The microtubule plus end tracking protein Orbit/MAST/CLASP acts downstream of the tyrosine kinase Abl in mediating axon guidance. Neuron 42:913-926.

Li F, Higgs HN (2003) The mouse Formin mDia1 is a potent actin nucleation factor regulated by autoinhibition. Curr Biol 13:1335-1340.

Li F, Higgs HN (2005) Dissecting requirements for auto-inhibition of actin nucleation by the formin, mDia1. J Biol Chem 280:6986-6992.

Li JY, Edelmann L, Jahn R, Dahlstrom A (1996) Axonal transport and distribution of synaptobrevin I and II in the rat peripheral nervous system. J Neurosci 16:137-147.

Liebl FL, Chen K, Karr J, Sheng Q, Featherstone DE (2005) Increased synaptic microtubules and altered synapse development in Drosophila sec8 mutants. BMC Biol 3:27.

Ligon LA, Shelly SS, Tokito M, Holzbaur EL (2003) The microtubule plus-end proteins EB1 and dynactin have differential effects on microtubule polymerization. Mol Biol Cell 14:1405-1417.

Lisman J, Raghavachari S (2006) A unified model of the presynaptic and postsynaptic changes during LTP at CA1 synapes. Sci. STKE 2006(356):re11

Lo Nigro C, Chong CS, Smith AC, Dobyns WB, Carrozzo R, Ledbetter DH (1997) Point mutations and an intragenic deletion in LIS1, the lissencephaly causative gene in isolated lissencephaly sequence and Miller-Dieker syndrome. Hum. Mol. Genet. 6:157-164

Lopez LA, Sheetz MP (1993) Steric inhibition of cytoplasmic dynein and kinesin motility by MAP2. Cell Motil Cytoskeleton 24:1-16.

Lu R, Wang H, Liang Z, Ku L, O'Donnell W T, Li W, Warren ST, Feng Y (2004) The fragile X protein controls microtubule-associated protein 1B translation and microtubule stability in brain neuron development. Proc Natl Acad Sci U S A 101:15201-15206.

Lucas FR, Goold RG, Gordon-Weeks PR, Salinas PC (1998) Inhibition of GSK-3beta leading to the loss of phosphorylated MAP-1B is an early event in axonal remodelling induced by WNT-7a or lithium. J Cell Sci 111 (Pt 10):1351-1361.

Luo L, O'Leary DD (2005) Axon retraction and degeneration in development and disease. Annu Rev Neurosci 28:127-156.

Ma Y, Shakiryanova D, Vardya I, Popov SV (2004) Quantitative analysis of microtubule transport in growing nerve processes. Curr Biol 14:725-730.

Mandelkow EM, Thies E, Trinczek B, Biernat J, Mandelkow E (2004) MARK/PAR1 kinase is a regulator of microtubule-dependent transport in axons. J Cell Biol 167:99-110.

Marie B, Sweeney ST, Poskanzer KE, Roos J, Kelly RB, Davis GW (2004) Dap160/intersectin scaffolds the periactive zone to achieve high-fidelity endocytosis and normal synaptic growth. Neuron 43:207-219.

Marques G (2005) Morphogens and synaptogenesis in Drosophila. J Neurobiol 64:417-434.

Martin M, Iyadurai SJ, Gassman A, Gindhart JG, Jr., Hays TS, Saxton WM (1999) Cytoplasmic dynein, the dynactin complex, and kinesin are interdependent and essential for fast axonal transport. Mol Biol Cell 10:3717-3728.

McCabe BD, Marques G, Haghighi AP, Fetter RD, Crotty ML, Haerry TE, Goodman CS, O'Connor MB (2003) The BMP homolog Gbb provides a retrograde signal that regulates synaptic growth at the Drosophila neuromuscular junction. Neuron 39:241-254.

Menon L, Mader SA, Mihailescu MR. (2008) Fragile X mental retardation protein interactions with the microtubule associated protein 1B RNA. RNA 14(8):1644-1655.

Mimori-Kiyosue Y, Shiina N, Tsukita S (2000) The dynamic behavior of the APC-binding protein EB1 on the distal ends of microtubules. Curr Biol 10:865-868.

Molk JN, Bloom K (2006) Microtubule dynamics in the budding yeast mating pathway. J Cell Sci 119:3485-3490.

Molk JN, Salmon ED, Bloom K (2006) Nuclear congression is driven by cytoplasmic microtubule plus end interactions in S. cerevisiae. J Cell Biol 172:27-39.

Morrison EE (2007) Action and interactions at microtubule ends. Cell Mol Life Sci 64:307-317.

Morrison EE, Moncur PM, Askham JM (2002) EB1 identifies sites of microtubule polymerisation during neurite development. Brain Res Mol Brain Res 98:145-152.

Morrison EE, Wardleworth BN, Askham JM, Markham AF, Meredith DM (1998) EB1, a protein which interacts with the APC tumour suppressor, is associated with the microtubule cytoskeleton throughout the cell cycle. Oncogene 17:3471-3477.

Munch C, Sedlmeier R, Meyer T, Homberg V, Sperfeld AD, Kurt A, Prudlo J, Peraus G, Hanemann CO, Stumm G, Ludolph AC (2004) Point mutations of the p150 subunit of dynactin (DCTN1) gene in ALS. Neurology 63:724-726.

Newsome TP, Schmidt S, Dietzl G, Keleman K, Asling B, Debant A, Dickson BJ (2000) Trio combines with dock to regulate Pak activity during photoreceptor axon pathfinding in Drosophila. Cell 101:283-294.

Nogales E (1999) A structural view of microtubule dynamics. Cell Mol Life Sci 56(1-2):133-142

Nunes P, Haines N, Kuppuswamy V, Fleet DJ, Stewart BA (2006) Synaptic vesicle mobility and presynaptic F-actin are disrupted in a N-ethylmaleimide-sensitive factor allele of Drosophila. Mol Biol Cell 17:4709-4719.

Odde DJ (2005) Chromosome capture: take me to your kinetochore. Curr Biol 15(9):R328-330

Otomo T, Otomo C, Tomchick DR, Machius M, Rosen MK (2005) Structural basis of Rho GTPase-mediated activation of the formin mDia1. Mol Cell 18:273-281.

Palazzo AF, Cook TA, Alberts AS, Gundersen GG (2001) mDia mediates Rho-regulated formation and orientation of stable microtubules. Nat Cell Biol 3:723-729.

Palazzo AF, Eng CH, Schlaepfer DD, Marcantonio EE, Gundersen GG (2004) Localized stabilization of microtubules by integrin- and FAK-facilitated Rho signaling. Science 303:836-839.

Parkes TL, Elia AJ, Dickinson D, Hilliker AJ, Phillips JP, Boulianne GL (1998) Extension of Drosophila lifespan by overexpression of human SOD1 in motorneurons. Nat Genet 19:171-174.

Pellegrin S, Mellor H (2005) The Rho family GTPase Rif induces filopodia through mDia2. Curr Biol 15:129-133.

Pennetta G, Hiesinger PR, Fabian-Fine R, Meinertzhagen IA, Bellen HJ (2002) Drosophila VAP-33A directs bouton formation at neuromuscular junctions in a dosage-dependent manner. Neuron 35:291-306.

Piehl M, Tulu US, Wadsworth P, Cassimeris L (2004) Centrosome maturation: measurement of microtubule nucleation throughout the cell cycle by using GFP-tagged EB1. Proc Natl Acad Sci U S A 101:1584-1588.

Pielage J, Fetter RD, Davis GW (2005) Presynaptic spectrin is essential for synapse stabilization. Curr Biol 15:918-928.

Pielage J, Fetter RD, Davis GW (2006) A postsynaptic spectrin scaffold defines active zone size, spacing, and efficacy at the Drosophila neuromuscular junction. J Cell Biol 175:491-503.

Pielage J, Cheng L, Fetter RD, Carlton PM, Sedat JW, Davis GW (2008) A presynaptic giant ankyrin stabilizes the NMJ through regulation of presynaptic microtubules and transsynaptic cell adhesion. Neuron 58:195-209.

Pruyne D, Evangelista M, Yang C, Bi E, Zigmond S, Bretscher A, Boone C (2002) Role of formins in actin assembly: nucleation and barbed-end association. Science 297:612-615.

Puls I, Jonnakuty C, LaMonte BH, Holzbaur EL, Tokito M, Mann E, Floeter MK, Bidus K, Drayna D, Oh SJ, Brown RH, Jr., Ludlow CL, Fischbeck KH (2003) Mutant dynactin in motor neuron disease. Nat Genet 33:455-456

Reddy S, Jin P, Trimarchi J, Caruccio P, Phillis R, Murphey RK (1997) Mutant molecular motors disrupt neural circuits in Drosophila. J Neurobiol 33:711-723.

Reichardt LF (2006) Neurotrophin-regulated signalling pathways. Philos Trans R Soc Lond B Biol Sci 361:1545-1564.

Reiner O, Carrozzo R, Shen Y, Wehnert M, Faustinella F, Dobyns WB, Caskey CT, Ledbetter DH (1993) Isolation of a Miller-Dieker lissencephaly gene containing G protein b-subunit-like repeats. Nature 364:717-721

Ridley AJ (2006) Rho GTPases and actin dynamics in membrane protrusions and vesicle trafficking. Trends Cell Biol 16:522-529.

Rochlin MW, Wickline KM, Bridgman PC (1996) Microtubule stability decreases axon elongation but not axoplasm production. J Neurosci 16:3236-3246.

Rodriguez OC, Schaefer AW, Mandato CA, Forscher P, Bement WM, Waterman-Storer CM (2003) Conserved microtubule-actin interactions in cell movement and morphogenesis. Nat Cell Biol 5:599-609.

Rogers SL, Rogers GC, Sharp DJ, Vale RD (2002) Drosophila EB1 is important for proper assembly, dynamics, and positioning of the mitotic spindle. J Cell Biol 158:873-884.

Roll-Mecak A, Vale RD (2005) The Drosophila homologue of the hereditary spastic paraplegia protein, spastin, severs and disassembles microtubules. Curr Biol 15:650-655.

Roll-Mecak A, Vale RD (2008) Structural basis of microtubule severing by the hereditary spastic paraplegia protein spastin. Nature 451:363-367.

Rolls MM, Satoh D, Clyne PJ, Henner AL, Uemura T, Doe CQ (2007) Polarity and intracellular compartmentalization of Drosophila neurons. Neural Develop 2:7.

Romero S, Le Clainche C, Didry D, Egile C, Pantaloni D, Carlier MF (2004) Formin is a processive motor that requires profilin to accelerate actin assembly and associated ATP hydrolysis. Cell 119:419-429.

Roos J, Kelly RB (1998) Dap160, a neural-specific Eps15 homology and multiple SH3 domain-containing protein that interacts with Drosophila dynamin. J Biol Chem 273:19108-19119.

Roos J, Hummel T, Ng N, Klambt C, Davis GW (2000) Drosophila Futsch regulates synaptic microtubule organization and is necessary for synaptic growth. Neuron 26:371-382.

Rose D, Chiba A (2000) Synaptic target recognition at Drosophila neuromuscular junctions. Micros Res Tech 49(1):3-13

Ruiz-Canada C, Budnik V (2006) Synaptic cytoskeleton at the neuromuscular junction. Int Rev Neurobiol 75:217-236.

Ruiz-Canada C, Ashley J, Moeckel-Cole S, Drier E, Yin J, Budnik V (2004) New synaptic bouton formation is disrupted by misregulation of microtubule stability in aPKC mutants. Neuron 42:567-580.

Sabry JH, O'Connor TP, Evans L, Toroian-Raymond A, Kirschner M, Bentley D (1991) Microtubule behavior durin guidance of pioneer neuron growth cones in situ. J Cell Biol 115(2):381-395

Sagot I, Rodal AA, Moseley J, Goode BL, Pellman D (2002) An actin nucleation mechanism mediated by Bni1 and profilin. Nat Cell Biol 4:626-631.

Salmon WC, Adams MC, Waterman-Storer CM (2002) Dual-wavelength fluorescent speckle microscopy reveals coupling of microtubule and actin movements in migrating cells. J Cell Biol 158:31-37.

Schaefer AW, Kabir N, Forscher P (2002) Filopodia and actin arcs guide the assembly and transport of two populations of microtubules with unique dynamic parameters in neuronal growth cones. J Cell Biol 158:139-152.

Schaefer AW, Schoonderwoert VT, Ji L, Mederios N, Danuser G, Forscher P (2008) Coordination of actin filament and microtubule dynamics during neurite outgrowth. Dev Cell 15:146-162.

Schuster CM (2006) Glutamatergic synapses of Drosophila neuromuscular juncitons: a high resolution model for the analysis of experience-dependent potentiation. Cell Tissue Res. 326(2):287-299.

Schuster CM, Davis GW, Fetter RD, Goodman CS (1996) Genetic dissection of structural and functional components of synaptic plasticity. I. Fasciclin II controls synaptic stabilization and growth. Neuron 17:641-654.

Schuyler SC, Pellman D (2001) Microtubule "plus-end-tracking proteins": The end is just the beginning. Cell 105:421-424.

Seitz A, Kojima H, Oiwa K, Mandelkow EM, Song YH, Mandelkow E (2002) Single-molecule investigation of the interference between kinesin, tau and MAP2c. Embo J 21:4896-4905.

Sherwood NT, Sun Q, Xue M, Zhang B, Zinn K (2004) Drosophila spastin regulates synaptic microtubule networks and is required for normal motor function. PLoS Biol 2:e429.

Shin H, Wyszynski M, Huh KH, Valtschanoff JG, Lee JR, Ko J, Streuli M, Weinberg RJ, Sheng M, Kim E (2003) Association of the kinesin motor KIF1A with the multimodular protein liprin-alpha. J Biol Chem 278:11393-11401.

Signor D, Scholey JM (2000) Microtubule-based transport along axons, dendrites and axonemes. Essays Biochem 35:89-102.

Somogyi K, Rorth P (2004) Evidence for tension-based regulation of Drosophila MAL and SRF during invasive cell migration. Dev Cell 7:85-93.

Spangler SA, Hoogenraad CC (2007) Liprin-alpha proteins: scaffold molecules for synapse maturation. Biochem Soc Trans 35:1278-1282.

Stepanova T, Slemmer J, Hoogenraad CC, Lansbergen G, Dortland B, De Zeeuw CI, Grosveld F, van Cappellen G, Akhmanova A, Galjart N (2003) Visualization of microtubule growth in cultured neurons via the use of EB3-GFP (end-binding protein 3-green fluorescent protein). J Neurosci 23:2655-2664.

Stewart BA, Pearce J, Bajec M, Khorana R (2005) Disruption of synaptic development and ultrastructure by Drosophila NSF2 alleles. J Comp Neurol 488:101-111.

Stewart BA, Mohtashami M, Rivlin P, Deitcher DL, Trimble WS, Boulianne GL (2002) Dominant-negative NSF2 disrupts the structure and function of Drosophila neuromuscular synapses. J Neurobiol 51:261-271.

Suter DM, Schaefer AW, Forscher P (2004) Microtubule dynamics are necessary for SRC family kinase-dependent growth cone steering. Curr Biol 14:1194-1199.

Svoboda K, Block SM (1994) Force and velocity measured for single kinesin molecules. Cell 77:773-784.

Svoboda K, Schmidt CF, Schnapp BJ, Block SM (1993) Direct observation of kinesin stepping by optical trapping interferometry. Nature 365:721-727.

Takemura R, Okabe S, Umeyama T, Kanai Y, Cowan NJ, Hirokawa N (1992) Increased microtubule stability and alpha tubulin acetylation in cells transfected with microtubule-associated proteins MAP1B, MAP2 or tau. J Cell Sci 103 (Pt 4):953-964.

Tanaka E, Ho T, Kirschner MW (1995) The role of microtubule dynamics in growth cone motility and axonal growth. J Cell Biol 128:139-155.

Tanaka EM, Kirschner MW (1991) Microtubule behavior in the growth cones of living neurons during axon elongation. J Cell Biol 115:345-363.

Tinsley JH, Minke PF, Bruno KS, Plamann M (1996) p150Glued, the largest subunit of the dynactin complex, is nonessential in Neurospora but required for nuclear distribution. Mol Biol Cell 7:731-742.

Tirnauer JS, Grego S, Salmon ED, Mitchison TJ (2002) EB1-microtubule interactions in Xenopus egg extracts: role of EB1 in microtubule stabilization and mechanisms of targeting to microtubules. Mol Biol Cell 13:3614-3626.

Tominaga T, Sahai E, Chardin P, McCormick F, Courtneidge SA, Alberts AS (2000) Diaphanous-related formins bridge Rho GTPase and Src tyrosine kinase signaling. Mol Cell 5:13-25.

Topp KS, Meade LB, LaVail JH (1994) Microtubule polarity in the peripheral processes of trigeminal ganglion cells: relevance for the retrograde transport of herpes simplex virus. J Neurosci 14:318-325.

Trotta N, Orso G, Rossetto MG, Daga A, Broadie K (2004) The hereditary spastic paraplegia gene, spastin, regulates microtubule stability to modulate synaptic structure and function. Curr Biol 14:1135-1147.

Tsui HT, Lankford KL, Ris H, Klein WL (1984) Novel organization of microtubules in cultured central nervous system neurons: formation of hairpin loops at ends of maturing neurites. J Neurosci 4:3002-3013.

Vallee RB, Tsai J-W (2006) The cellular roles of the lissencephaly gene LIS1, and what they tell us about brain development. Genes Dev. 20:1384-1393

VanBerkum MF, Goodman CS (1995) Targeted disruption of Ca(2+)-calmodulin signaling in Drosophila growth cones leads to stalls in axon extension and errors in axon guidance. Neuron 14:43-56.

Vaughan KT, Tynan SH, Faulkner NE, Echeverri CJ, Vallee RB (1999) Colocalization of cytoplasmic dynein with dynactin and CLIP-170 at microtubule distal ends. J Cell Sci 112 (10):1437-1447.

Viquez NM, Li CR, Wairkar YP, DiAntonio A (2006) The B' protein phosphatase 2A regulatory subunit well-rounded regulates synaptic growth and cytoskeletal stability at the Drosophila neuromuscular junction. J Neurosci 26:9293-9303.

Wadsworth P (1999) Regional regulation of microtubule dynamics in polarized, motile cells. Cell Motil Cytoskeleton 42:48-59.

Wagh DA, Rasse TM, Asan E, Hofbauer A, Schwenkert I, Durrbeck H, Buchner S, Dabauvalle MC, Schmidt M, Qin G, Wichmann C, Kittel R, Sigrist SJ, Buchner E (2006) Bruchpilot, a protein with homology to ELKS/CAST, is required for structural integrity and function of synaptic active zones in Drosophila. Neuron 49:833-844.

Wallar BJ, Alberts AS (2003) The formins: active scaffolds that remodel the cytoskeleton. Trends Cell Biol 13:435-446.

Wallar BJ, Stropich BN, Schoenherr JA, Holman HA, Kitchen SM, Alberts AS (2006) The basic region of the diaphanous-autoregulatory domain (DAD) is required for autoregulatory interactions with the diaphanous-related formin inhibitory domain. J Biol Chem 281:4300-4307.

Wang S, Liu Y, Adamson CL, Valdez G, Guo W, Hsu SC (2004) The mammalian exocyst, a complex required for exocytosis, inhibits tubulin polymerization. J Biol Chem 279:35958-35966.

Watanabe N, Kato T, Fujita A, Ishizaki T, Narumiya S (1999) Cooperation between mDia1 and ROCK in Rho-induced actin reorganization. Nat Cell Biol 1:136-143.

Waterman-Storer CM, Salmon ED (1997a) Microtubule dynamics: treadmilling comes around again. Curr Biol 7(6):R369-372

Waterman-Storer CM, Salmon ED (1997b) Actomyosin-based retrograde flow of microtubules in the lamella of migrating epithelial cells influences microtubule dynamic instability and turnover and is associated with microtubule breakage and treadmilling. J Cell Biol 139:417-434.

Waterman-Storer CM, Desai A, Bulinski JC, Salmon ED (1998) Fluorescent speckle microscopy, a method to visualize the dynamics of protein assemblies in living cells. Curr Biol 8:1227-1230.

Wen Y, Eng CH, Schmoranzer J, Cabrera-Poch N, Morris EJ, Chen M, Wallar BJ, Alberts AS, Gundersen GG (2004) EB1 and APC bind to mDia to stabilize microtubules downstream of Rho and promote cell migration. Nat Cell Biol 6:820-830.

Williams MJ, Habayeb MS, Hultmark D (2007) Reciprocal regulation of Rac1 and Rho1 in Drosophila circulating immune surveillance cells. J Cell Sci 120:502-511.

Wittmann T, Desai A (2005) Microtubule cytoskeleton: a new twist at the end. Curr Biol 15:R126-129Wyszynski M, Kim E, Dunah AW, Passafaro M, Valtschanoff JG, Serra-Pages C, Streuli M, Weinberg RJ, Sheng M (2002) Interaction between GRIP and liprin-alpha/SYD2 is required for AMPA receptor targeting. Neuron 34:39-52.

Yan Y, Broadie K (2007) In vivo assay of presynaptic microtubule cytoskeleton dynamics in Drosophila. J Neurosci Methods 162:198-205.

Zhang YQ, Broadie K (2005) Fathoming fragile X in fruit flies. Trends Genet 21:37-45.

Zhang YQ, Bailey AM, Matthies HJ, Renden RB, Smith MA, Speese SD, Rubin GM, Broadie K (2001) Drosophila fragile X-related gene regulates the MAP1B homolog Futsch to control synaptic structure and function. Cell 107:591-603.

Zhen M, Jin Y (1999) The liprin protein SYD-2 regulates the differentiation of presynaptic termini in C. elegans. Nature 401:371-375.

Zhou FQ, Waterman-Storer CM, Cohan CS (2002) Focal loss of actin bundles causes microtubule redistribution and growth cone turning. J Cell Biol 157:839-849.

Zigmond SH (2004) Formin-induced nucleation of actin filaments. Curr Opin Cell Biol 16:99-105.

Zigmond SH, Evangelista M, Boone C, Yang C, Dar AC, Sicheri F, Forkey J, Pring M (2003) Formin leaky cap allows elongation in the presence of tight capping proteins. Curr Biol 13:1820-1823.

Zito K, Parnas D, Fetter RD, Isacoff EY, Goodman CS (1999) Watching a synapse grow: noninvasive confocal imaging of synaptic growth in Drosophila. Neuron 22:719-729.

Zweifel LS, Kuruvilla R, Ginty DD (2005) Functions and mechanisms of retrograde neurotrophin signalling. Nat Rev Neurosci 6:615-625.

Publishing Agreement

It is the policy of the University to encourage the distribution of all theses, dissertations, and manuscripts. Copies of all UCSF theses, dissertations, and manuscripts will be routed to the library via the Graduate Division. The library will make all theses, dissertations, and manuscripts accessible to the public and will preserve these to the best of their abilities, in perpetuity.

Please sign the following statement:

I hereby grant permission to the Graduate Division of the University of California, San Francisco to release copies of my thesis, dissertation, or manuscript to the Campus Library to provide access and preservation, in whole or in part, in perpetuity.

Rawson

Author Signature

1/6/2009

Date